

5-2015

The Effect Of Activation Induced Cytidine Deaminase Phosphorylation And Herpes Virus Uracil Dna Glycosylase On Antibody Diversification

Marc Macaluso

Follow this and additional works at: https://digitalcommons.library.tmc.edu/utgsbs_dissertations

 Part of the [Immunology of Infectious Disease Commons](#), [Medicine and Health Sciences Commons](#), [Molecular Biology Commons](#), and the [Virology Commons](#)

Recommended Citation

Macaluso, Marc, "The Effect Of Activation Induced Cytidine Deaminase Phosphorylation And Herpes Virus Uracil Dna Glycosylase On Antibody Diversification" (2015). *Dissertations and Theses (Open Access)*. 560.

https://digitalcommons.library.tmc.edu/utgsbs_dissertations/560

This Dissertation (PhD) is brought to you for free and open access by the MD Anderson UTHealth Houston Graduate School at DigitalCommons@TMC. It has been accepted for inclusion in Dissertations and Theses (Open Access) by an authorized administrator of DigitalCommons@TMC. For more information, please contact digcommons@library.tmc.edu.

**THE EFFECT OF ACTIVATION INDUCED CYTIDINE DEAMINASE PHOSPHORYLATION
AND HERPES VIRUS URACIL DNA GLYCOSYLASE ON ANTIBODY
DIVERSIFICATION**

BY

Marc Daniel Macaluso, B.S.

APPROVED:

Kevin M. McBride, Ph.D., Supervisory Professor

Rick A. Finch, Ph.D.

Ellen R. Richie, Ph.D.

Richard D. Wood, Ph.D.

Mark T. Bedford, Ph.D.

APPROVED:

Dean, The University of Texas
Graduate School of Biomedical Sciences at Houston

THE EFFECT OF ACTIVATION INDUCED CYTIDINE DEAMINASE PHOSPHORYLATION
AND HERPES VIRUS URACIL DNA GLYCOSYLASE ON ANTIBODY DIVERSIFICATION

A

Dissertation

Presented to the Faculty of

The University of Texas Health Science Center at Houston

And

The University of Texas M.D. Anderson Cancer Center

Graduate School of Biomedical Sciences

in Partial Fulfillment

of the Requirements

for the degree of

DOCTOR OF PHILOSOPHY

By

Marc Daniel Macaluso, B.S.

Houston, Texas

May 2015

THE EFFECT OF ACTIVATION INDUCED CYTIDINE DEAMINASE PHOSPHORYLATION AND HERPES VIRUS URACIL DNA GLYCOSYLASE ON ANTIBODY DIVERSIFICATION

Marc Daniel Macaluso, Ph.D.

Supervisory Professor: Kevin M. McBride, Ph.D.

Activation-induced cytidine deaminase (AID) is a mutagenic enzyme that is expressed in mammalian B-cells and initiates the antibody diversification processes of somatic hypermutation (SHM) and isotype class switch recombination (CSR). AID is targeted to the immunoglobulin gene locus where it deaminates cytosines to generate uracil residues in DNA. This generates guanine-uracil (U:G) mismatch lesion which are recognized by uracil DNA glycosylase (UNG), a DNA repair enzyme that removes uracil from DNA and triggers downstream repair of the lesion. While UNG is a ubiquitously expressed DNA repair enzyme, its recognition and removal of AID introduced uracils is essential in both SHM and CSR. Mice lacking AID or UNG are deficient in SHM and CSR resulting in a compromised immune system.

Due to its mutagenic activity AID is heavily regulated by diverse mechanisms including post-translational modification. Here we investigate the effect of AID phosphorylation in CSR, and identify potential phospho-AID interacting factors. Using an *in vitro* CSR assay we show that preventing AID phosphorylation at novel sites threonine-150, serine-169 and tyrosine-184 significantly reduces CSR efficiency. We identified potential phospho-AID binding proteins using a protein domain array screen, which may prove to be important in modulating AID activity.

Herpes viruses possess a large double stranded DNA genome and many carry a form of uracil DNA glycosylase. Many of these viruses, such as Epstein-Barr virus (EBV), infect mammalian B-cells. Our experiments show that viral UNGs are able to partially restore CSR

when expressed in B-cells from *Ung* deficient mice. Intriguingly we discovered that viral UNGs suppress CSR when expressed in wild-type B-cells, and that UNG catalytic activity is not required for this suppressive effect. We also found that viral UNG expression in mouse B-cells reduces the frequency of AID induced IgH-cMYC translocations, suggesting that viral UNG may play a role in protecting the host cell genome from damage. These studies have revealed a novel mechanism by which herpes viruses might impede the host immune system.

TABLE OF CONTENTS

	PAGE
APPROVAL PAGE	i
TITLE PAGE	ii
ABSTRACT	iii
TABLE OF CONTENTS	v
LIST OF FIGURES	viii
LIST OF TABLES	x
LIST OF ABBREVIATIONS	xi
CHAPTER 1: INTRODUCTION	1
1.1 Adaptive Immunity and the Antibody Diversification Processes	1
1.2 V(D)J Recombination	2
1.3 Somatic Hypermutation	3
1.4 Class Switch Recombination	6
1.5 Activation Induced Cytidine Deaminase (AID)	9
1.6 DNA Glycosylases	10
1.7 Mammalian DNA Glycosylases	13
1.8 Mammalian Uracil DNA Glycosylase (UNG)	14
1.9 Base Excision Repair	15
1.10 Base Excision Repair in B-cells	16
1.11 Herpesviridae	19
1.12 EBV Life Cycle	22
1.13 Mouse Models of Gamma Herpes Virus Infection	26

1.14 Oncoviruses	27
1.15 The Function of Viral Uracil DNA Glycosylase	31
CHAPTER 2: RATIONALE AND HYPOTHESIS	
2.1 The Role of AID Phosphorylation	36
2.2 The Involvement of γ Herpes Virus UNG in Antibody Diversification Processes	36
CHAPTER 3: THE DETECTION AND EFFECT OF AID PHOSPHORYLATION	
3.1 Class Switch Recombination Assay Characterization and Optimization	38
3.2 Chromatin Associated AID is Highly Modified	42
3.3 Generation of Phospho-Specific Antibodies	44
3.4 The Effect of AID Phosphorylation on Class Switch Recombination	48
3.5 Putative Phospho-AID Interacting Proteins	50
3.6 Differential Regulation of The PI3 Kinase Pathway on AID-S38 Phosphorylation	55
3.7 Chapter 3 Summary	57
CHAPTER 4: THE EFFECT OF VIRAL URACIL DNA GLYCOSYLASE ON ANTIBODY DIVERSIFICATION PROCESSES IN MAMMALINA B-CELLS	
4.1 Viral UNGs are Able to Partially Restore Isotype Class Switch Recombination in <i>Ung</i> ^{-/-} Mice	59
4.2 Viral UNGs Suppress Class Switch Recombination when Expressed in <i>wt</i> Mouse B-cells	62

4.3 UNG Catalytic Activity is Nonessential for Suppressing CSR in <i>wt</i> Mouse B-cells	67
4.4 Viral UNG Suppresses IgH-cMYC Translocations When Expressed in Mouse B-cells	72
4.5 Viral UNG Suppresses AID Induced Mutation in NTZ-3T3 Reporter Cells	77
4.6 Chapter 4 Summary	85
 CHAPTER 5: MATERIALS AND METHODS	
5.1 Antibodies and Reagents	86
5.2 Experimental Methods	87
 CHAPTER 6: DISCUSSION	
6.1 AID Phosphorylation	101
6.2 The Role of Herpes Virus UNG	104
 BIBLIOGRAPHY	
VITA	125

LIST OF FIGURES

Figure 1	A Depiction of the Somatic Hypermutation Process at the Immunoglobulin Heavy Chain (IgH) Locus	5
Figure 2	Class Switch Recombination Process at the IgG Locus	8
Figure 3	Crystal Structure of Human Uracil DNA Glycosylase	12
Figure 4	A Model for Class Switch Recombination and Somatic Hyper Mutation	17
Figure 5	The Cycle of Epstein-Barr Infection	24
Figure 6	Crystal Structure of Epstein-Barr Virus Uracil DNA Glycosylase	32
Figure 7	Alignment of Human, Mouse, and Gamma Herpes Virus UNG Amino Acid Sequences	33
Figure 8	Plating Density Effects Switch to IgG1 in Primary Mouse B-cells	39
Figure 9	The Lot of Serum used During the CSR Assay can Effect Switch Efficiency	41
Figure 10	Chromatin Associated AID is More Negatively Charge than Whole Cell AID	43
Figure 11	Anti p-184 and Anti p-150 are Specific for Phosphorylated AID Peptide	45
Figure 12	The Anti 184-Antibody Specifically Recognizes Phospho-Y184 AID Isolated from Mouse B-cells	47

Figure 13	Class Switch Recombination Efficiency is Effected by AID Phosphorylation	49
Figure 14	Phospho-AID Peptides Interact with Phospho-Binding Protein Domains	52
Figure 15	Phospho-Tyrosine Binding Protein SH3BP2 is Expressed in <i>wt</i> Mouse B-cells	53
Figure 16	SH3BP2 can be Detected from Cell Lysate by Western Blot	54
Figure 17	The PI3Kinase Inhibitor LY29004 Stimulates AID-S38 Phosphorylation in 3T3 Cells but not B-cells	56
Figure 18	Expression of Viral UNG in <i>Ung</i> ^{-/-} B-cells Provides Partial Compensation During CSR <i>in vitro</i>	60
Figure 19	Expression of Viral UNG in <i>wt</i> mouse B-cells Suppresses CSR <i>in vitro</i>	63
Figure 20	Two Potential Models to Explain the Ability of Viral UNG to Rescue CSR in <i>Ung</i> ^{-/-} B-cells and Suppress CSR in <i>wt</i> B-cells	65
Figure 21	UNG Catalytic Mutants are Generated by Site Directed Mutagenesis	68
Figure 22	UNG Catalytic Activity is Necessary for <i>Ung</i> ^{-/-} CSR Compensation But Dispensable for Suppression of CSR in <i>wt</i> B-Cells	71
Figure 23	Experimental Design for the IgH-cMYC Translocation Assay	

Figure 24	MHV-UNG Expression Decreases IgH-Myc Translocations in <i>wt</i> mouse B-Cells	75
Figure 25	Error Prone Repair at the GFP-STOP Codon in NTZ-3T3 Cells is Needed to Initiate GFP Transcription After AID Deamination	78
Figure 26	NTZ-3T3 Experimental Time Line	80
Figure 27	EBV-UNG and KSV-UNG Suppress AID Induced GFP Reversion Rates in NTZ-3T3 Cells Over Time	81
Figure 28	Expression of Viral UNGs in NTZ-3T3 Cells Suppresses GFP Reversion	82
Figure 29	EBV-UNG, KSV-UNG and MHV-UNG all Suppress AID Induced GFP Reversion in NTZ-3T3 Cells	84

LIST OF TABLES

Table 1	Known Human Herpes Viruses and Their Associated Pathologies	21
Table 2A	IgH-cMYC Translocation Data from Four Independent Experiments	76
Table 2B	Statistical Analysis of Translocation Data	76

LIST OF ABBREVIATIONS

AID	activation induced cytidine deaminase
AP	abasic site
BCR	B-cell receptor
BER	base excision repair
NHEJ	non-homologous end joining
cDNA	complementary DNA
CDR	complementarity determining region
CSR	class switch recombination
CMV	cytomegalovirus
DNA	deoxyribonucleic acid
dsDNA	double stranded DNA
DSB	double-strand break
EBV	Epstein-Barr virus
EBNA	Epstein-Barr nuclear antigen
FACS	fluorescence-activated cell sorting
GC	germinal center
HSV	herpes simplex virus
LMP	latent membrane protein
KSV	Kaposi's sarcoma associated herpesvirus
Ig	immunoglobulin
IgH	Immunoglobulin heavy chain
IgL	Immunoglobulin light chain
IL-4	Interleukin - 4

LPS	Lipopolysaccharide
LCL	Lymphoblastoid cell line
MEF	mouse embryonic fibroblast
MHCII	major histocompatibility complex II
MHV68	mouse herpes virus 68
PCR	polymerase chain reaction
RAG	recombination activating gene
SHM	somatic hypermutation
ssDNA	single stranded DNA
dUTP	deoxyuridine triphosphate
UNG	uracil DNA glycosylase

Chapter 1 - Introduction

1.1 Adaptive Immunity and the Antibody Diversification Processes

B-cells and the antibodies they produce are one of the primary mechanisms used by the mammalian immune system to respond to infections such as parasites, bacteria and viruses. B-cells are also one of the two cell types that are responsible for adaptive immunity and immunological memory. They generate an antibody repertoire with the ability to recognize a diverse spectrum of antigens as well as several different effector functions through three distinct mechanisms. V(D)J recombination is a process that occurs in the bone marrow involving different gene segments of the immunoglobulin variable region that are recombined stochastically to produce unique combinations of the antibody variable region. The second major process known as somatic hypermutation (SHM), involves the deliberate introduction of random mutations into the previously recombined V(D)J region, greatly increasing the antigen recognition potential of the immune system (Delker, 2009). The third mechanism of antibody diversification is Isotype Class Switch Recombination (CSR) whereby the antigen binding specificity of the antibody remains the same but the isotype class of the constant region is changed thus allowing for a differential response from immune system to the same antigen (McHeyzer-Williams and McHeyzer-Williams, 2005). Both SHM and CSR occur in mature B-cells found in the secondary lymphoid tissues and both are initiated at the molecular level by unique mechanisms that involve of self-induced DNA damage. A mutagenic enzyme known as Activation Induced Cytidine Deaminase (AID) is recruited to the Ig locus to initiate both the SHM and CSR process (Delker, 2009). For reasons that are not yet fully understood AID-induced DNA damage in B-cells is not repaired in a high fidelity manner. Taken together these three immunological diversification mechanisms allow the immune system to produce a diverse antibody repertoire that is capable of identifying and adapting to novel antigens, and able to stimulate a response from the different branches of the immune system.

1.2 V(D)J recombination

The germ line immunoglobulin gene consists of both heavy and light chain loci that encode multiple copies of nonfunctional gene segments. The heavy chain locus contains three types of gene segments, the variable(V) , the diversity(D) , and the joining(J) segment. While the light chain locus only contains variable(V) and joining(J) gene segments. In order to make a functional immunoglobulin gene locus these gene segments must be reordered in a process called V(D)J recombination that occurs during B-cell development in the bone marrow (Schatz and Ji, 2011). The human heavy chain locus is located on chromosome 14 and each chromosome contains approximately 123-129 variable, 27 diversity, and 9 joining segments (Watson, 2013) and in order to produce an expressible immunoglobulin variable region one gene segment from each type must be brought together to form a functional V(D)J exon. The V(D)J recombination process is initiated by protein complex containing recombination activating gene 1 and 2 (RAG1,RAG2) that targets and cleaves DNA at a RAG recombination signal that flank both ends of the V, D and J segments (Schatz and Ji, 2011). These double strand breaks (DSBs) are then repaired by the classical non-homologous end joining (NHEJ) pathway. The Immunoglobulin heavy chain (IgH) locus is processed first and upon its successful recombination the Immunoglobulin light chain (IgL) locus is then processed. This gene recombination connects the V, D and J segments resulting in a functional V(D)J exon. This recombined V(D)J exon is then expressed along with the constant region exon to produce a functional B-cell receptor (BCR). Non-productive V(D)J gene rearrangements are also possible such as gene inversion, gene duplication, and translocations. Normally translocations trigger programmed cell death, however it is possible for some translocation events from V(D)J recombination, such as Bcl2-IgG fusion, to lead to B-cell lymphomas (Schatz and Ji, 2011). After successful V(D)J recombination and BCR expression the cells are considered naïve adult B-cells and leave the bone marrow to infiltrate the periphery.

1.3 Somatic Hypermutation

The random assortment of V(D)J gene segments during B-cell development in the bone marrow provides some limited diversification to the antibody binding repertoire, but these antibodies are ultimately only able to recognize a finite number of antigens. However the antigen binding repertoire can be greatly expanded through a secondary process known as somatic hypermutation in which the antigen binding domain is actively mutated, thereby altering the affinity and specificity for a given antigen. After naïve B-cells enter the periphery they, along with T-cells, are attracted to the secondary lymphoid tissues by CXCL13 that is secreted by follicular dendritic cells (Cyster, 2010). Once B-cells have entered the secondary lymphoid tissue they enter a sub-structure known as the germinal center (GC) where B-cells both proliferate and begin the somatic hypermutation process. The expression of AID, the initiating factor of SHM, is highly restricted and requires direct stimulation from T helper cell contact via the CD40-CD40L signaling pathway. Once AID is expressed in GC B-cells it is targeted to the V(D)J region of the Ig locus during gene transcription, potentially by interaction with PCNA, where it deaminates cytosine residues to produce uracils (Delker, 2009). While most uracils present in DNA are repaired in a high fidelity fashion by the Base Excision Repair (BER) pathway, uracils introduced into the Ig locus by AID are not. Error prone DNA polymerases are recruited to the Ig locus where they replicate the DNA introducing mutations in the process. The molecular mechanisms that suppress classical high fidelity repair, and lead to the recruitment of low fidelity factors are still largely unknown. After the random mutation of the variable region in the somatic hypermutation process GC B-cells then compete for survival signals in a process known as clonal selection. First the GC B-cells compete for the ability to bind to antigens that are presented by follicular dendritic cells. GC B-cells that have a strong binding affinity for antigen will receive pro-survival signals through their B-cell receptor, while GC B-cells that have low antigen binding

affinity will not receive those survival signals and be deleted (Shlomchik and Weisel, 2012). After GC B-cells have successfully competed for and bound antigen they internalize the antigen, digest it into peptides and present it to T-helper cells via Major Histocompatibility Complex II (MHCII) (Shlomchik and Weisel, 2012). B-cells that are reactive to self-antigen are deleted by the T-helper cells, those that are not are given survival and proliferation signals by the T-helper cells. B-cells that bind to antigen with high affinity and have received the proper signals from T-helper cells then go on to proliferate and differentiate into long-lived memory B-cells or effector plasma cells that actively secrete antibody.

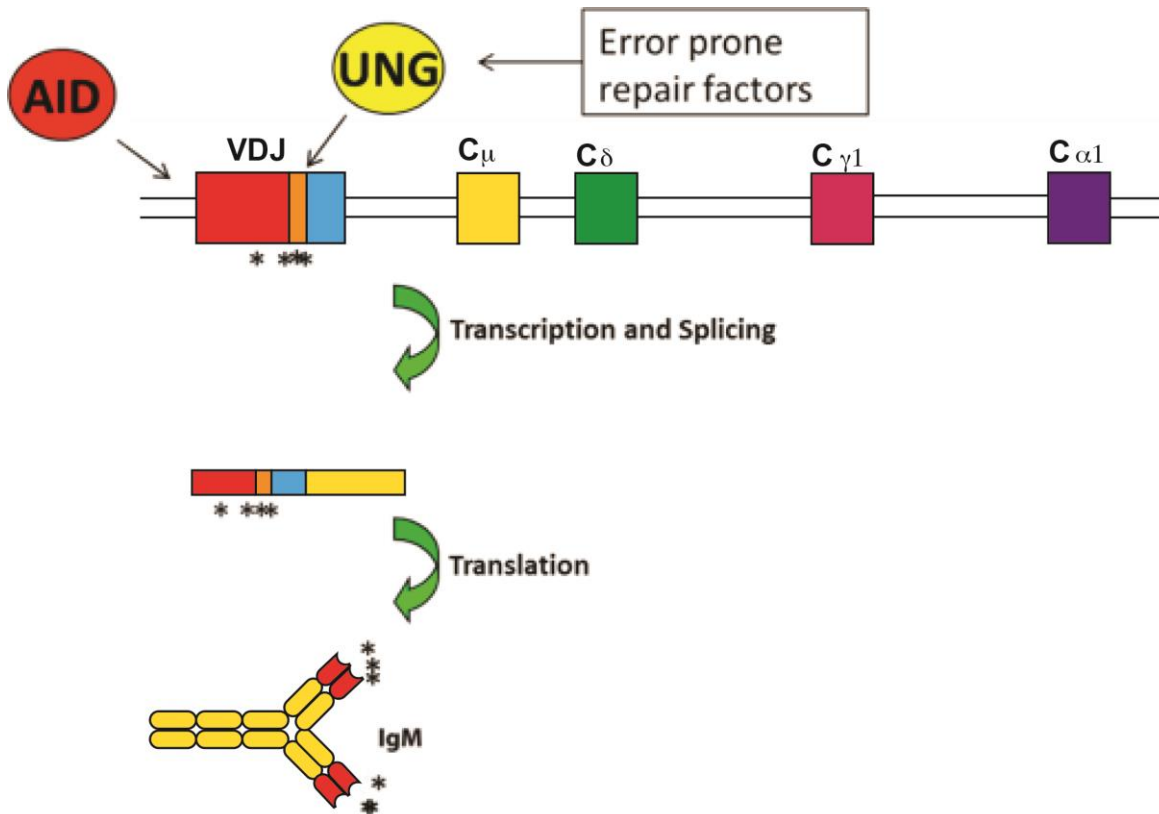


Figure 1

A Depiction of the Somatic Hypermutation Process at the Immunoglobulin Heavy Chain (IgH) Locus

AID is expressed in germinal center B-cells and is targeted to the V(D)J exon of the IgH locus. During transcription of the V(D)J exon AID deaminates cytosine to uracil in single stranded DNA introducing mutations into the gene sequence. Uracil DNA Glycosylase (UNG) scans the Ig locus detects and removes the uracils introduced by AID leaving an abasic site. Error prone polymerases are then recruited to the locus which repair the locus by low fidelity replication, thereby introducing more mutations into the V(D)J exon. The mutations at the V(D)J exon lead to changes in protein primary sequence and tertiary structure of the antigen binding portion of the antibody, thus diversifying the spectrum of potential antigens that can be recognized.

1.4 Class Switch Recombination

Mammalian antibodies are categorized into five different isotypes depending on the structure of their constant region domain, the portion of the protein that allows for differential effector function; the stimulation of the immune system in response to the antigen recognized by the variable region of the antibody. The Ig locus consists of two main types of exons, the variable region exon that is made functional after successful V(D)J rearrangement, and constant region exons that code for the constant region of the protein. The transcription of the Ig locus is regulated in such a way that the immediate downstream constant region exon is spliced to the variable region exon to produce a mature mRNA transcript. In the germ line gene arrangement of the Ig gene the μ exon is immediately downstream of the variable region exon, followed by the δ exon. Thus all naïve B-cells start as IgM or IgD, differential splicing regulates the expression of these two constant region exons in naïve B-cells. In order for B-cells to express any other immunoglobulin isotype they must undergo Class Switch Recombination (CSR), a process in which the Ig gene locus is rearranged and a new constant region exon is moved to the adjacent downstream position. AID deamination is also the first step of the CSR process, although it is targeted to another region of the Ig locus known as switch regions. Switch regions are long stretches of GC rich tandem repeat DNA located between the constant region exons. The CSR process is initiated by stimulation from external signals that lead to AID expression, the transcription of specific switch regions, and the targeting of AID to those actively transcribed switch regions. AID induced uracils at the actively transcribed switch regions are processed by uracil DNA glycosylase (UNG), this then leads to two double strand breaks and non-homologous end joining between different switch regions, deleting the intervening sequence in the process (Fig. 2). The end result of this is the insertion of a new constant region exon adjacent to the variable region exon, thus resulting in the expression of a new antibody isotype in that cell.

How UNG processing of AID induced uracils at the switch region initiates double strand breaks in this process has yet to be resolved.

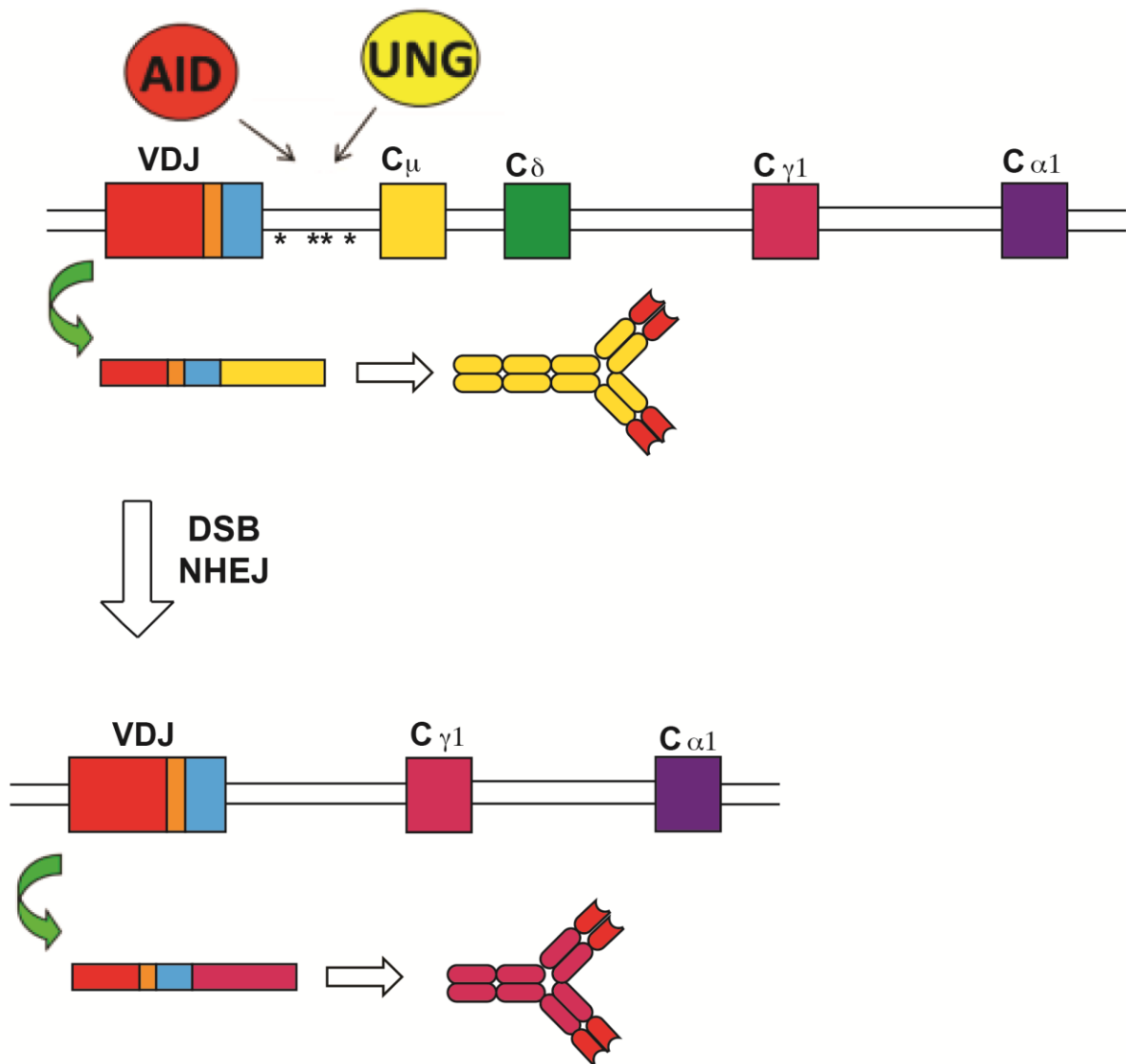


Figure 2

Class Switch Recombination Process at the IgG Locus

During normal Ig heavy chain expression the V(D)J exon is expressed, spliced to adjacent to the “C” constant region exon, producing a functional antibody upon translation. During the Class Switch Recombination process AID deaminates switch regions between the V(D)J and the first constant region exon (C μ) and switch regions between C exons.

1.5 Activation Induced Cytidine Deaminase

AID belongs to the APOBEC gene family of deaminases, enzymes that possess the ability to deaminate cytosine to uracil in RNA and DNA. While AID functions in adaptive immunity it is one of the oldest members of the gene family, suggesting it may have other functions (Conticello, 2008). Other APOBEC family members perform different functions. The gene family is named after apolipoprotein B editing complex 1 (APOBEC1) which functions as an mRNA editing enzyme that deaminates apolipoprotein B transcripts introducing a stop codon (Conticello, 2008). This mRNA editing of apolipoprotein B serves as a mechanism of regulating lipid uptake in the intestines. APOBEC3 serves as an intracellular anti-retroviral defense system, introducing mutations into retroviral RNA as the virus attempts to replicate in host cells (Conticello, 2008). AID is a single stranded DNA deaminase that catalyzes the deamination of cytosine to uracil in DNA. AID was originally discovered in the mouse B-cell lymphoma cell line CH12 which is known to be able to efficiently undergo class switch recombination *in vitro* upon stimulation (Nakamura, 1996). AID was discovered using a PCR screen to differentiate between transcripts that are expressed in resting CH12 cells and transcripts that are only expressed when the cells are exposed to switch stimulation (Muramatsu, 1999). An *Aid* knockout mouse line was soon generated, B-cells from these mice showed a complete inability to undergo CSR *in vitro* and *in vivo*, displaying a hyper-IgM phenotype (Muramatsu, 2000). These mice also showed an inability to produce antibodies in response to inoculation, demonstrating the essential role of AID in the SHM process (Muramatsu, 2000). The loss of AID in human patients results in a rare genetic condition known as Hyper-IgM syndrome type 2. These patients have compromised immune systems because their B-cells cannot undergo CSR or SHM (Revy, 2000). While essential for a healthy immune system AID actively damages DNA and can cause genomic instability. It has been demonstrated that AID is necessary for the formation of the IgH-cMYC translocation, the oncogenic translocation that is the hallmark of Burkitt's

lymphoma, suggesting that AID deamination is the first step in the transformation process (Ramiro, 2006). Due to its potential oncogenic activity AID is heavily regulated by a number of different mechanisms, including cellular localization, transcriptional regulation through microRNAs, and posttranslational modification (Delker, 2009). Many studies have shown that AID is heavily regulated through posttranslational modification, particularly phosphorylation. AID contains at least six serine/threonine phosphorylation sites and one tyrosine phosphorylation site that have been detected by mass spectrometry (McBride, 2006). Of these sites the majority of research has been focused on Serine 38 and to a lesser extent Serine 3. It has been suggested that serine 38 phosphorylation has a positive regulatory effect on both class switch recombination as well as somatic hypermutation, as mice that possess a S38A mutation show significant reduction in both processes (Cheng, 2009). Conversely phosphorylation of serine 3 of AID has been shown to be a negative regulator of its activity. The S3A substitution mutation causes an increase in CSR levels, as well as an increase in off target AID activity and c-myc/IgH translocations (Gazumyan, 2011).

1.6 DNA Glycosylases

DNA glycosylases are a large family of enzymes that excise damaged DNA bases as part of the base excision repair pathway. They are found in *E.coli* up to higher eukaryotes. A highly conserved mechanism of “base flipping” is used to remove the damaged base. They are categorized into six super families based on their structure and crystal structures have been solved for at least one protein from each family, showing that the six super families evolved DNA glycosylase activity from different ancestral genes (Conticello, 2008). Mammals have 11 DNA glycosylases, some recognize a specific substrate, while others are capable of recognizing and removing multiple substrates (Conticello, 2008). Bases can be damaged through a number of different chemical mechanisms. Oxidation can result in 8-

oxoguanine, 5-hydroxycytosine, or thymine glycol and alkylation can result in 3-methylguanine or 3-methyladenine (Krokan and Bjoras, 2013). Deamination of adenine results in hypoxanthine, and deamination of cytosine results in uracil. DNA glycosylases have specificity for particular lesions as well as the context of DNA, single or double stranded, in which the lesion is found (Krokan and Bjoras, 2013). Mammalian UNG is also regulated by subcellular localization and are capable of acting on nuclear or mitochondrial DNA. The mechanism of UNG localization is dependent on the presence of a mitochondrial localization signal generated by alternate splicing (Krokan and Bjoras, 2013).

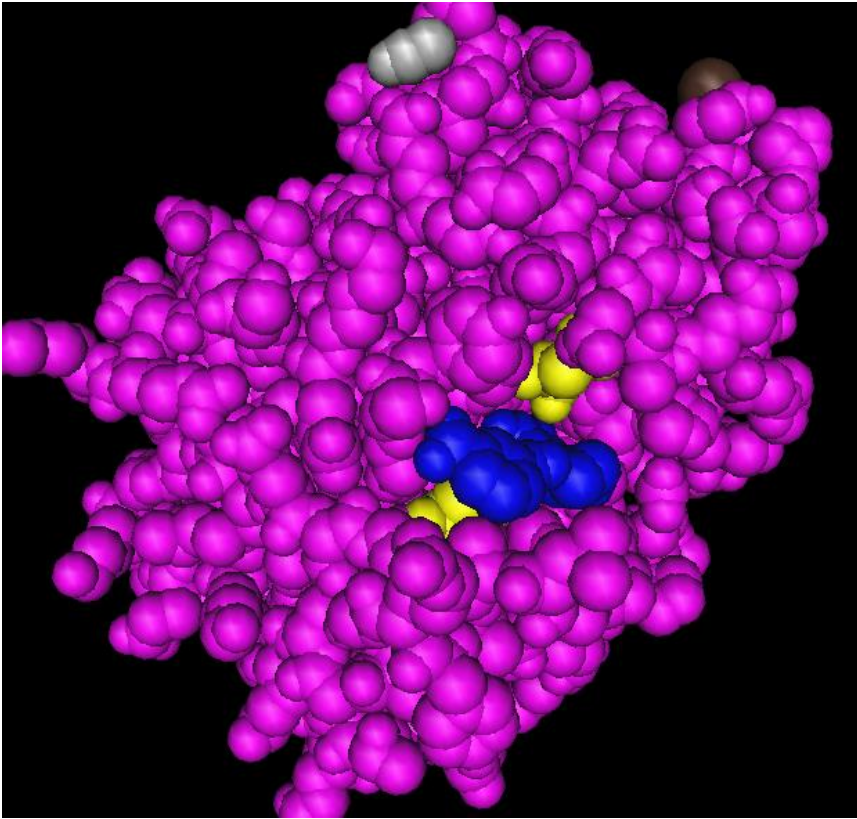


Figure 3

Crystal Structure of Human Uracil DNA Glycosylase 2

A space filling model of human UNG bound to substrate analog 6-[4-[(3-Carboxybenzylamino)butyl amino]methyl]uracil (blue). Two highly conserved residues essential for catalysis, Aspartic Acid-154 in the water activating loop, and Histidine-277 in the DNA interacting leucine loop, are highlighted in yellow (Mol, 1995).

1.7 Mammalian DNA Glycosylases

Uracil exist in double stranded DNA in two main forms U:G mismatches and U:A pairs both of which are recognized and removed by uracil DNA glycosylases. U:A mismatches occur due to the incorporation of free dUTP during DNA replication; dUTP exists in the cytosol in small quantities and is necessary in pyrimidine metabolism pathways (Krokan and Bjoras, 2013) . Free dUTP can be read by the replicative DNA polymerase as a dTTP and incorporated across from an adenine during DNA replication. U:G mismatches

occur in dsDNA when the amine group of cytosine is replaced with an oxygen, this deamination results in a uracil. When read by a DNA polymerase a U:G mismatch will result in a transition mutation C:G mutated to a A:T if the mismatch is not repaired before replication. Uracil in mammalian DNA is recognized and removed by four monofunctional DNA glycosylases methyl-CpG binding domain protein 4 (MBD4), Thymine DNA glycosylase (TDG), Single-strand selective monofunctional uracil DNA glycosylase (SMUG), and Uracil-DNA glycosylase (UNG) (Krokan and Bjoras, 2013). MBD4 is capable of recognizing and removing U:G and T:G mismatches in double stranded DNA and possesses a methyl-CpG binding domain that targets its binding to methylated DNA (Krokan and Bjoras, 2013). MBD4 may play an important role in maintaining genomic integrity in the intestines as evidenced by the loss of MBD4 in many colorectal cancers that show microsatellite instability (Ricchio, 1999), (Howard, 2009). Thymine DNA glycosylase, as the name suggests is capable of removing thymine from G:T and U:G mismatches in double stranded DNA. Interestingly the deletion of *Tdg* in mice causes an embryonic lethal phenotype, most likely due to its involvement in gene methylation during development (Cortazar, 2011). SMUG is capable of recognizing U:G and U:A mismatches with a strong preference for single stranded DNA and is thought to serve as a backup for other DNA glycosylases (Kavli, 2002).

1.8 Mammalian Uracil DNA Glycosylase (UNG)

UNG is the primary mammalian uracil DNA glycosylase. UNG exists in two isoforms UNG1 and UNG2, both encoded by the same gene and regulated by alternate splicing of the amino terminus (Krokan and Bjoras, 2013). UNG1 contains a mitochondrial localization signal and is the only known mitochondrial DNA glycosylase. UNG2 is targeted to the nucleus and contains both PCNA and RPA binding sites that are thought to target it to the replication fork machinery so it can process uracils as they are incorporated into DNA during

polymerization (Krokan and Bjoras, 2013). UNG is a globular enzyme consisting of eight alpha helices surrounding a centralized four stranded parallel beta sheet where the active site groove is located (Mol, 1995). UNG detects uracils in double stranded DNA through contact with the minor groove and a specific amino acid Leu 272 is essential for scanning and contacting the DNA backbone (Mol, 1995). Once the enzyme encounters a uracil leu 272 penetrates the minor groove, bending the DNA slightly and flipping out the uracil from the core of the double helix and into the binding pocket of the UNG active site (Mol, 1995). The flipping of uracil base and the distortion of the DNA backbone by UNG causes strain in the DNA, and once the uracil is situated in the binding pocket it is coordinated by catalytic amino acids. The enzyme then changes conformation cleaving the glycosidic bond between the uracil and the 1'-carbon of the deoxyribose base. A water molecule, coordinated by aspartate 145 (in human UNG), makes a nucleophilic attack on the 1'-carbon replacing the uracil with a hydroxyl group (Mol, 1995). The cleavage of this bond releases the strain and distortion in the DNA backbone and leaves an abasic site and a free uracil. After cleavage UNG remains tightly bound to the fragile abasic site that is later processed by downstream pathways (Mol, 1995). It has been demonstrated that the substitution of key amino acids in the catalytic motifs of the water activating loop (D147N), the uracil recognition strand (N206V) and the leucine loop (H270L) can significantly reduce the glycosylase activity of mouse UNG (Begum, 2007). While the combination of at least two of these mutations results in the complete loss of UNG glycosylase activity (Di Noia, 2007). Genetic deletion of *Ung* in mice shows that while they do not have a significant increase in genomic mutation or cancer they do have a deficiency in adaptive immunity (Nilsen, 2000). When *Ung* null mice are crossed to *Smug1* and *Msh2* double knockout have a significantly shorter lifespans and a high prevalence of lymphomas, suggesting a high degree of redundancy to detect and remove uracil from DNA (Kemmerich, 2012).

1.9 Base Excision Repair

The recognition of a chemically damaged base by a DNA glycosylase is the first step in the Base Excision Repair process. The chemically damaged base is recognized by a DNA glycosylase which catalyzes the cleavage of the N-glycosydic bond between the base and the 1' carbon of the deoxyribose sugar leaving an abasic site (Krokan and Bjoras, 2013). The abasic site is then further processed by cleaving the phosphodiester bond in the backbone causing a single strand break. This nicking of the DNA backbone is catalyzed by bifunctional DNA glycosylases, which possess both glycosylase and endonuclease catalytic activity, or by an AP endonuclease that is recruited to the abasic site (Krokan and Bjoras, 2013). The single-strand break is then processed and repaired by either short patch repair, where the missing nucleotide is replaced, or long patch repair where up to 10 adjacent nucleotides are replaced (Krokan and Bjoras, 2013). The choice between short patch and long patch repair depends on the initiating glycosylase, and cell type, and cofactors present. Short patch repair is thought to take place primarily in resting cells, after the glycosylase removes the base AP endonuclease APE1 is recruited to nick and process the abasic site, and then the abasic site is filled in by DNA pol β , and ligated by DNA ligase 1 or 3 (Fortini and Dogliotti, 2007). Base excision repair occurs during DNA replication and utilizes many of the same factors involved in DNA replication (Akbari, 2009). After AP endonuclease nicks the strand the site is then processed by DNA pol β , or pol δ , depending on the original glycosylase that recognized the lesion (Tichy, 2011).

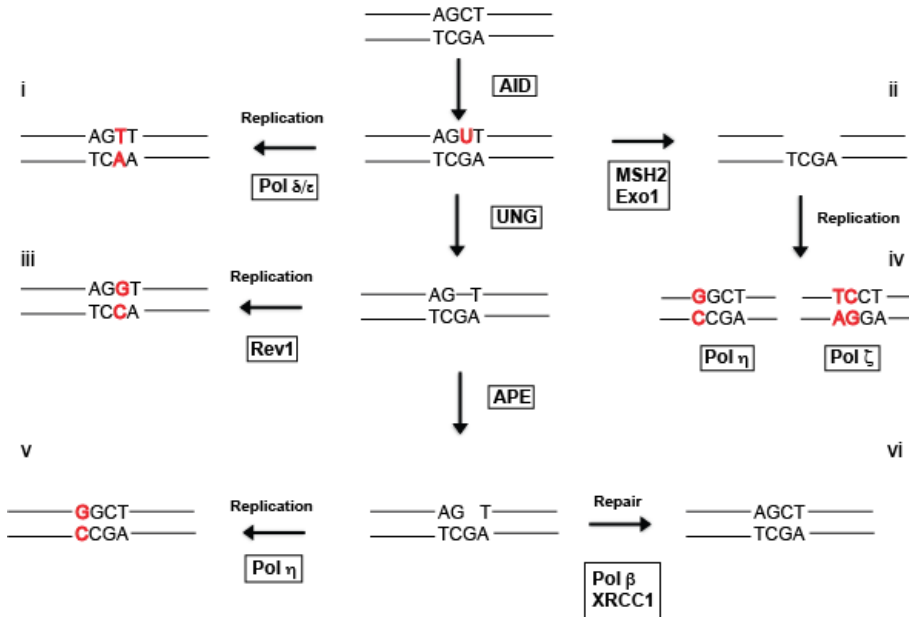
1.10 Base Excision Repair in B-cells

B-cells express the mutagenic AID that actively deaminates cytosines in the immunoglobulin gene locus creating the mutations needed for antibody diversity (Delker, 2009). After AID deamination UNG2 is actively recruited to the Immunoglobulin locus where it removes AID induced uracils (Delker, 2009). However AID induced uracils in the Ig locus

are not repaired by the normal high fidelity BER pathway. Through mechanisms that are still unknown low fidelity DNA polymerases are recruited to process abasic sites in the VDJ region during the somatic hypermutation process, diversifying the mutation spectrum more than simple U:G mismatches would (Diaz and Storb, 2003). UNG2 is also involved with removing AID induced uracils at switch regions during the class switch recombination process (Delker, 2009). The processing of these abasic sites leads to a double strand break and non-homologous end joining. Thus B-cells from mice lacking UNG are almost completely unable to undergo class switch recombination *in vitro* (Shen, 2006). The small amount of cells able to switch is due to compensation from the MSH1/MSH2 pathway as evidenced by *Ung/Msh1/Msh2* triple knockout mice being completely unable to undergo class switch (Shen, 2006).

Somatic Hyper Mutation

B



Class Switch Recombination

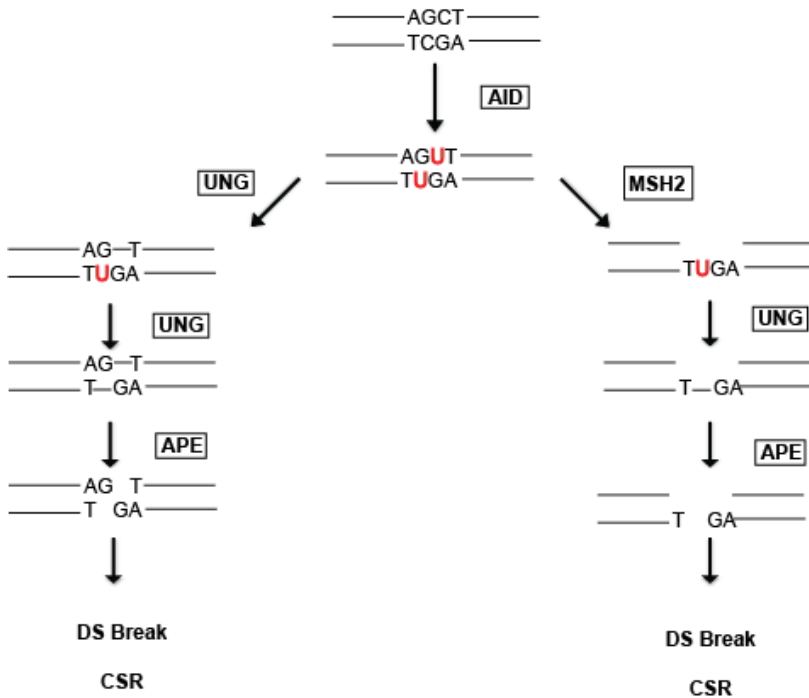


Figure 4

A Model for Class Switch Recombination and Somatic Hyper Mutation

A) The class switch recombination process is initiated by AID deamination adjacent of cytosines on opposite strands at switch region loci. These uracils are then removed by UNG or MSH2. The abasic sites are then nicked by AP endonuclease resulting in a double strand break at the switch region leading the class switch recombination. **B)** Somatic Hypermutation is initiated AID deamination in the switch regions. If the uracil is undetected it will be read as a T during replication resulting in an A/T mutation (i). The uracil can be detected by the MSH2/6 complex and processed by Exo1 (ii), the resulting sequence gap is then replicated by error prone DNA polymerases such as pol η or pol ζ leading to transition or transversion mutations (iv). The uracil can be detected and removed by UNG leaving an a basic site, the abasic site can then be processed by AP endonuclease and then repaired by pol β resulting in high fidelity repair (vi). The abasic site can also be repaired by translesion synthesis where in Rev1 recruits error prone polymerases to the abasic site before or after processing by AP endonuclease, resulting in the introduction of mutations (iii, v).

1.11 Herpesviridae

Herpes viruses are a large family of viruses that infect a wide variety of host species (Huff and Barry, 2003). They possess a linear double stranded DNA genome that encodes for 100-200 genes, and a lipid bilayer envelope with membrane glycoproteins that they use to gain entry to the host cell (Baer, 1984). After the virus enters the host cell the viral DNA enters the nucleus, circularizes and begins transcribing viral genes (Young and Rickinson, 2004). Herpes viruses follow a pattern of infection usually involving an initial lytic infection for the mucosal epithelium, the virus infects the host and an acute symptomatic infection can occur during which the virus transcribes lytic genes (Young and Rickinson, 2004). After the initial lytic stage of infection the virus enters its primary host cell and enters the latent stage of its life cycle where it can persist asymptomatically for many years causing no symptoms in the host (Young and Rickinson, 2004). Some herpes viruses are capable of reactivation after long-term latency, which can lead to serious secondary conditions such as shingles or cancer (Young, 1989). Herpes viruses are classified into three major subgroups Alpha, Beta, and Gamma according to their rate of growth and, the primary cell of latent infection.

Alpha herpes viruses include human herpes simplex viruses 1, 2, and varicella zoster virus. Both human herpes simplex viruses cause skin blisters at the site of infection, HSV1 causes primarily oral "cold" sores and HSV2 causes genital herpes. While v.zoster primary infection causes chicken pox resulting in red sores covering the body (Cohen, 2013). During the latent phase of the viral life cycle these viruses infect the neurons of the peripheral ganglia where they remain for the lifespan of the host usually asymptomatically (Grinde, 2013). However these viruses are capable of reactivation leading to herpes outbreaks or in the case of varicella zoster reactivation results in shingles, a condition characterized by skin rashes and severe pain caused by the virus damaging peripheral neurons (Kawai, 2014).

Beta herpes viruses infect and establish latency in leukocytes; the most thoroughly studied and clinically relevant human beta herpes virus is cytomegalovirus (CMV). A commonly occurring infection CMV usually produces no symptoms and remains latent. However in patients with suppressed immune systems CMV reactivation can occur and lead to serious conditions such as hepatitis, pneumonitis, and retinitis (Gupta, 2014), (Chiotan, 2014).

Gamma herpes viruses the third subfamily contains two human viruses Epstein-Barr virus and Kaposi's sarcoma virus, as well as mouse herpes virus 68 the standard laboratory model. Gamma herpes viruses are transmitted orally or sexually and establish an acute epithelial infection followed by a long-term latent infection in memory B-cells. Epstein-Barr (EBV) perhaps the most well studied human herpes virus is known to cause acute mononucleosis and is associated with several types of B-cell lymphoma (Young and Rickinson, 2004). Kaposi's sarcoma virus (KSV) was originally discovered in AIDS patients during the 1990's as the causative agent in the rare cancer Kaposi's sarcoma (Chang, 1994). Both EBV and KSV infect host cells and evade the immune system through complex mechanisms and contribute to the prevalence of several types of cancer worldwide.

Table 1 – Known Human Herpes Viruses and Their Associated Pathologies

Common name	Number	Subfamily	Cell type of latency	Associated diseases
Herpes Simplex Virus 1	HHV-1	α	Neuron	Oral/genital herpes
Herpes Simplex Virus 2	HHV-2	α	Neuron	Oral/genital herpes
Varicella Zoster Virus	HHV-3	α	Neuron	Chicken pox, shingles
Epstein Barr Virus	HHV-4	γ	B-cells	Infectious mononucleosis, post transplant lymphoma, Hodgkin's lymphoma, Burkitt's lymphoma, nasopharyngeal carcinoma
Cytomegalovirus	HHV-5	β	Leukocytes	Mononucleosis like syndrome
Human B lymphotropic virus, Roseolovirus	HHV-6	β	T cells	Roseola infantum
	HHV-7	β	T cells	Roseola infantum
Kaposi's sarcoma virus	HHV-8	γ	B-cells	Kaposi's sarcoma, primary effusion lymphoma, Castleman's disease

1.12 EBV Life Cycle

Epstein-Barr virus is the most thoroughly studied of the gamma herpes virus family due to its early discovery in 1964 and its association with a number of human diseases (Epstein, 1964). It has been suggested that 90 – 95% of adults have been infected at some point in their lives (Ascherio, 2001). Acute infection can cause infectious mononucleosis, however the majority of infected individuals are asymptomatic (Young and Rickinson, 2004). Transmitted orally EBV initially enters the host by infecting the epithelial cells of the oral mucosa where the virus is thought to undergo lytic replication, shedding more virus into the oropharynx (Fig. 5). The host immune system responds to the initial mucosal infection whereby the virus is able to infect its main host cell type, mature B-cells (Anagnostopoulos, 1995). EBV enters host B-cells by binding to CD21 (also known as Complement type 2 receptor) and to the MHC-II molecules present on the cell surface (Nemerow, 1987). After gaining entry into the host B-cell the EBV genome circularizes and enters the nucleus where it remains episomally (Young and Rickinson, 2004). During the B-cell stage of the infection the virus enters the latency III phase of its life cycle, where it activates a distinct gene expression program to stimulate the host B-cells to proliferate, including 6 EBV nuclear antigens (EBVNAs) and latent membrane proteins LMP-1, LMP-2A, and LMP-2B (Anagnostopoulos, 1995). The infected B-cells then enter into the latency II gene expression program which includes the expression of EBNA-LP, LMP-1, LMP-2, and induces the host B-cells to differentiate into memory cells (Odumade, 2011). The host cell finally reaches the latency I program where only viral gene expressed is EBNA-1, which simply replicates the viral genome during host cell division (Humme, 2003). The EBNAs replicate the viral genome and activate expression of other EBV genes (Young and Rickinson, 2004). LMP-1 expression activates the CD40 pathway, a signal normally provided by T-cells during the germinal center selection process (Uchida, 1999). This leads to downstream activation of NF- κ B target genes such as anti-apoptotic Bcl-2 genes and AID and allows EBV infected

cells to escape the normal negative selection process that takes place in germinal centers (Henderson, 1991). LMP-2 mimics the activation of the B-cell Receptor pathway to stimulate tyrosine kinase pathways leading to cell proliferation (Caldwell, 1998). *In vitro* infection of B-cells with EBV is capable of transforming cells into lymphoblast cell lines (LCL) that express EBV latent cycle genes. Viral genome mutation studies have shown that EBNA2 and LMP-1 expression is essential for the *in vitro* transformation of B-cells (Rowe, 1987).

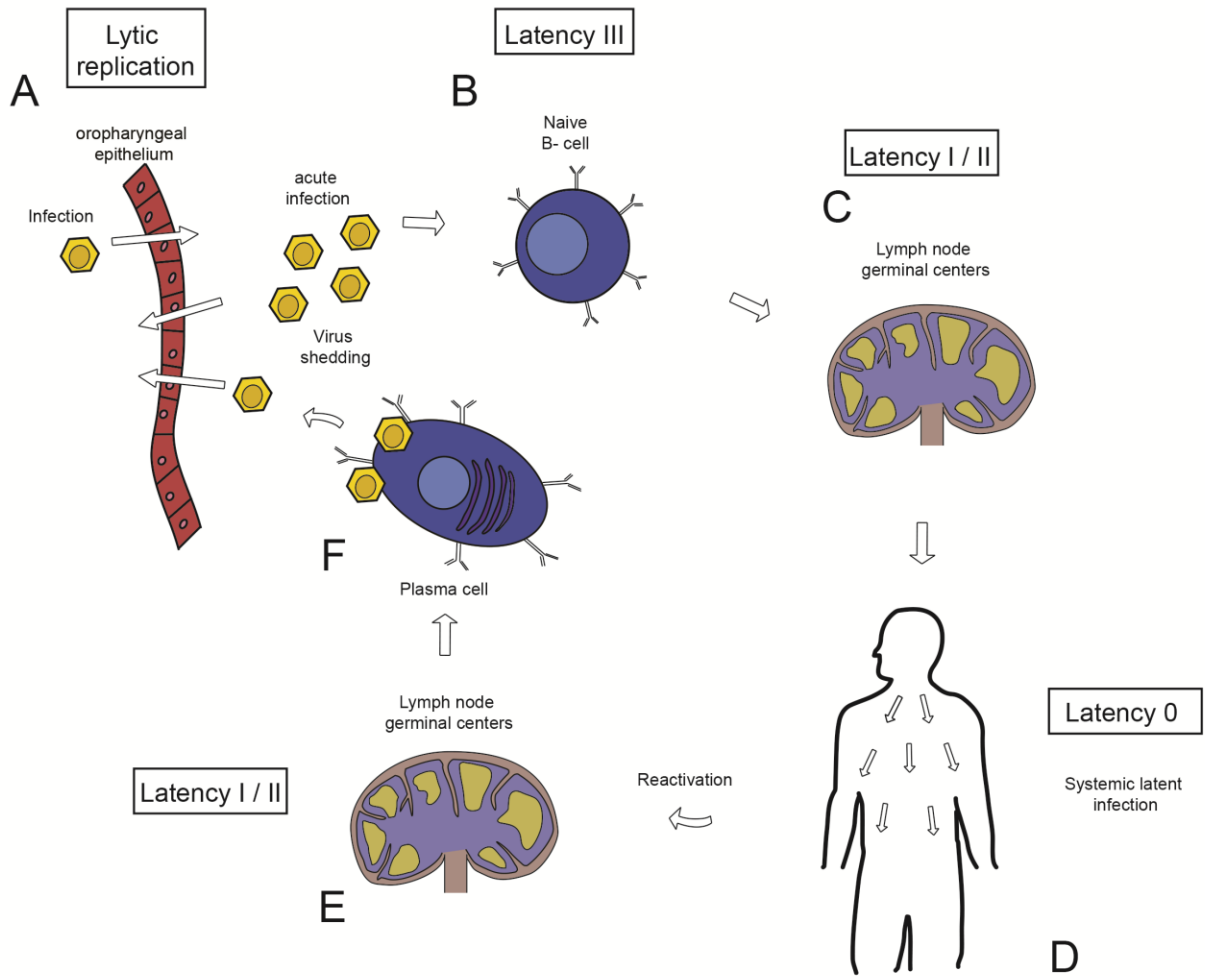


Figure 5

The Cycle of Epstein-Barr Infection

A) The virus enters the host through the nasopharyngeal mucosa where the virus establishes an acute primary infection and undergoes lytic replication and sheds virus. **B)** The virus then infects peripheral B-cells where it goes into type III latency, activating all of the EBNA's and LMP's **C)** Some of these infected B-cells make their way to the secondary lymphoid tissue where they enter type II latency where they express LMP's and EBNA-1, or type I latency only expressing EBNA-1. **D)** Infected B-cells then enter the latency 0 stage, where none of the viral genes are expressed, and can remain in this state for several decades unless reactivated. **E)** Rarely these EBV infected B-cells may respond to an infection and re-enter the germinal center and activate type I/II latency genes. **F)** The reactivated infected cells can differentiate into memory or plasma cells and can be recruited to the oral mucosa where they can enter they lytic stage of replication and begin shedding virus.

1.13 Mouse Models of Gamma Herpes Virus Infection

Murine gamma herpes virus 68 is rodent herpes virus that has become the standard model for studying gamma herpes virus family members in the laboratory. Originally isolated from voles in northern Europe, MHV68 enters the host through the nasal epithelium and the virus undergoes proliferation and replication in the lung during the acute phase of infection, it then establishes acute infection in B-cells as well as T-cells where it causes a pathology similar to human mononucleosis (Blaskovic, 1980). Germinal center B-cells are the main host cell type during the latent phase of infection (Simas and Efstathiou, 1998). MHV68 has been shown to cause lymphoproliferative disorders and high grade mixed T and B-cell lymphomas (Sunil-Chandra, 1994). However, it has been suggested that MHV68 may only play a role in initiating transformation of these cell since the viral genome was not detectable in the majority of MHV68 associated lymphomas (Usherwood, 1996). The MHV68 genome encodes for several genes that lead to host cell proliferation. Like KSV and EBV, MHV68 carries its own version of the anti-apoptotic protein bcl-2 that has been shown to interfere with pro-apoptotic pathways, and inhibit apoptosis *in vitro* (Weck, 1997), and also encodes for its own homolog of cyclin D, which it may use to stimulate host cell proliferation (Jung, 1994). MHV68 ORF-4 is homologous to host CD59 (Rother, 1994), a protein that inhibits the complement membrane attack complex, and is likely used by the virus to evade the host immune system. MHV68 also encodes for a uracil DNA glycolyase in ORF46 (Mackett, 1997). Like the other herpes viruses there is little known about the role viral UNG plays at the lytic or latent stages of viral infection, if viral UNG helps maintain the host genome, or in some way aids in manipulating host cell processes.

1.14 Oncoviruses

Oncoviruses are viruses that are known to cause cancer in the host cells they infect. There are seven known human oncoviruses that infect a variety of cell types and transform them through direct and indirect mechanisms. Hepatitis B and C are both known to infect hepatocytes and chronic infection can lead to hepatocellular carcinoma (El-Serag and Rudolph, 2007). Hepatitis B is a DNA virus that is transmitted through bodily fluids or from mother to child at the time of birth. Those infected before one year of age are highly susceptible to developing chronic hepatitis, which may lead to hepatocellular carcinoma later in life (Chang, 2007). Hepatitis B possesses a partially double stranded DNA genome, but replicates its genome via reverse transcription (Beck and Nassal, 2007). It is not clear if the hepatitis virus contributes to hepatocellular transformation directly, it is thought that cancer arises after years of chronic liver inflammation (Chang, 2007). In contrast the Hepatitis C virus is a single stranded RNA virus that is transmitted sexually or through intravenous drug use. While acute infection symptoms are usually mild, approximately 80% of cases develop chronic infection and inflammation that can lead to cirrhosis and hepatocellular carcinoma (Rosen, 2011).

Human papilloma virus (HPV) is a double stranded DNA virus that is responsible for cancers of the cervix, genitals, tonsils and oropharynx (Schiffman and Castle, 2003). HPV transforms host cells through direct two mechanisms, HPV protein E7 binds and sequesters the tumors suppressor gene Rb which allows the transcription factor E2F to stimulate cell cycle and proliferation (Ganguly and Parihar, 2009). While HPV protein E6 binds to tumor suppressor p53, the major regulator of apoptosis, and primes it for ubiquitination via MDM2 E3 ligase and subsequent proteasomal degradation (Ganguly and Parihar, 2009). In 2005 a vaccine for HPV was introduced to the market, which may lead to a significant reduction in HPV associated cancers in the future (Who, 2009).

Two human herpes viruses Epstein-Barr (HHV-4) and Kaposi's sarcoma virus (HHV-8) are known oncoviruses, and are known to cause a number of different malignancies in the host they infect. Epstein-Barr virus (EBV) was the first identified human oncovirus (Epstein, 1964). It is well documented that EBV infection is associated with the initiation and progression of nasopharyngeal carcinoma and three types of lymphoma including Hodgkin's lymphoma, post-transplant lymphomas and Burkitt's lymphoma, the tumor where the virus was first identified in electron micrographs (Young and Rickinson, 2004). Although EBV infection is associated with these three types of lymphoma, the viral genes expressed in these tumor types can vary greatly (Young and Rickinson, 2004), (Epstein, 1964). EBV infection is associated with approximately 40% of Hodgkin's lymphoma cases in industrialized countries and in EBV positive cases of Hodgkin's lymphoma expression of latent genes LMP1, LMP2 and EBNA1 has been found in Reed-Sternberg cells, a characteristic cell type used to diagnose Hodgkin's lymphoma (Portis, 2003). Reed-Sternberg cells are thought to be multinucleated B-cells that have gone through "failed" germinal center reactions and have escaped negative selection (Portis, 2003). It has been suggested that the expression of these viral genes allow these cells to bypass germinal center selection since LMP-1 and LMP-2 mimic CD40 and BCR signaling respectively (Young and Rickinson, 2004). EBV is also associated with B-cell lymphomas that arise in immunosuppressed individuals, EBV genes can be detected in approximately 60% of lymphomas in AIDS patients (Boshoff and Weiss, 2002). Post-transplant lymphomas (PTLs) can arise after a bone marrow transplant, which severely suppresses the immune system until the white blood cell population is able to regrow. PTLs usually occur within the first year after allografting, and almost all of them express EBV latency genes EBVNA2 or LMP-1, suggesting an important role for adaptive immunity in keeping latent EBV infections suppressed (Young, 1989). Burkitt's lymphoma is the cancer that is most commonly associated with EBV infection. There are three main classifications of Burkitt's lymphoma,

endemic, sporadic and immunodeficiency associated. All forms of Burkitt's lymphoma are B-cell lymphomas that are defined by a reciprocal translocation from the Ig locus to the cMYC gene (Polack, 1996). The resulting chromosomal fusion drives over-expression of the cMYC proto-oncogene, leading to proliferation and transformation. Burkitt's lymphomas do not show active expression of LMP-1 or EBNA2 like other EBV associated lymphomas, thus it has been suggested that LMP-1 plays a role in the initiation Burkitt's lymphoma and the generation of the Ig-MYC translocation, but is later turned off (Kelly, 2002). EBV infection is found in almost all cases of endemic Burkitt's lymphoma, which effects children in West Africa in areas where malaria is also endemic, while EBV is present in only a small number of "sporadic" cases which are more common in the developed world (Brady, 2008). Lastly Burkitt's lymphoma can arise in patients with severe immune system deficiency, and AIDS patients frequently. Perhaps the most famous example of this was David Vetter, the so called bubble boy afflicted with severe combined immunodeficiency (SCIDs). He died of Burkitt's lymphoma 15 days after receiving a bone marrow transplant from his sister that was later found to be contaminated with trace amounts of EBV (Aloj, 2012). Nasopharyngeal carcinoma (NPC) is a rare cancer associated with EBV infection. It is most commonly found in south East Asia where it has a peak prevalence of approximately 0.003% (Yu and Yuan, 2002). NPCs can show expression of EBNA1 as well as LMP1 and usually show an undifferentiated pathology with a high amount of lymphocytic infiltrate which may be involved in the progression of the tumor (Raab-Traub, 2002).

Kaposi's sarcoma was first described in 1872 by Moritz Kaposi, however the herpes virus that is now known to cause the disease was not discovered until 1994 (Chang, 1994). The virus often leads to tumors in AIDS patients, where it was first identified; KSV infection is normally asymptomatic in patients with a healthy immune system (Chang, 1994). The virus itself has a high prevalence in Africa, and it is estimated 3 - 10% of the population in the United States has been exposed to the virus that is thought to be spread by sexual

transmission (Neipel, 1997b). Along with Kaposi's sarcoma, KSV infection is also associated with other malignancies such as primary effusion lymphoma and rare lymphoproliferative disorder Castleman's disease (Soulier, 1995). Castleman's disease, also known as angiofollicular lymph node hyperplasia, can be unicentric and confined to one lymph node, or multicentric involving multiple sites throughout the body (Soulier, 1995). Unicentric Castleman's disease can normally be cured by the simple surgical removal of the afflicted lymph node, while multicentric Castleman's disease is a much more serious condition that can involve organ malfunction due to hyperactivation of the immune-system and cytokine overexpression (Fajgenbaum, 2014). Primary effusion lymphoma is a B-cell lymphoma almost always associated with KSV infection and is primarily found in large body cavities such as the abdominal or retroperitoneal cavity (Cesarman, 1995). All three KSV associated diseases Kaposi's sarcoma, Castleman's disease, and Primary effusion lymphoma are also associated with simultaneous HIV-AIDS infection, showing the importance of the immune system in suppressing KSV associated pathology. KSV stimulates growth and transformation of host cells through different pathways, KSV encodes a homolog of cyclin D which when expressed can stimulate host cell cycle progression by interacting with host cyclin dependent kinases such as Cdk6 (Cesarman, 1996). And like Epstein-Barr virus KSV encodes a gene in ORF16 that is homologous to host *bcl-2* and suppresses apoptosis by binding to pro-apoptotic *bcl-2* family members like Bax (Cai, 2010). Although KSV does infect a wider variety of host cells than EBV does it also infects B-cells where it enters the latent phase of its cycle. KSV encodes and expresses its own homolog of IL-6, a growth factor known to stimulate the proliferation and differentiation of B-Lymphocytes (Neipel, 1997a). Whether or not KSV-UNG plays a role in viral genome maintenance or any pathology associated with the virus remains unknown.

1.15 The Function of Viral Uracil DNA Glycosylase

Herpes Viruses are a family of double stranded DNA viruses with large genomes of approximately 200kb in length (Amon and Farrell, 2005). The genomes of mammalian herpes viruses contain a uracil DNA glycosylase that shows strong homology to mammalian UNG2 (Geoui, 2007). Other large double stranded DNA genome viruses families like poxviridae viruses such as vaccinia virus and lumpy skin disease virus also carry a copy of uracil DNA glycosylase (Millns, 1994), (Tulman, 2001). The structure of herpes virus UNG contains four motifs directly involved with coordinating reactants that are identical to mammalian UNG2 suggesting there is a highly conserved catalytic mechanism used by all of these proteins (Fig. 6) (Geoui, 2007). There are two major structural differences between herpes virus UNGs and their host homologs; most viral UNGs lack the N-terminal domain that contains regulatory phosphorylation sites and RPA and PCNA interacting motifs that are thought to help recruit mammalian UNG2 to the site of DNA replication, suggesting viral UNG may not be recruited to the mammalian replication fork (Hagen, 2008). Herpes virus UNGs have a seven amino acid insert near the minor groove interacting motif known as the leucine loop (Fig. 7) that does play a role in contacting the minor groove of DNA, however this insertion does not seem to significantly effect the activity of the enzyme and its function, if any, remains unresolved (Geoui, 2007). While the role of many viral UNG during infection is unclear it has been shown that HSV-1 UNG and simian varicella virus UNG are needed for these viruses to efficiently infect and replicate in neurons *in vivo*, suggested that these UNGs are needed to maintain the integrity of the viral genome during the replication process (Pyles and Thompson, 1994), (Ward, 2009). Intriguingly host UNG been shown to act on the genome of the human retrovirus hepatitis B and counteract the antiviral effects of APOBEC3G (Kitamura, 2013).

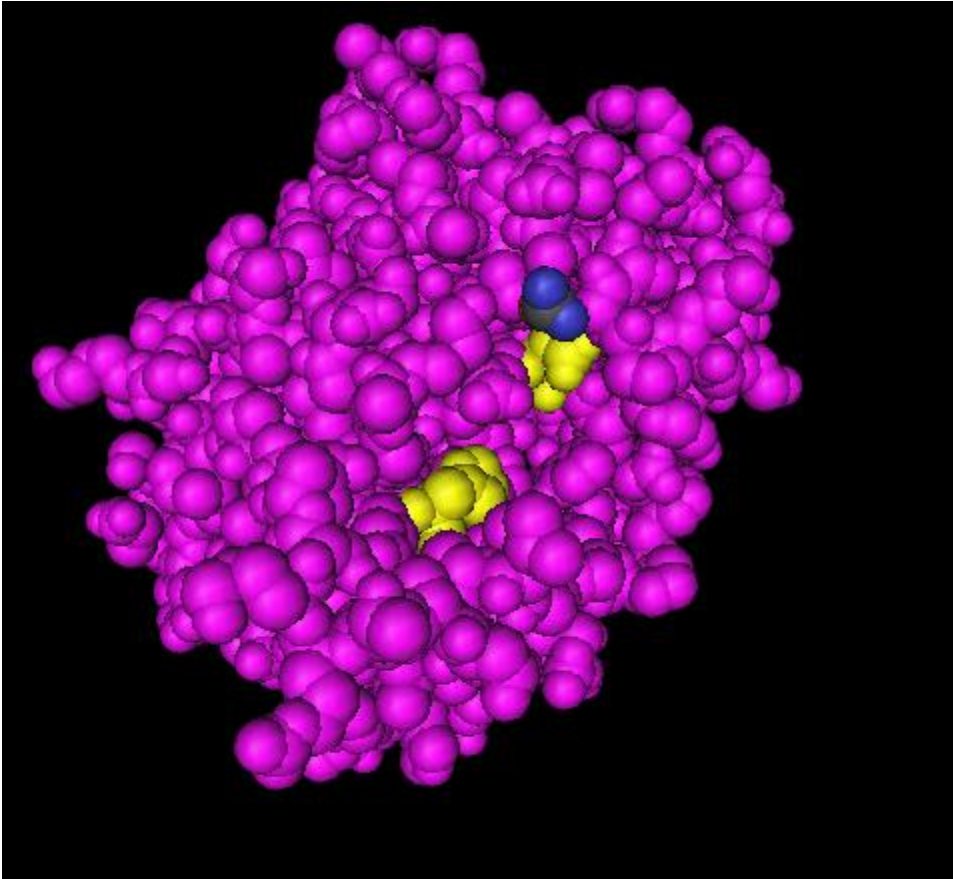


Figure 6

Crystal Structure of Epstein-Barr Virus Uracil DNA Glycosylase

A space-filling model of Epstein Barr UNG facing the catalytic pocket, two highly conserved residues essential for catalysis, Aspartic Acid-91 in the water activating loop (water molecule shown in black and blue), and Histidine -213 in the DNA backbone interacting loop, are highlighted in yellow. These residues are analogous to Aspartic Acid-154 and Histidin-277 in human UNG (Geoui, 2007).

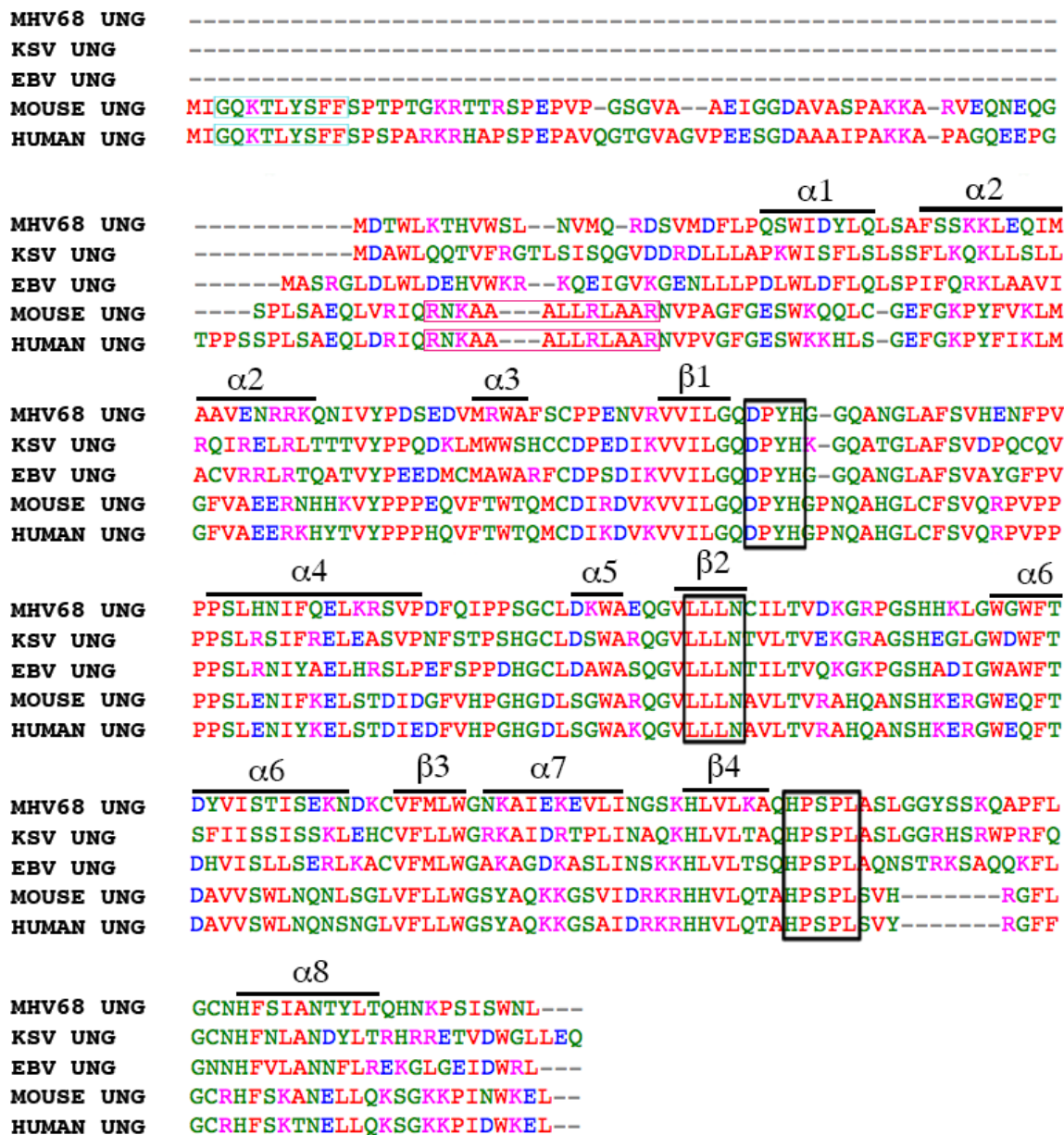


Figure 7

Alignment of Human, Mouse, and Gamma Herpes Virus UNG Amino Acid Sequences

Alignment of mouse herpes virus 68 (MHV68) UNG, Kaposi sarcoma associated herpes virus (KSV) UNG, Epstein Barr (EBV) UNG, mouse UNG2 and Human UNG2. Small hydrophobic amino acids are shown in red, acidic amino acids in blue, basic in magenta, and hydroxyl sulfhydryl and amine shown in green. Bars above the sequence indicate conserved secondary structures. Black boxed regions indicate regions conserved domains involved in catalysis. Blue box indicates the PCNA interacting motif, the purple box indicates the RPA interacting motif. (Obtained from clustal Omega).

A recently published report showed that MHV68, a key model of mammalian herpes virus infection *in vivo*, needs viral UNG in order to replicate effectively during infection and establish latency in mice. This study is the first to demonstrate that MHV-UNG is capable of complementing *Ung*^{-/-} mouse B-cells, the main host cell type during latency. Using an *in vitro* class switch recombination assay they showed that *Ung*^{-/-} B-cells expressing mUNG or MHV-UNG are capable of switching to IgG1 while *Ung*^{-/-} B-cells expressing empty vector control are not, demonstrating that viral UNG is capable of participating in the CSR process at the immunoglobulin locus (Minkah, 2015). They then created a mutant MHV68 virus (Δ UNG) incapable of expressing UNG by inserting a stop codon in the UNG open reading frame. Using this Δ UNG virus they show that viral UNG is needed for efficient viral genome replication *in vitro*. When immortalized 3T3 cells or primary mouse embryonic fibroblasts are infected with either wt MHV or Δ UNG-MHV virus in a single step plaque assay the Δ UNG-MHV expressing cells show a significantly lower number of plaque forming units. However both wt MHV both the Δ UNG-MHV infected cells both express viral proteins at similar levels, suggesting a defect in viral gene transcription or expression, is not responsible for the impaired ability of virus to replicate (Minkah, 2015). Using an *in vitro* biochemical assay they showed that lysates from MHV infected fibroblasts are capable of removing uracil from the middle of a 19 base pair long substrate. While lysates from cells expressing Δ UNG-MHV did not show significantly different enzymatic activity compared to the uninfected control (Minkah, 2015). Significantly they show that viral UNG is essential for MHV replication during the initial infection in the lungs of mice. Mice infected intranasally with Δ UNG-MHV showed significantly lower viral titers compared to MHV infected when infected lungs were homogenized and tittered by plaque assay, suggesting an essential role for viral UNG during the early stages of mucosal infection (Minkah, 2015). It was also demonstrated that the loss of MHV-UNG delays the establishment of latency in the spleen of mice, as well as the ability

of infected splenic cells to reactivate (Minkah, 2015). However they go on to show that infecting mice with a higher dose of Δ UNG-MHV can partially overcome the defects in latency establishment and reactivation. Interestingly when mice are infected via intraperitoneal inoculation and tested for latency establishment and splenocyte reactivation Δ UNG-MHV infected mice show no significant difference from MHV infected mice (Minkah, 2015). When they examined the effect of viral UNG in other host cell types such as peritoneal exudate macrophages they found that loss of MHV-UNG had no effect on the ability of the MHV virus to establish latency or undergo reactivation (Minkah, 2015). They then showed using a biochemical assay that lysates from MHV infected tissue such as spleen, and peritoneal exudate cells, retain their UNGase activity, suggesting the active expression of viral UNG protein in those cell types (Minkah, 2015).

It is however still unknown if herpes virus UNGs play any sort of role in counteracting intracellular antiviral responses. While UNG is not essential for viability in mammals it plays an important role in the antibody diversification process in B-cells, one of the major host cell types these viruses infect (Nilsen, 2000), (Shen, 2006). While EBV infection has been shown to be associated with autoimmune disorders, suggesting it may play a role in autoantibody formation (Draborg, 2013). It is not yet known if viral UNGs are capable of acting on the host genome in any way to enhance or interfere with normal host UNG processes, or suppress the host immune response to the infection.

Chapter 2 - Rationale and Hypothesis

2.1 The Role of AID Phosphorylation

We hypothesized that novel phosphorylation sites in AID exist in B-cells that are important in regulating AID function, and that novel phospho-AID binding proteins interact with AID to regulate its function. To detect the presence of novel phosphorylation on AID we developed phospho-specific antibodies to detect p-T150-AID or p-Y184-AID. We predicted that these phosphorylation events would be detectable using phospho-specific antibodies, however did not know the conditions needed to induce a detectable level of AID phosphorylation at these sites. To address this we tested for the presence of these phosphorylation events in mouse B-cells and 3T3 cells and flag B-cells, and use small molecule inhibitors in order to understand the signaling pathways that influence AID phosphorylation. We also treated AID expressing cells with the tyrosine phosphatase inhibitor NaVO₄ in order to produce a robust level of p-Y184-AID that could be detected using our p-Y184-AID specific antibody. We predicted that these novel AID phosphorylation sites may be involved with regulating the CSR process. To test this we created non-phosphorylatable mutants of AID to evaluate the effect of AID phosphorylation in CSR *in vitro*. We then set up a screen for potential phospho-AID binding partners using a phospho-binding protein domain array. This led us to the prediction that AID might have phospho-specific binding partners that regulate its function. We then cloned these genes into plasmids to use in later experiments.

2.2 The Involvement of γ Herpes Virus UNG in Antibody Diversification Processes

We hypothesized that Uracil DNA Glycosylases from γ herpes viruses are capable of processing uracils in the host genome, and by doing so may interfere with AID initiated

mutagenic events in mammalian B-cells. We tested for the ability of viral UNG to influence AID mediated mutagenic events such as Class Switch Recombination, Somatic Hypermutation, Non-Ig locus somatic mutations, and reciprocal translocations. To determine the effect of viral UNG on AID driven SHM *in vitro*. We predicted that viral UNG is capable of acting on AID induced uracils in the mammalian genome. To test this we used a fibroblast indicator cell line, 3T3-NTZ that express a single GFP copy with a premature STOP codon. We co-expressed viral UNG and AID in these cells to determine the direct effect of viral UNG on AID hypermutation. Mutation rates were measured by the reversion rate of the GFP stop that results in GFP expression. We predicted that viral UNG might be capable of acting on the host genome B-cells, participating in the CSR process. To determine if viral UNG can participate in the CSR process we transduced *Ung*^{-/-} mouse B-cells *in vitro* with viral UNGs, and stimulated CSR in the cells. We also predicted that viral UNG may interfere with the function of host UNG in the CSR process. To test this we transduced naïve B cells from *wt* mice with a retrovirus expressing viral UNG and stimulated CSR *in vitro*. We predicted that the presence of viral UNG in the CSR process may also lead to an increase or decrease in off target genomic damage caused by AID. To test this we set up an assay to determine if viral UNG expression affected translocation rate. We transduced naïve B-cells from mice with viral UNG and measured translocation frequency using a PCR/Southern blot assay that selectively amplifies *c-myc* to *IgH* chromosome fusions. Reciprocal translocations were detected and confirmed with southern probes specific to regions of *c-myc* and *IgH* within the amplified region.

Chapter 3 - The Detection and Effect of AID Phosphorylation

3.1 Class Switch Recombination Assay Characterization and Optimization

Naïve primary mouse B-cells can be stimulated to switch isotypes from IgM to IgG1 *in vitro* by treating the cells with Lipopolysaccharide (LPS) and Interleukin-4 (IL-4). LPS activates the TLR-4 receptor, which triggers the expression of AID, while IL-4 receptor stimulation initiates targeting of AID to the S μ and S γ 1 switch regions to initiate the CSR process. There are however many variable that can affect the ability of B-cells to switch *in vitro* such as the lot of serum used and the density at which the cells are plated. In order to determine the affect cell plating density on CSR primary mouse B-cells were plated and maintained at varying densities in a six well plate in 2ml of B-cell media with LPS and IL-4. B-cells were plated at 3M, 2M, 1M, 500K or 250K cells per ml. The cells were counted using a hemocytometer daily, cells were removed from wells and replaced with new B-cell media to maintain the wells at their given cell density. After three days of *in vitro* stimulation cells were stained with an anti-IgG antibody and analyzed by FACS to measure the percentage of cells switched to IgG1 (Fig. 8). We observed that the B-cells maintained at a lower cell density over three days have an increased percentage of cell switched IgG1. 6.73% of cells plated at 3M cells per ml switched to IgG1 while 24.7% of cells plated at 250K per ml switched to IgG1 (Fig. 8). For all future switch assays cells were maintained at a density of 500K per ml to ensure both a robust percentage of cells switch (21.5% after 3 days), as well as ensuring at least 2M cells per well are present.

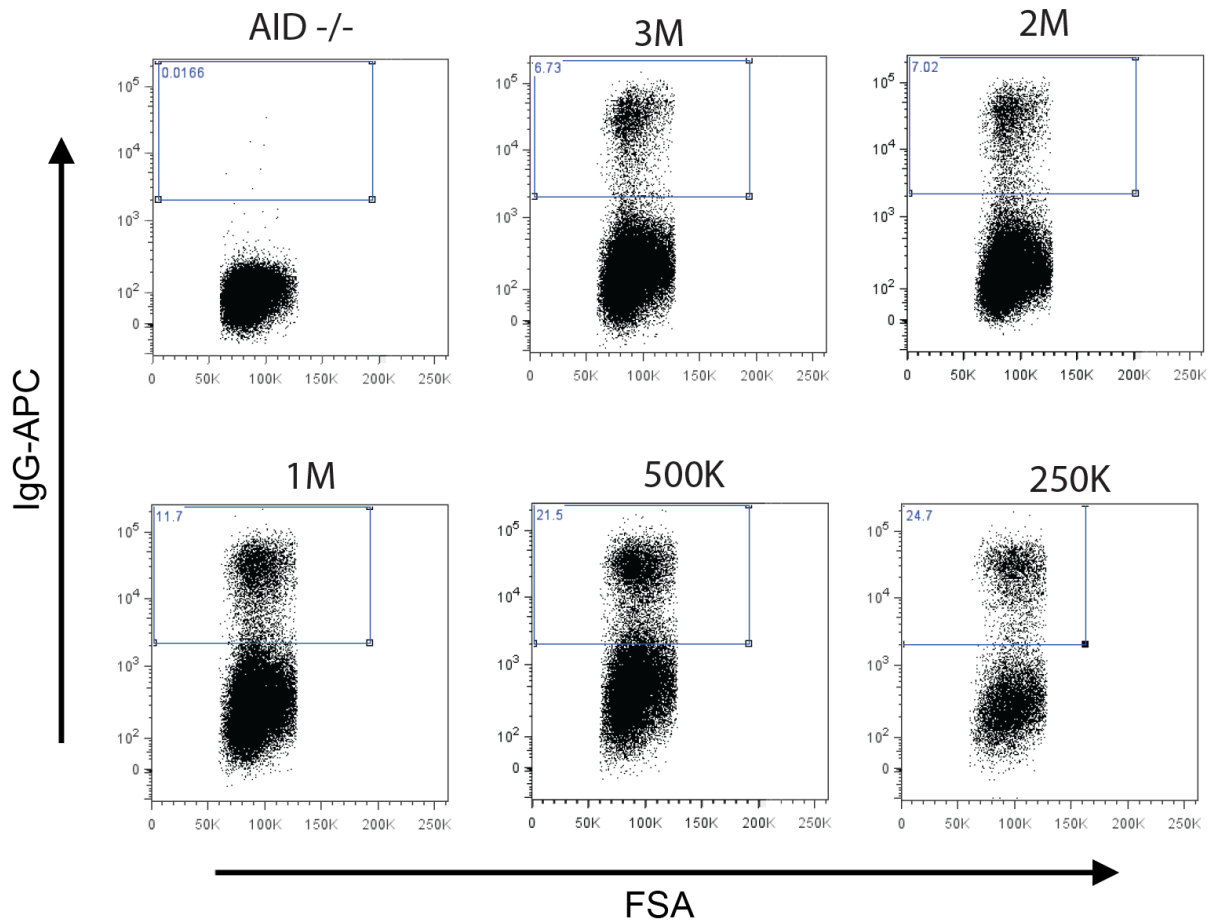


Figure 8

Plating Density Effects Switch to IgG1 in Primary Mouse B-cells.

Primary mouse B-cells are maintained at different densities show difference in switch after three days *in vitro*, percent switch to IgG shown in the upper left quadrant. *wt* B-cells maintain at lower cells densities have increased switch levels, *Aid*^{-/-} B-cells maintained at 500K cells per ml do not switch. All cells were plated in 6 well plates with 2ml of B-cell media with 10 µg/ul IL-4 and 25µg/ml LPS.

While LPS and IL-4 stimulation are essential for switch, other growth factors present in FBS are also capable of having a significant impact on the ability of B-cells to switch *in vitro*. In order to determine which lot of serum consistently allows for the highest percentage of cells to switch, we tested several lots from different companies. Primary mouse B-cells were plated at a density of 500K per ml in a six well plate, along with LPS and IL-4 in B-cell media containing 10% FBS. After 3 days *in vitro* cells were stained with an anti-IgG1 antibody and measured by FACS (Fig. 9). While all of the sera tested caused at least 20% of cells to switch, fetal bovine serum from Sigma-Aldrich (Sigma-Aldrich, St. Louis, MO. Catalog# F6178) stimulated the highest percent switch at 26%. This serum was used for all future experiments.

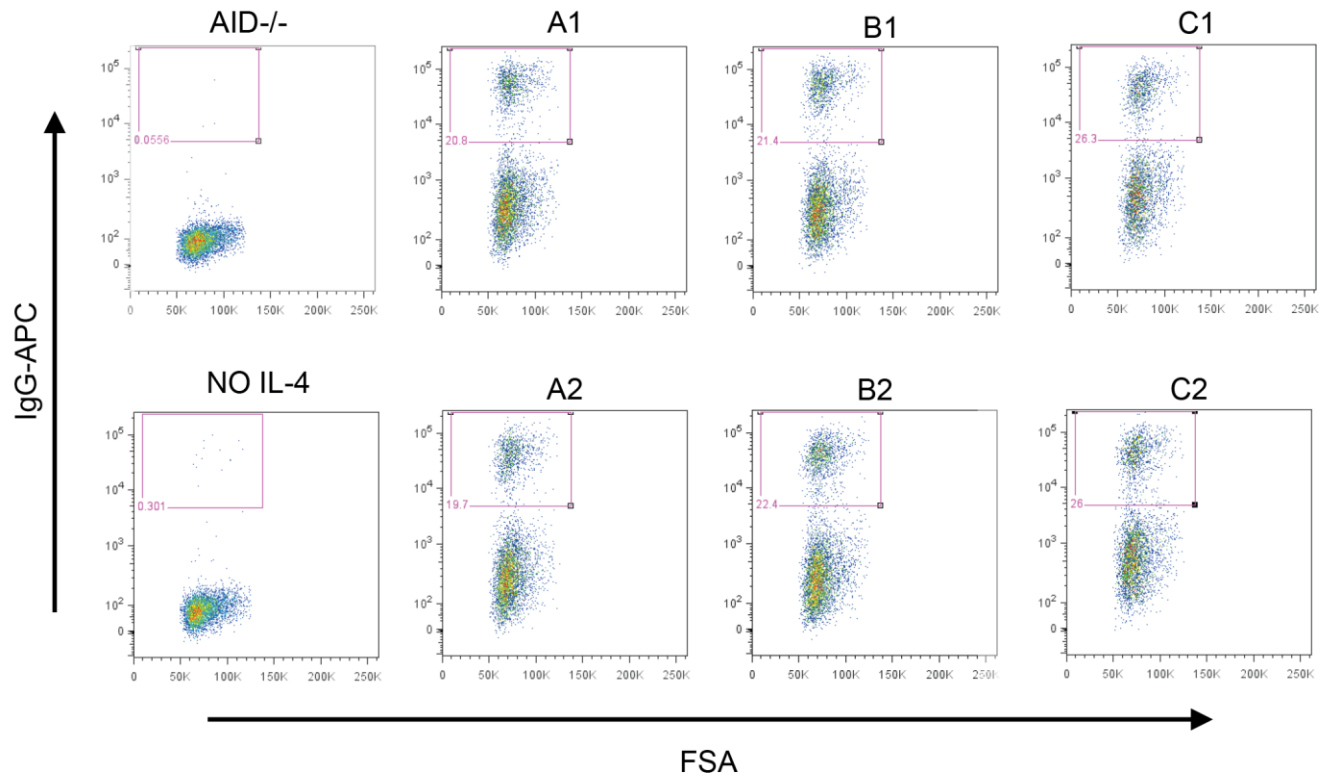


Figure 9

The Lot of Serum used During the CSR Assay can Effect Switch Efficiency

Fetal Bovine Serum from at least 4 different suppliers was tested for its ability to effect CSR efficiency. The cells were maintained at 500K per ml in B-cell media with 10%FBS +IL-4 +LPS and measured by FACS after 3 days *in vitro*. As a negative control, *Aid*^{-/-} and *wt* B-cells with no IL-4 do not undergo CSR. Percent switch to IgG is show in the lower right quadrant.

3.2 Chromatin Associated AID is Highly Modified

Previous studies had shown that most AID is localized in the cytosol (McBride, 2004). In order to determine the posttranslational modification state of AID relative to its subcellular localization a two-dimensional gel analysis and immunoblot was performed. 3T3 were cells infected with virus containing pMX-FLAG-AID. Three days after infection the cells were lysed on ice with RIPA with NaF and Calyculin in order to isolate protein lysates while preserving protein phosphorylation states. Cell lysates were then subjected to sucrose gradient equilibrium density ultracentrifugation to isolate chromatin-associated proteins. FLAG-AID was then immuno-precipitated from whole cell lysates and chromatin associated fraction using anti-FLAG beads. FLAG-AID protein was then eluted off of the bead and run on an immobilized pH gradient acrylamide gel strip to separate proteins by charge then run orthogonally on a SDS-PAGE gel and to separate proteins by size. The proteins are then transferred to a nitrocellulose membrane and immunoblotted for AID (Fig. 10). The results indicate that while FLAG-AID from whole cell lysate and from the chromatin associated fraction have the same molecular mass, there is a large differential in the range of isoelectric points between species in the whole cell extract and species in the chromatin associated fraction. Overall FLAG-AID from the chromatin-associated fraction had a more negative isoelectric point than the whole cell extract, which suggests that chromatin associated AID is highly phosphorylated. Given these results posttranslational modification is likely a mechanism in regulating the functional activity of AID at the chromatin level.

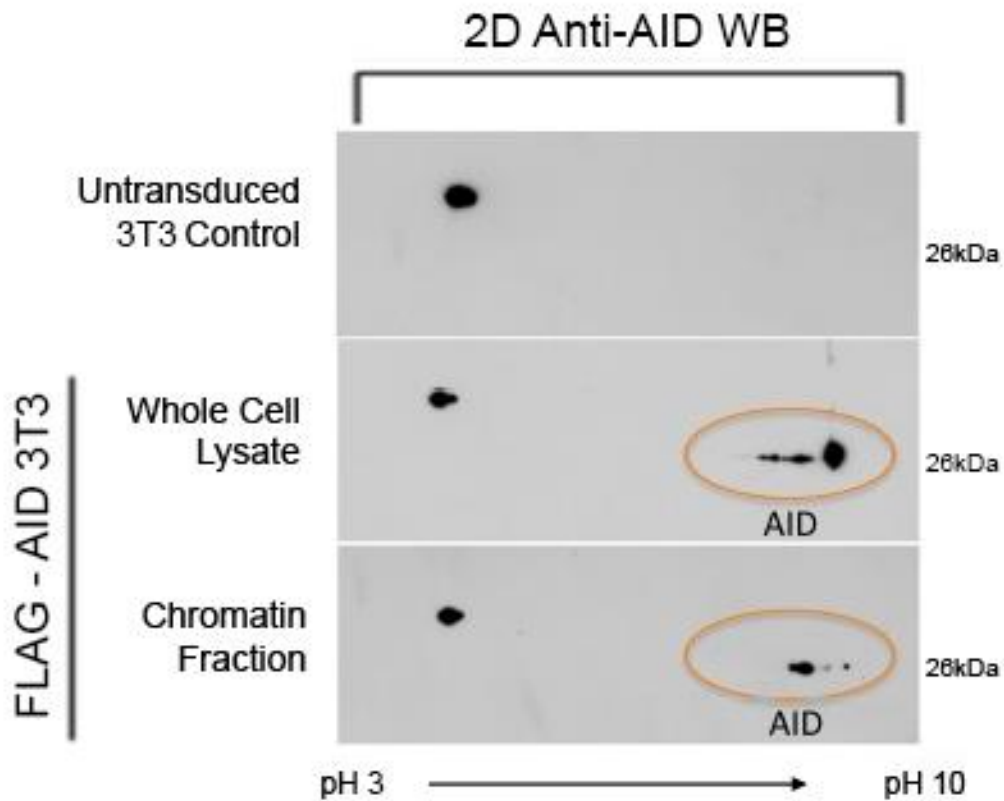


Figure 10

Chromatin Associated AID is More Negatively Charged than Whole Cell AID

Flag-AID isolated from the chromatin associated fraction reaches its isoelectric point at a lower pH than, Flag-AID isolated from whole cell extracts, indicating that it is more negatively charged, most likely do to protein phosphorylation. 3T3 MEF cells transduced with Flag-AID, and lysed with RIPA buffer after 3 days *in vitro*. Chromatin was isolated by equilibrium density centrifugation from Flag-AID expressing cell lysates. Flag-AID was then immuno-precipitated with anti-Flag beads from either whole cell extract or the isolated chromatin fraction. Immuno-precipitated lysates were then separated on a 3-10 immobilized pH gradient, then separated by molecular weight by SDS-PAGE. Proteins were then transferred to a membrane and blotted with an anti-AID antibody (courtesy of Sean Hensley).

3.3 Generation of Phospho-Specific Antibodies

In order to detect p-Y184 AID and p-T150 AID we developed two poly-clonal mouse antibodies that specifically recognizes p-Y184 AID or p-T150 AID. To test the sensitivity and the specificity of these antibodies for their specific epitope peptides containing p-Y184 AID, p-T150 AID, or recombinant AID were serially diluted and spotted onto an activated nitrocellulose membrane. The membranes were then blocked and incubated with either the anti p-Y184 or the anti p-T150 antibody for one hour, washed three times, incubated with a anti mouse-HRP secondary and developed with ECL. The results showed that each respective anti-phospho-AID antibody specifically recognized its intended epitope (Fig. 11). The anti p-Y184 AID antibody was able to detect the p-Y184 substrate at a concentration of about $2 \times 10^{-2} \mu\text{g}$, while the anti p-T150 AID antibody was able to specifically detect the p-T150 AID peptide at a concentration of $2 \times 10^{-8} \mu\text{g}$.

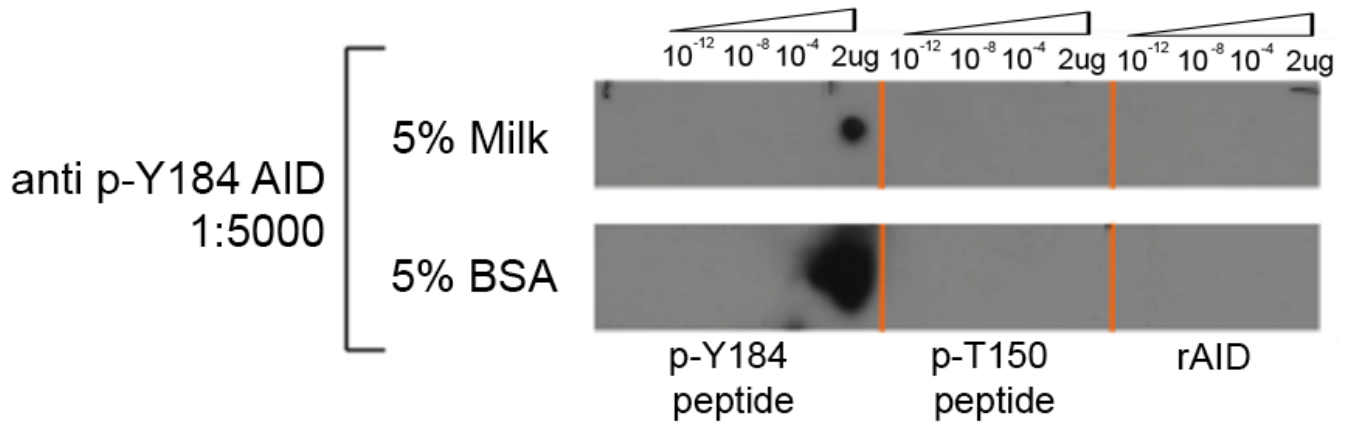


Figure 11

Anti p-Y184 AID is Specific for Phosphorylated AID Peptide

AID peptides containing p-Y184, p-T150 or un-phosphorylated recombinant AID (rAID) were serially diluted from 2 μg to 2 X 10⁻¹² μg spotted onto a nitrocellulose membrane, blocked with either 5% BSA or 5% Milk in TBST, and probed with anti p-184 AID antibody at a dilution of 1:5000. The anti p-184 AID antibody specifically recognizes p-Y184 AID peptide at concentrations approximately 2 X 10⁻² μg in 5% milk. The antibody does not recognize the p-T150 peptide or the un-phosphorylated rAID at any concentration.

While the sensitivity and specificity of the phospho-specific antibodies has been demonstrated, it is not known if AID is indeed phosphorylated at these sites cells. In order to test this primary mouse B-cells from *Aid*^{-/-} mice were isolated, plated, and retrovirally transfected with either FLAG-AID or FLAG-AID^{Y184F}. The cells were stimulated with LPS and IL-4 for three days. To induce tyrosine phosphorylation cells were exposed to NaVO₄ for thirty minutes before the cells are pelleted and lysed with RIPA. Western blots of the lysates were then performed using the anti p-Y184 AID antibody (Fig. 12) showing that the p-Y184 AID species is detectable after NaVO₄ treatment, but not in the FLAG-AID^{Y184F} expressing cells. This data demonstrates that the p-Y184 AID species does exist in mouse B-cells, and therefore tyrosine kinase pathways that are capable of targeting and phosphorylating AID in B-cells.

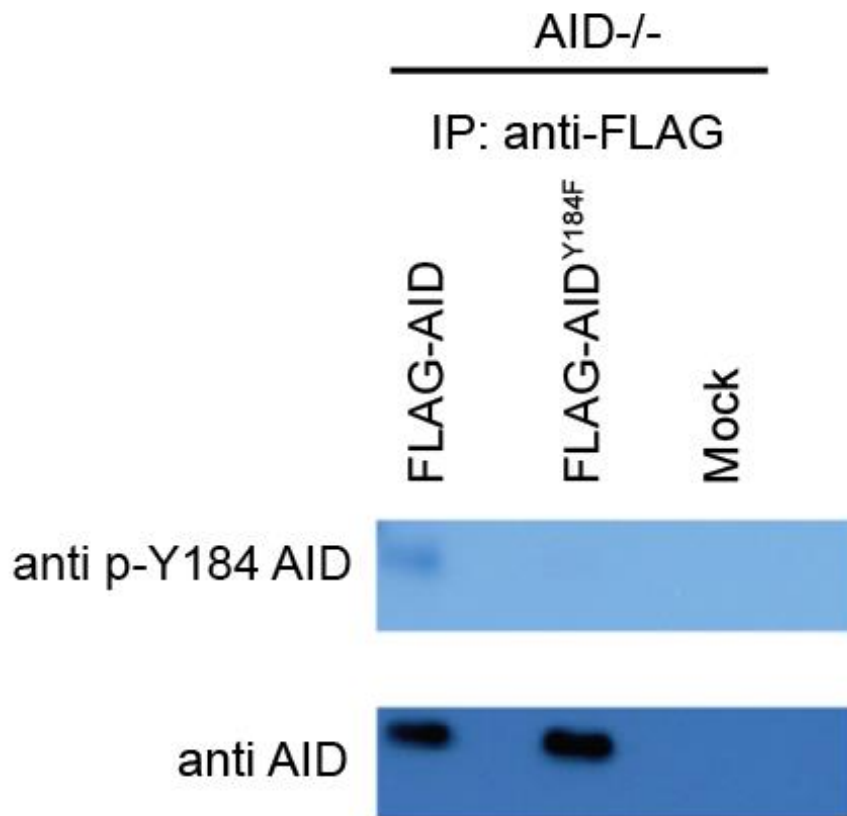


Figure 12

The Anti 184-Antibody Specifically Recognizes p-Y184 AID Isolated from Mouse

B-cells

Western blot showing the presence of p-T184 AID in B-cells. Primary mouse splenocytes isolated from *Aid*^{-/-} mice were transduced with flag-AID or flag-AID^{Y184F}, and simulated *in vitro* with LPS and IL-4. Transduced or uninfected cells were treated with NaVO₄ for 30 minutes to induce tyrosine phosphorylation prior to lysis, immuno-precipitation and immunoblotting with the anti p-Y184 AID antibody.

3.4 The Effect of AID Phosphorylation on Class Switch Recombination

The effect of AID phosphorylation on CSR has been studied in detail for phosphorylation sites such as serine 38 and serine 3, however there are other putative phosphorylation sites on AID that have yet to be thoroughly characterized. In order to understand the influence that phosphorylation of Y184, T150, T158, and S169 may have on CSR isolated *Aid*^{-/-} B-cells were retrovirally transduced with FLAG-AID-Y184F, FLAG-T150A, FLAG-T158A and FLAG-S169A and stimulated to switch with LPS and IL-4. FACS analysis of the AID mutant infected cells showed that the T158A mutation over all showed little effect on switch, the S169A and the Y184F mutations reduced switch by 30 - 60%, while the T150A mutation caused almost complete loss of the ability of cells to switch (Fig. 13). We can conclude from these findings that phosphorylation of T150, S169 and Y184 of AID may be necessary steps in the CSR pathway in order to obtain maximum switching efficiency. T150 of AID in particular seems to be an important residue for the CSR process and further study is needed to understand its role in this process *in vitro* and *in vivo*. Our results indicate the AID^{Y184F} mutation reduces switch slightly, indicating that tyrosine kinase pathways may be a distinctive regulatory mechanism for AID regulation.

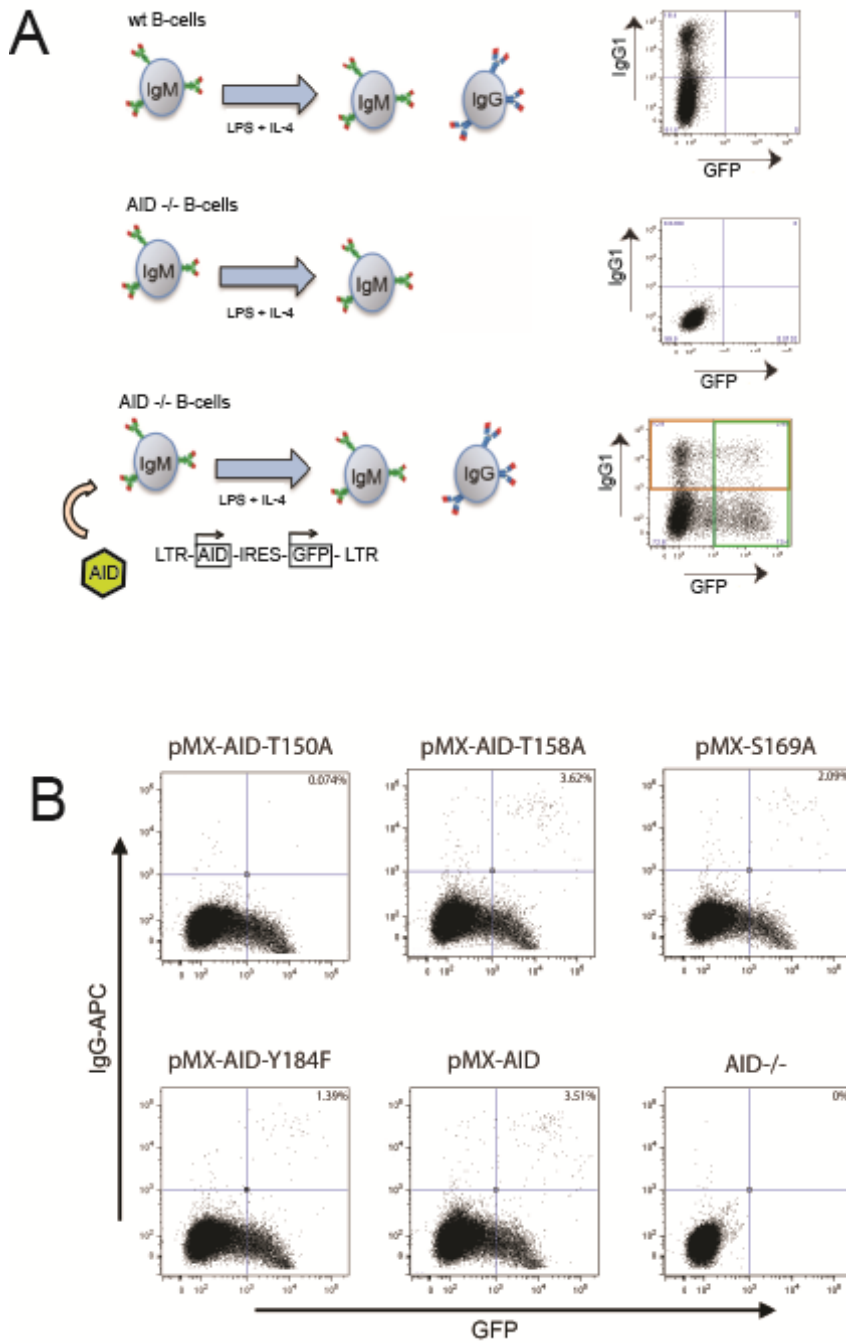


Figure 13

Class Switch Recombination Efficiency is Effected by AID Phosphorylation (A) wt B-cells stimulated with LPS + IL-4 *in vitro* switch from IgM to IgG which can be measured by FACS. *Aid*^{-/-} B-cells do not undergo switch *in vitro* when stimulated with LPS + IL-4. *Aid*^{-/-} B-cells can be transduced with virus containing pMX-AID. AID expression from pMX allows *Aid*^{-/-} B-cells to switch when stimulated with LPS + IL-4 *in vitro*; orange box. The

transduction efficiency can be measured by the expression of the IRES driven GFP; green box **(B)** *Aid*^{-/-} B-cells are infected with virus containing AID, or AID with point mutations preventing phosphorylation at T150, T158, S169, or Y184. FACS plots showing the effect of phosphorylation on switch, wt AID shows the greatest ability to switch, while all of the nonphosphorylatable mutant forms of AID show reduced switch.

3.5 Putative Phospho-AID Interacting Proteins

In order to discover potential phospho-AID binding proteins we employed phospho-protein binding array that contained immobilized SH2 phospho-tyrosine binding domains. We probed this array with a fluorochrome tagged peptide of the AID c-terminus containing phosphorylated Y184. If the phospho-peptide binds to the phospho-binding domain it will be detectable upon fluorescent imaging of the array (Fig. 14). The results revealed four potential AID-p-Y184 binding partners two tyrosine kinases FYN and ABL2, a guanine nucleotide exchange factor VAV2, and an adaptor protein SH3BP2 that also contains an SH2 domain. A previous report showed that *Sh3bp2* knock out mice showed unexpected B-cell phenotype that included a defect in CSR (Chen, 2007). Due to this fact we decided to focus on SH3BP2 to understand the potential roles phospho-binding proteins may play in regulating AID function.

To test for the expression of SH3BP2 in mouse B-cells we isolated and purified mRNA, then used oligo-dT and reverse transcriptase to generate a cDNA library of genes actively transcribed by mouse B-cell under LPS and IL-4 stimulated conditions. Using specific primers we were able to amplify SH3BP2 from this cDNA library (Fig. 15),

demonstrating it is actively transcribed in mouse B-cell. We purified these PCR products and ligated them into the pMX-expression vector to be able to express SH3BP2 protein in future experiments.

In order to detect SH3BP2 protein in cells we purchased two separate anti-SH3BP2 polyclonal goat antibodies Clone C-19 and N-18 (Sanata Cruz Bio, Dallas, TX). We used these antibodies to perform western blots on protein lysates from LPS and IL-4 stimulated mouse B-cells, HEK cells, and HEK cells transfected with pMX-SH3BP2 (Fig. 16). Of the three groups tested we were only able to detect SH3BP2 protein in the pMX-SH3BP2 group, and although SH3BP2 protein was detectable using both antibodies the N-18 clone proved to be significantly more sensitive than the C-19 clone. While the mRNA of SH3BP2 was detectable in mouse B-cells we were unable to identify protein from them using these antibodies. These results suggest that SH3BP2 may be expressed in B-cells but at a level too low to be detected, at least with the current antibodies available on the market.

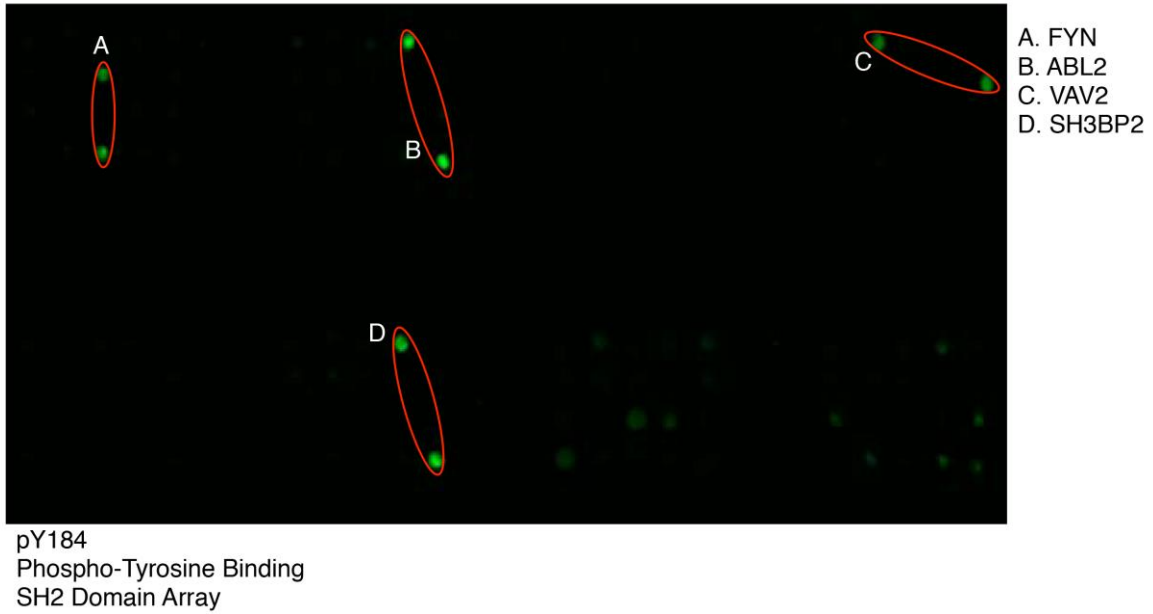


Figure 14

Phospho-AID Peptides Interact with Phospho-Binding Protein Domains

An AID peptide containing phosphorylated Y184 interacts with SH2 domains from four different proteins. An array of protein phospho-binding domains were immobilized on a nitrocellulose coated slide. Arrays are then probed with Cy3 tagged phospho-AID peptides and washed. Protein domains that strongly bind phospho-AID peptides are identified by Cy3 fluorescence. (Courtesy of the Bedford lab)

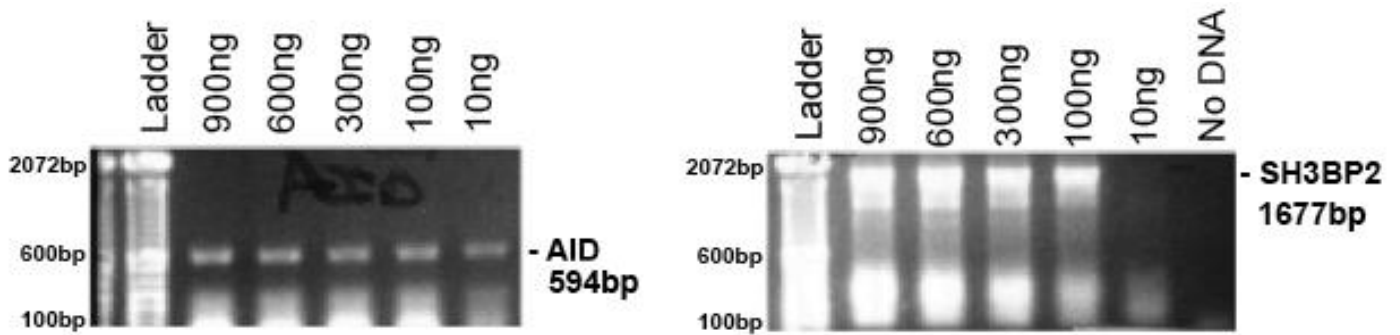


Figure 15

Phospho-Tyrosine Binding Protein SH3BP2 is Expressed in *wt* Mouse B-cells

Ethidium-bromide gel staining showing SH3BP2 PCR products amplified from mouse B-cell cDNA. cDNA from mouse B-cells was isolated using oligo-dT primers to amplify mRNA. Specific primers for SH3BP2 were able to amplify the 1677bp gene at cDNA concentrations from 900ng to 100ng. As a positive control 594bp AID was amplified from the same cDNA with AID specific primers. SH3BP2 gel bands were then isolated and cloned into vectors for later use.

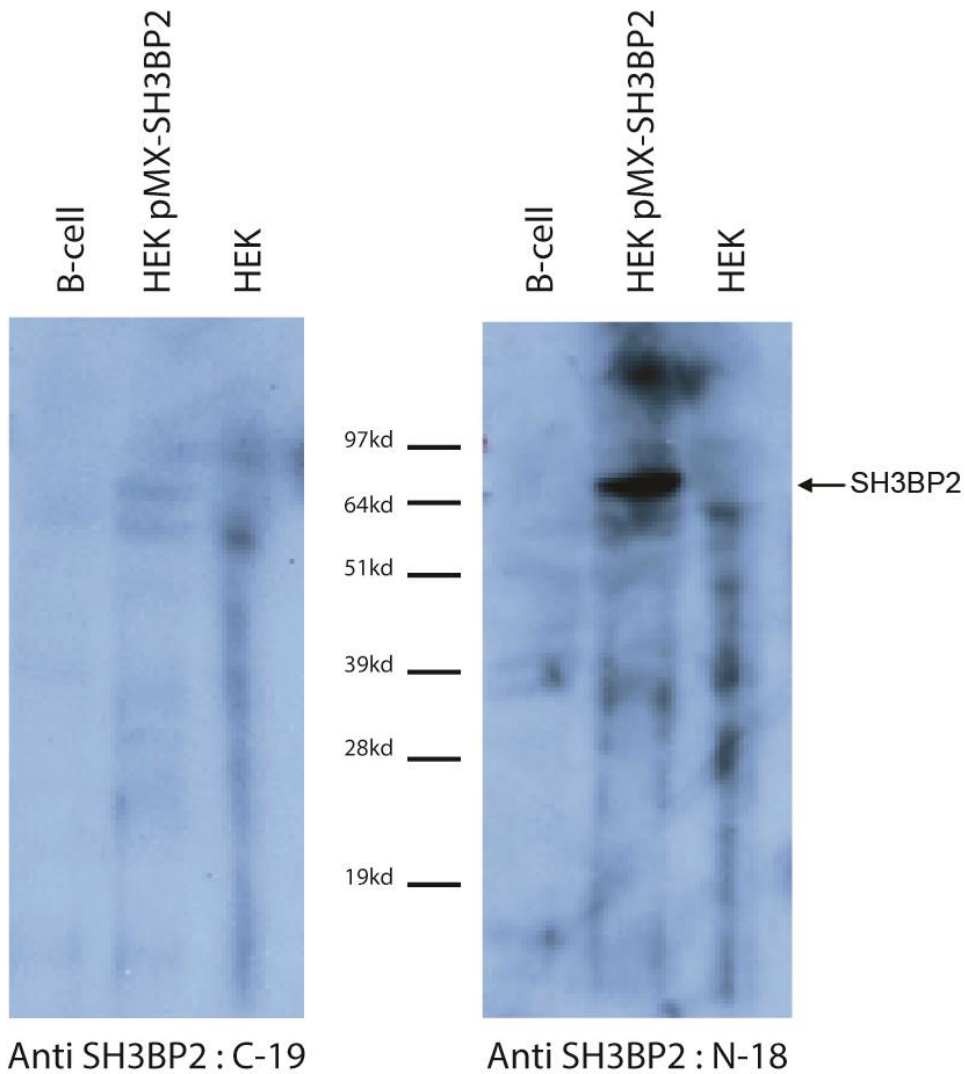


Figure 16

SH3BP2 can be Detected from Cell Lysate by Western Blot

Western blots testing two different anti-SH3BP2 antibodies. SH3BP2 can be detected using the N-18 antibody in cells transfected to over express SH3BP2. Bands were not visible in extracts from *wt* B-cells or untransduced HEK cells, suggesting that these antibodies are not able to detect SH3BP2 protein at endogenous levels.

3.6 Differential Regulation of The PI3 Kinase Pathway on AID-S38 Phosphorylation

In order to better understand the signal transduction pathways that lead to or inhibit AID phosphorylation we treated AID expressing cells with a number of different small molecule inhibitors. We discovered that a small molecule inhibitor of the PI3Kinase pathway LY29004 was able to cause an increase in the amount of AID-S38 phosphorylation when 3T3 cells expressing FLAG-AID were exposed to the chemical for several minutes (Fig. 17). Intrigued by these results, we repeated the same experiment using LPS and IL-4 stimulated mouse B-cell, however exposure to LY29004 had no effect on FLAG-AID S38 phosphorylation, suggesting a difference in the signaling pathways that regulate AID-S38 phosphorylation between these two cell types.

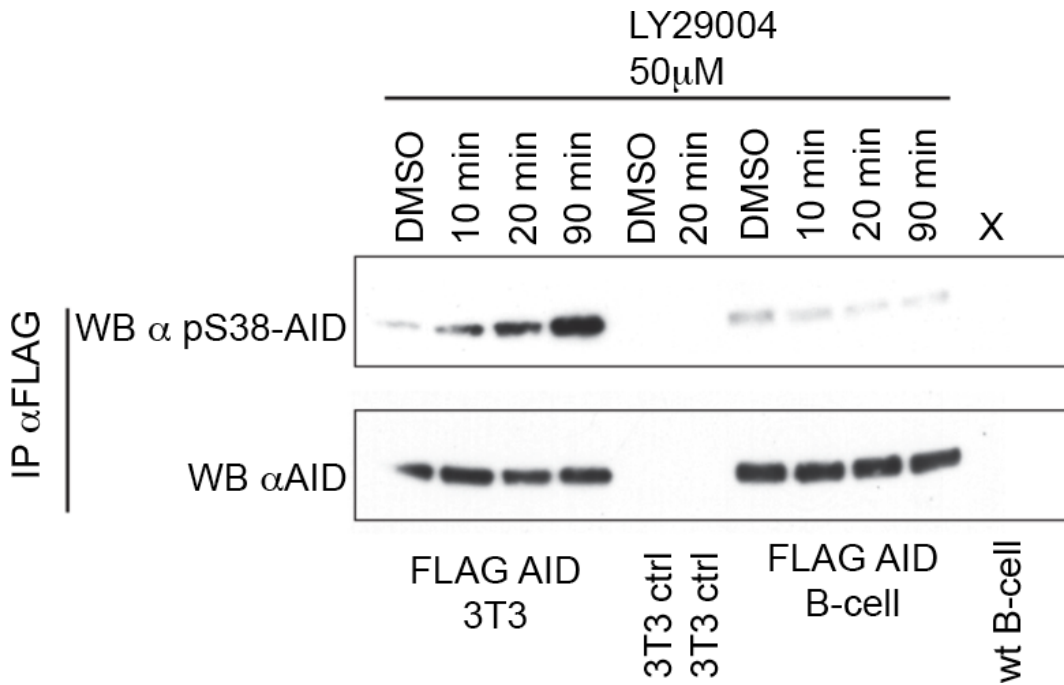


Figure 17

The PI3Kinase Inhibitor LY29004 Stimulates AID S38 Phosphorylation in 3T3 Cells but not B-cells

3T3 cells are transfected with pMX-FLAG-AID, or left untransfected as a control. The PI3Kinase inhibitor LY29004 was applied for varying lengths of time. The cells were then lysed and immuno-precipitated using anti-FLAG beads, then eluted and western blotted with an anti p38-AID antibody. Cells showed an increase in S38 phosphorylation that was time dependent. However when the experiment was repeated with FLAG-AID expressing B-cells LY29004 treatment produced no effect on AID S38 phosphorylation. Both membranes were then stripped and re-probed with an anti-AID antibody to ensure equal loading.

3.7 Chapter 3 Summary

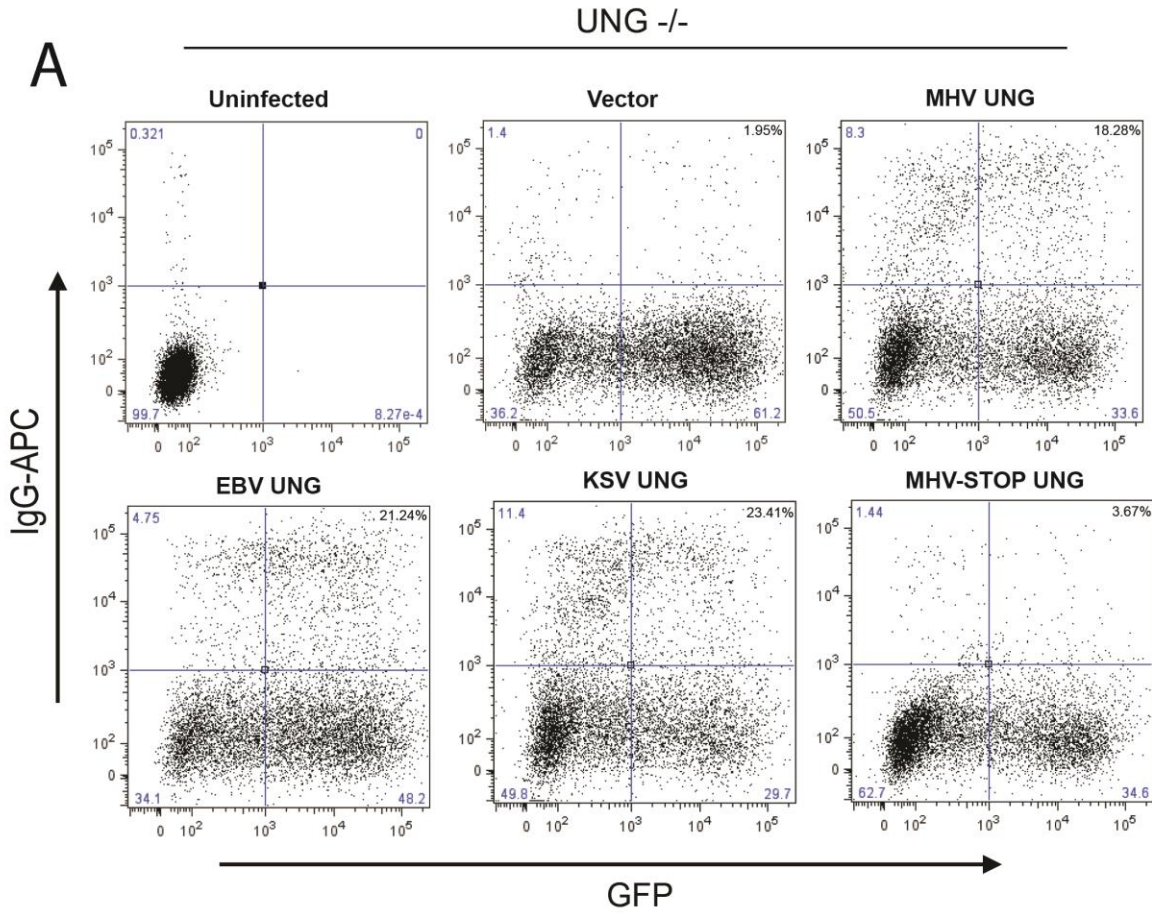
While the *in vitro* CSR assay is a powerful tool to study the isotype class switching process, our initial characterization experiments demonstrate the sensitivity of this system to variables such as serum lot, and cell plating density. These factors are capable of having a significant influence on the CSR process *in vitro*, and therefore need to be controlled in order to ensure consistent experimental results. Using a two-dimensional gel analysis we found that chromatin associated AID has a significantly lower isoelectric point than AID isolated from whole cell extracts, implying that chromatin associated AID is heavily phosphorylated. These results suggest that proper phosphorylation of AID is necessary before it can associate with genomic DNA. There are several phosphorylation sites on AID whose function is unknown. In order to determine if these AID phosphorylation sites regulate the CSR process we tested the effect of their absence in the *in vitro* CSR process. We found that three of these site mutations T150A, S169A, Y184F reduced the ability of cells to switch, suggesting phosphorylation at these sites is needed for optimum CSR efficiency. Where as the T158A mutation had no measurable effect on switch, implying it plays no role in the regulation of CSR. We also developed antibodies that specifically recognize p-T150-AID or p-Y184-AID, and show that it is possible to detect p-Y184-AID in mouse B-cells after treatment with tyrosine phosphatase inhibitor NaVO₄. However the signaling pathways that lead to AID phosphorylation at these sites remain unresolved. We also used a protein domain array to screen for potential phospho-AID specific binding partners, a completely untouched area in the AID field. The screen revealed four potential phospho-AID interacting proteins, some of which are known to be important in other B-cell pathways. We were able to show that the adaptor protein SH3BP2 is actively expressed in mouse B-cells, although not at levels high enough to be detected by western blot with commercially available antibodies. Our data demonstrate a regulatory role for multiple phosphorylation sites in the CSR process, and that there may be factors that interact with AID in a

phosphorylation specific manner. While these results are intriguing, further research is needed to understand the significance of these findings, and how they influence B-cell biology.

Chapter 4 - The Effect of Viral Uracil DNA Glycosylases on Antibody Diversification Processes in Mammalian B-cells

4.1 Viral UNGs are Able to Partially Restore Isotype Class Switch Recombination in *Ung*^{-/-} Mice

Detection and removal of uracil in the switch region DNA is a crucial step in the CSR process, therefore *Ung*^{-/-} mice are almost completely deficient in their ability to switch isotypes. B-cells are known to be the main host cell type for gamma herpes viruses, it was however unknown if their viral UNGs are able to act on the host cell genome and participate in antibody diversification processes such as CSR that rely heavily on the host UNG. In order to determine if viral UNGs are able to participate in the CSR process, *Ung*^{-/-} B-cells were isolated and transduced with retrovirus containing pMX-MHV68-UNG, pMX-EBV-UNG, pMX-KSV-UNG or an empty pMX control vector. The infected B-cells were then cultured in the presence of LPS and IL-4 for four days, then stained with an anti-IgG-APC antibody and analyzed by FACS. To our surprise expressing any of the viral UNGs in the *Ung*^{-/-} B-cells was able to induce approximately 20% of the cells to switch to IgG1 (Fig. 18), in comparison to the empty vector control which had negligible percentage of cells switch. We can conclude from these experiments that viral UNGs are capable of acting on the host genome in B-cells and are able to participate in the class switch recombination process at the Ig locus.



B

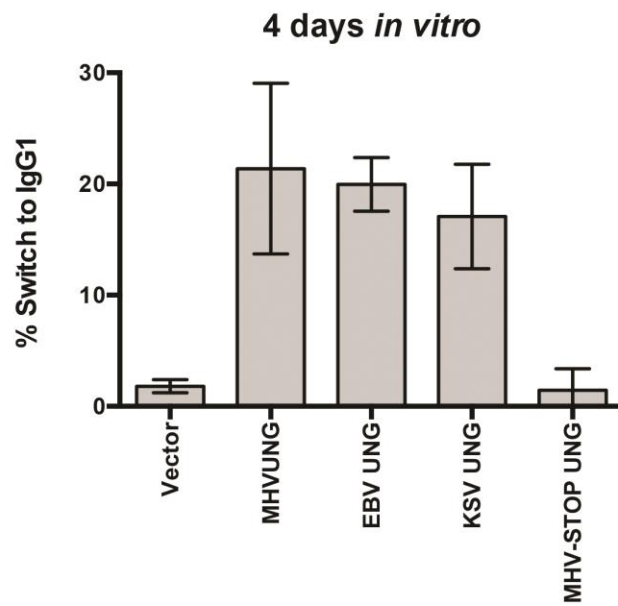


Figure 18

Expression of Viral UNG in *Ung*^{-/-} B-cells Provides Partial Compensation During CSR *in vitro*

UNG is introduced to the cells by retroviral infection, after 4 days of LPS and IL-4 stimulation *in vitro*, the cells are analyzed for UNG-IRES-GFP expression and switch to IgG1 by FACS.

(A) Representative FACS plots of *Ung*^{-/-} cells expressing viral UNG. *Ung*^{-/-}

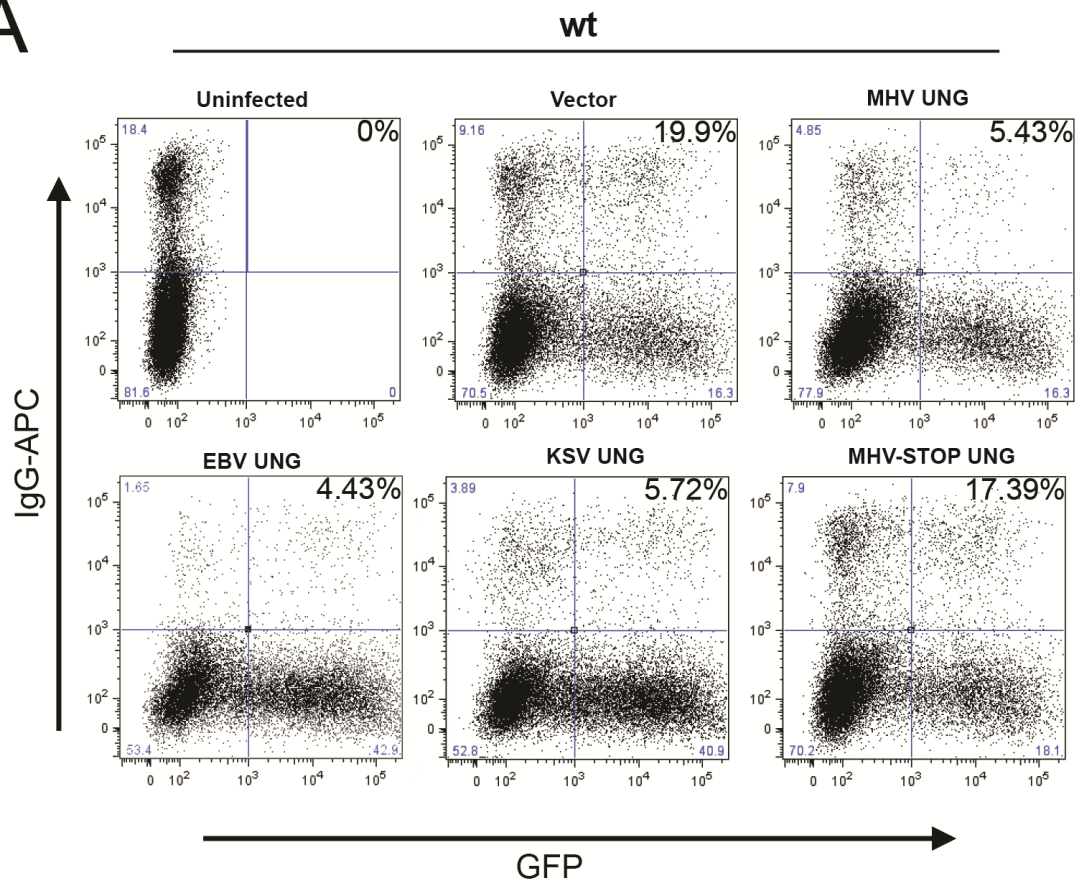
B-cells expressing MHV UNG, EBV UNG or KSV UNG are able to switch to IgG1 at a level significantly higher than cells expressing the vector control or the truncated protein MHV-STOP UNG. The percent of infected cells that have switched to IgG1 are shown in the upper right corner. (B) Average switch of *Ung*^{-/-} cells expressing viral UNG to IgG1, averaged of three separate experiments. $p < 0.001$ for viral UNG expressing cells compared to the vector control.

4.2 Viral UNGs Suppress Class Switch Recombination when Expressed in *wt* Mouse

B-cells

After discovering that viral UNGs are capable of participating in the CSR process in *Ung*^{-/-} cells we wanted to more accurately model the gamma herpes virus infection. To model this we purified and infected *wt* B-cells and transduced them with retrovirus containing pMX-MHV68-UNG, pMX-EBV-UNG, pMX-KSV-UNG, empty pMX control vector, or pMX-MHV-STOP UNG a nonfunctional truncated form of MHV-UNG. After four days of *in vitro* stimulation with LPS and IL-4, the percentage of cells switched to IgG1 was measured by FACS analysis. To our surprise all the expression of full length viral UNGs suppressed the ability of *wt* B-cells to switch isotypes by approximately 50% compared to the empty vector control (Fig. 19). We can conclude from these results that the expression of viral UNG in *wt* B-cells is somehow interfering with the molecular processes involved in CSR. Given these surprising results we developed two models in an attempt to explain the effects of viral UNG in the CSR process (Fig. 20). In the first model, referred to as the scaffolding model, we propose that viral UNG competes with endogenous host UNG for binding partners involved in the CSR process, thereby reducing the number of fully functional UNG complexes and the efficiency of the CSR process (Fig. 20). The second model, the enhanced clearance of uracil model, proposes that with the additional expression of viral UNG there is too much UNG catalytic activity, and this excess UNG activity does not allow enough uracils to accumulate at the switch regions to lead to a double strand break (Fig. 20).

A



B

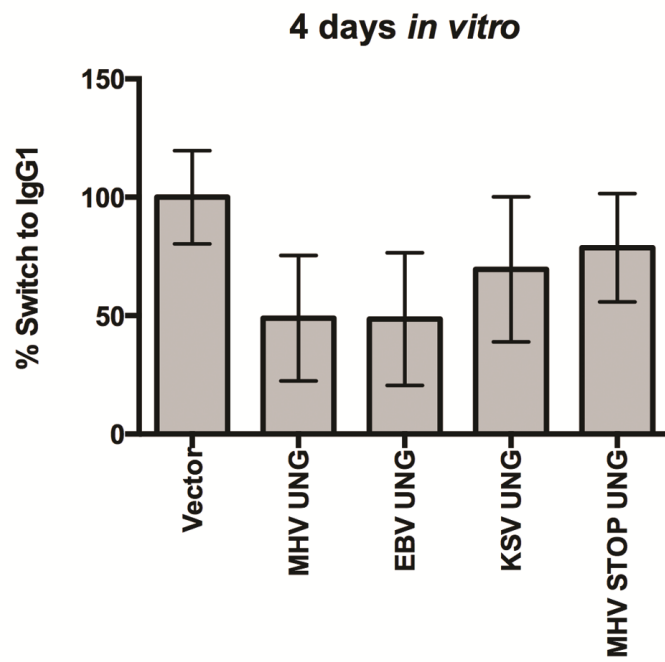


Figure 19

Expression of Viral UNG in *wt* mouse B-cells Suppresses CSR *in vitro*

(A) Representative FACS plots of *wt* mouse B-cells expressing viral UNG. After 4 days of LPS and IL-4 stimulation *in vitro* B-cells expressing MHV-UNG, EBV-UNG or KSV-UNG show significantly reduced ability to switch to IgG1. The percent of infected cells that have switched to IgG1 are shown in the upper right corner. (B) Average switch of *wt* B-cells expressing viral UNG to IgG1, averaged of three separate experiments. $p < 0.001$ for viral UNG expressing cells compared to the vector control.

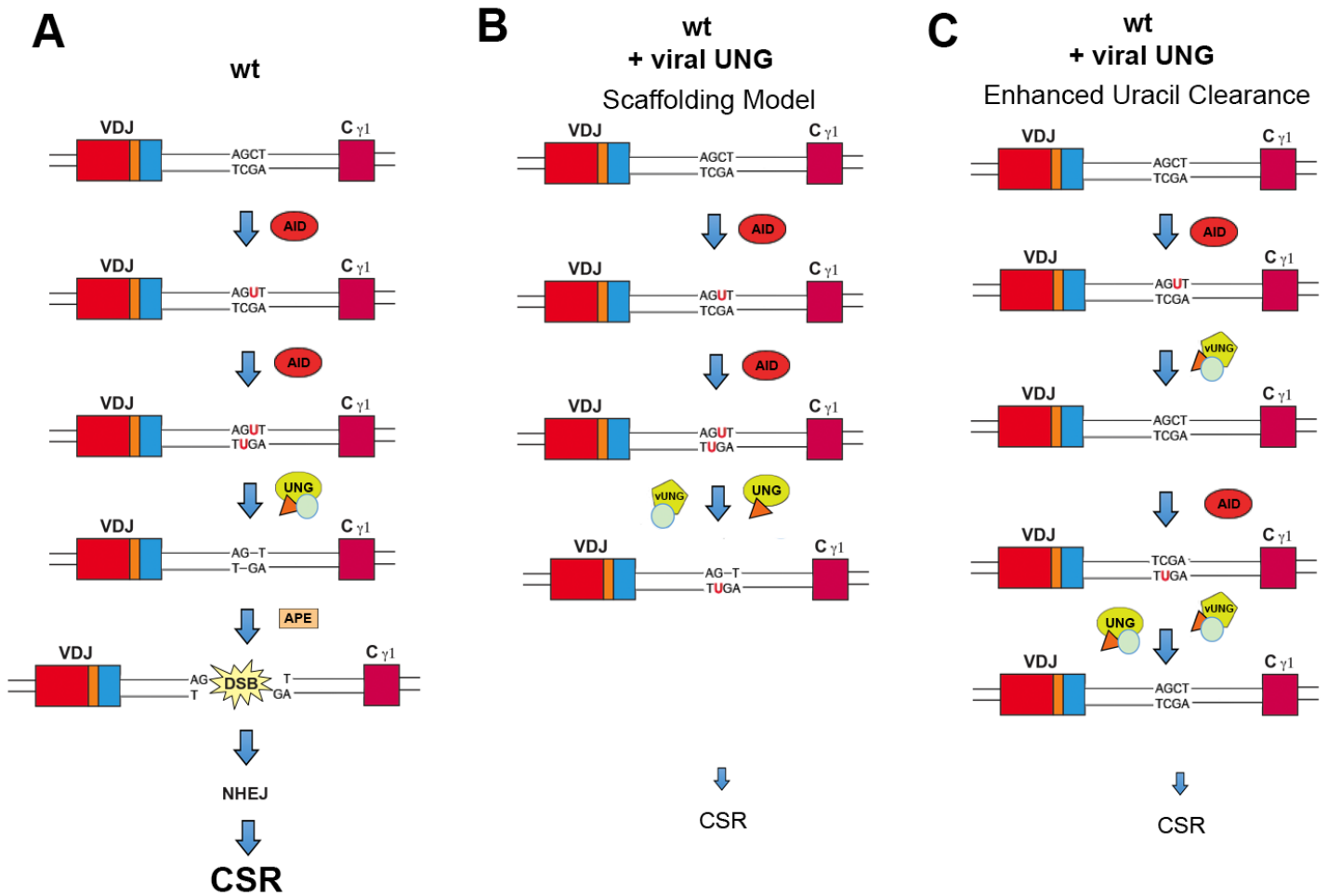


Figure 20

Two Potential Models to Explain the Ability of Viral UNG to Suppress CSR in wt B-cells.

A) A model for CSR in wt B-cells; AID is targeted to the switch regions where it introduces uracils on both strands of DNA. UNG then removes these uracils to produce abasic sites that are then nicked by AP-endonuclease (APE), resulting in a double strand break.

Processing and ligation of the break to another switch region by the NHEJ pathway leads to CSR. **B)** The scaffolding model; viral UNG is able to form a partially functional complex with UNG associated cofactors compensate for the loss of mUNG when expressed in *Ung*^{-/-} B-cells. However in when viral UNG is expressed in wt B-cells it competes for binding factors (represented by green circles and orange triangles) with mUNG leading to less efficient removal of uracils, limiting downstream processes and reducing ability of cells to complete the CSR process. **C)** The enhanced clearance of uracil model; in wt B-cells when viral UNG is expressed with endogenous UNG, the over abundance of UNG does not allow AID induced uracils to accumulate to the critical level needed to cause a double strand break; the abundance of UNG removes and repairs uracils in a high fidelity manner before downstream CSR mechanisms can be initiated.

4.3 UNG Catalytic Activity is Nonessential for Suppressing CSR in *wt* Mouse B-cell

To determine the mechanism of action of viral UNG interference in the CSR process, we produced two UNG mutants, a catalytically inactive form of mUNG, and a catalytically inactive form of MHV-UNG. Previous studies had shown that it was necessary to mutate at least two residues essential for catalysis in order to completely eliminate catalytic activity from mouse UNG (Di Noia, 2007). We replicated two of these mutations in mouse UNG, one in the water activating loop (¹⁴¹VVILGQDPYH¹⁵¹), and one in the DNA backbone interacting leucine loop (²⁷⁰HPSPL²⁷⁴) using site directed mutagenesis (Fig. 21). Although it had never been attempted, the identical sequence conservation of catalytic motifs in MHV-UNG allowed us to make identical point mutations by site directed mutagenesis.

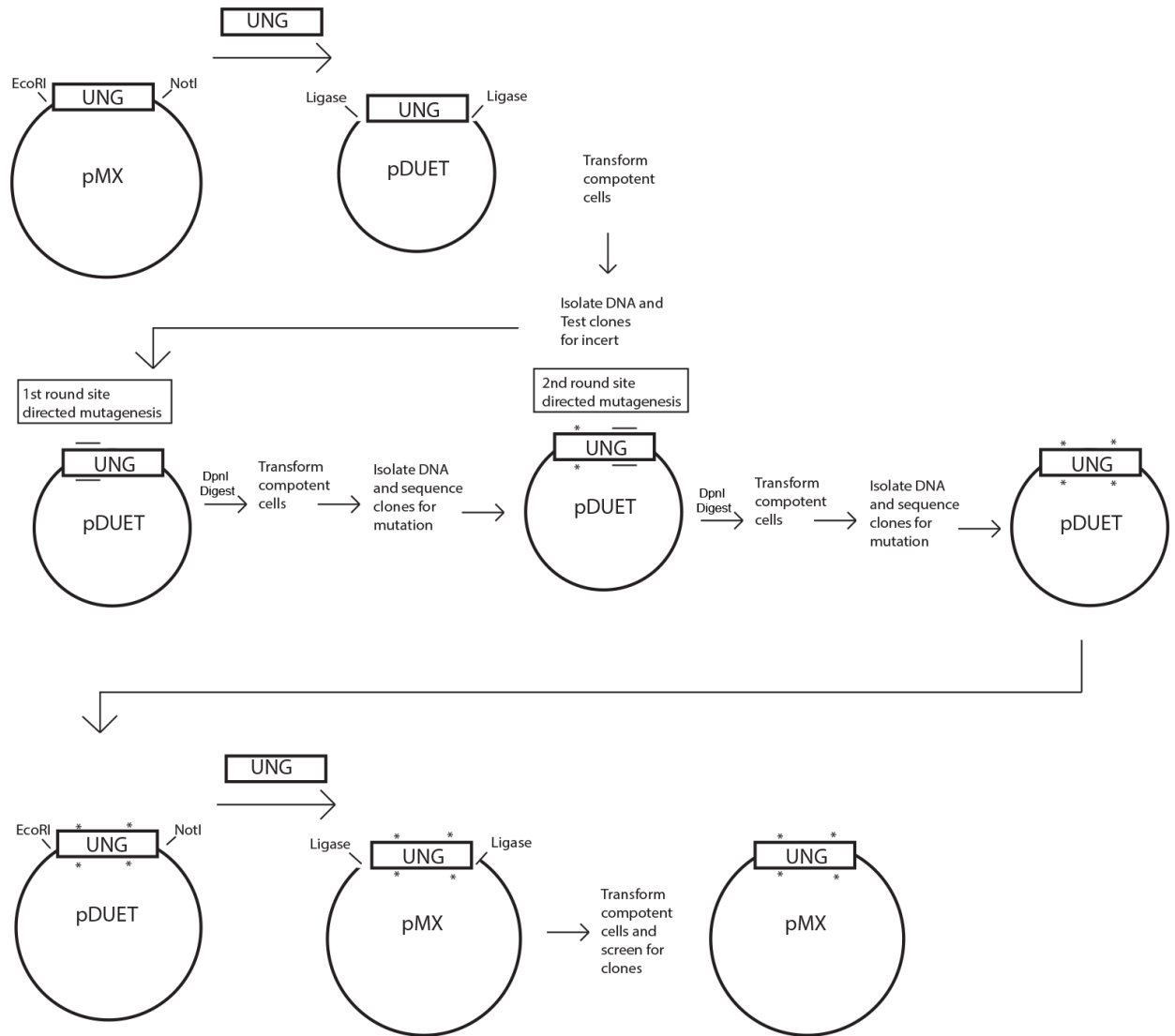


Figure 21

UNG Catalytic Mutants are Generated by Site Directed Mutagenesis

Either mUNG or MHV-UNG were excised from pMX by restriction endonucleases. Then was ligated in to the smaller vector pDUET, and used to transform competent bacteria. Plasmids then undergo PCR with the site directed primers and high-fidelity pfuTurbo DNA polymerase. The PCR products are then digested with DpnI in order to remove the methylated unmutated template DNA. The Digested PCR product is then used transform competent bacteria, from which individual clones are picked, and purified for plasmid DNA. The DNA is then sequenced to check for the presence of the mutation. Plasmids containing the mutation are then subjected to a second round of site directed PCR using the second set of primers to induce the second mutation. Purified plasmids are then sequenced to test for the presence of both mutations. Once both mutations are verified by sequencing the mutated UNG insert is excised and ligated into pMX.

We then transduced both *Ung*^{-/-} B-cells and *wt* B-cells with catalytically inactive mUNG, catalytically inactive MHV-UNG, mUNG or MHV-UNG and stimulated them for four days in vitro in the presence of LPS and IL-4 then measured by FACS for switch. We found that catalytic activity is necessary for either mUNG or MHV-UNG to stimulate class switching in *Ung*^{-/-} cells, however both the catalytically active and inactive forms of the proteins are able to suppress switch in *wt* B-cells (Fig. 22). These results suggest that viral UNG is interfering with the endogenous class switch process via a scaffolding mechanism that does not require UNG catalytic activity.

A

mUNG	141-VVILGQDPYHG-151	270- <u>H</u> PSPL-274
MHV UNG	79-VVILGQDPYHG-89	207- <u>H</u> PSPL-211
cat. mut mUNG	141-VVILGQNPYHG-151	270- <u>L</u> PSPL-274
cat. mut MHV UNG	79-VVILGQNPYHG-89	207- <u>L</u> PSPL-211

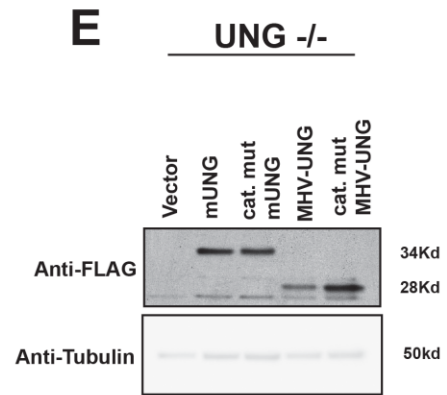
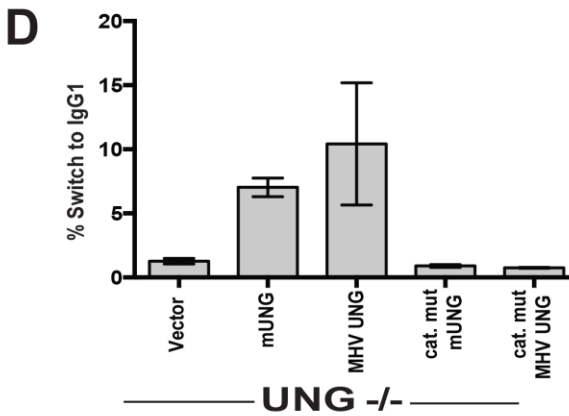
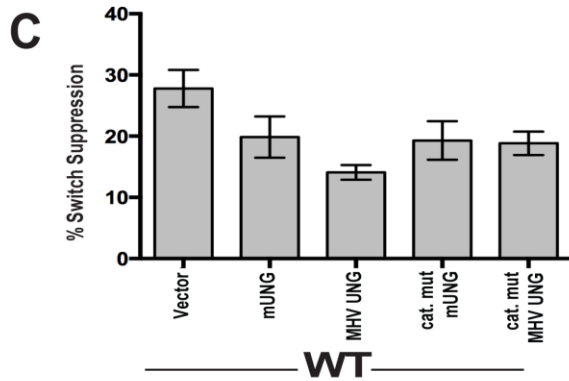
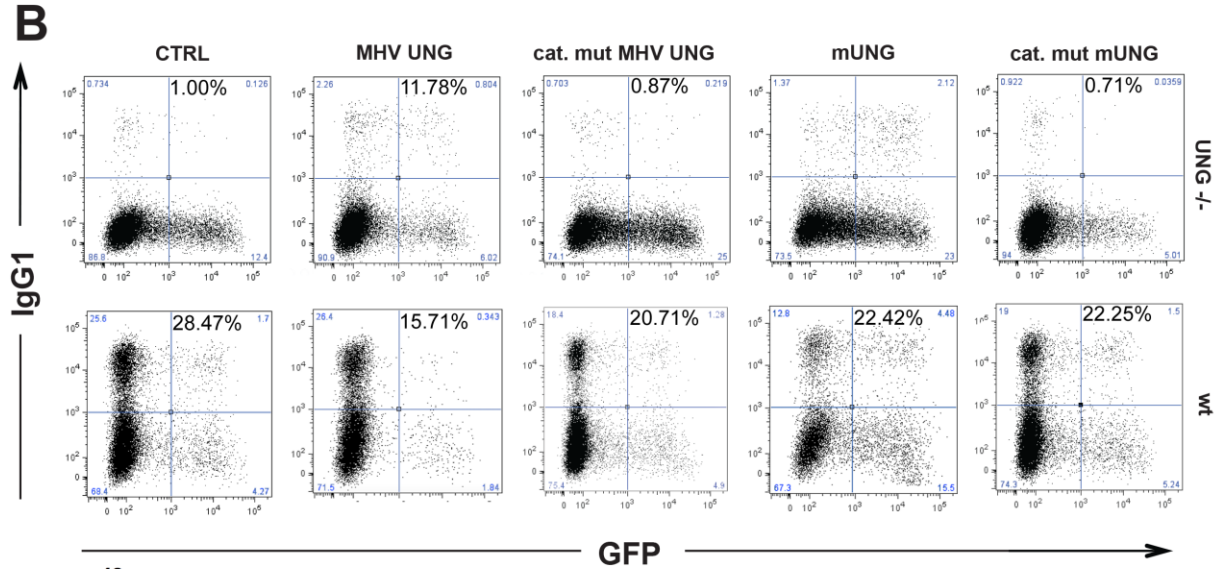


Figure 22

UNG Catalytic Activity is Necessary for *Ung*^{-/-} CSR Compensation But Dispensable for Suppression of CSR in *wt* B-Cells

(A) Alignment of the amino acid sequence of mUNG and MHV68-UNG showing the conservation of the catalytic domain between the host and virus UNG (B) Representative FACS plots showing the ability of catalytically active UNG to increase switch in *Ung*^{-/-} B-cells, while catalytic activity of UNG is not necessary for suppression of switch in *wt* B-cells. (C) Graphical representation of the average effect on CSR when catalytically active and inactive UNGs are expressed in *Ung*^{-/-} (D) or *wt* mouse B- cells. Average of three separate experiments (E) Catalytically inactive mUNG and MHV68 UNG are stably translated in *Ung*^{-/-} cells. Anti-FLAG WB of lysates from cells expressing mUNG-FLAG, MHV-FLAG, mUNG-CAT.MUT-FLAG or MHV-CAT. MUT-FLAG.

4.4 Viral UNG Suppresses IgH-cMYC Translocations When Expressed in Mouse

B-cells

There is as large body of evidence linking Epstein-Barr infection to the development of Burkitt's lymphoma (Young and Rickinson, 2004). It has also been established that the molecular events that initiate CSR are also responsible for the formation of the IgH-cMYC translocation, the hallmark of Burkitt's lymphoma (Ramiro, 2006). Upon the discovery that viral UNGs interfere with the CSR process we wanted to determine if IgH-cMYC translocation rates were also affected by viral UNGs. In order to test this we infected *wt* B-cells with retrovirus containing either pMX MHV-UNG or an empty pMX control vector. The cells were stimulated for four days *in vitro* with LPS and IL-4 then analyzed by FACS. GFP positive cells expressing the pMX vector were sorted and collected (Fig. 23). Genomic DNA from the GFP positive cells collected was amplified by PCR using IgG and cMYC specific primers which amplify IgH-cMYC reciprocal translocations. The PCR products were then run on an agarose gel and transferred to a nylon membrane for southern blotting. The membranes were then probed with probes specific for IgH or cMYC, and spots positive for both IgH and cMYC probes were counted as reciprocal translocations (Fig. 24). The frequency of translocations in *wt* B-cells infected with pMX MHV-UNG was reduced by approximately 60% compared to the empty pMX control infected cells (Fig. 24)(Table 4-1). From these results we conclude that the expression of viral UNGs in B-cells may in fact reduce the probability of oncogenic translocations, therefore loss of viral UNG expression may be a necessary step in the transformation of gamma herpes virus infected cells.

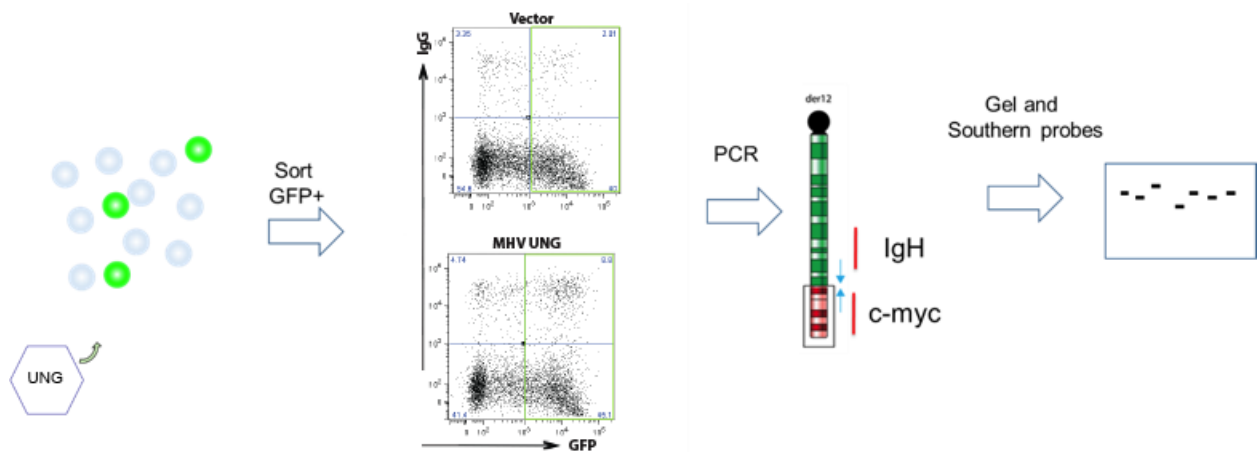


Figure 23

Experimental Design for the IgH-cMYC Translocation Assay

Primary mouse B-cells isolated and plated at a density of 1×10^6 cells per ml for 12 hours. The cells are then re-plated into 6 well plates at a density of 500K per ml and infected with either pMX MHV-UNG virus or pMX empty vector control virus. The cells are kept at 500K per ml until 60 hours after infection at which point they are sorted for GFP expression (green boxes). After sorting genomic DNA is isolated from the GFP positive cells and long range PCR is performed using cMYC and IgH specific primers using 500ng of DNA per reaction. The PCR products are then run on a 1% agarose gel, imaged using ethidium bromide then transferred to a nylon membrane and probed for cMYC and IgH.

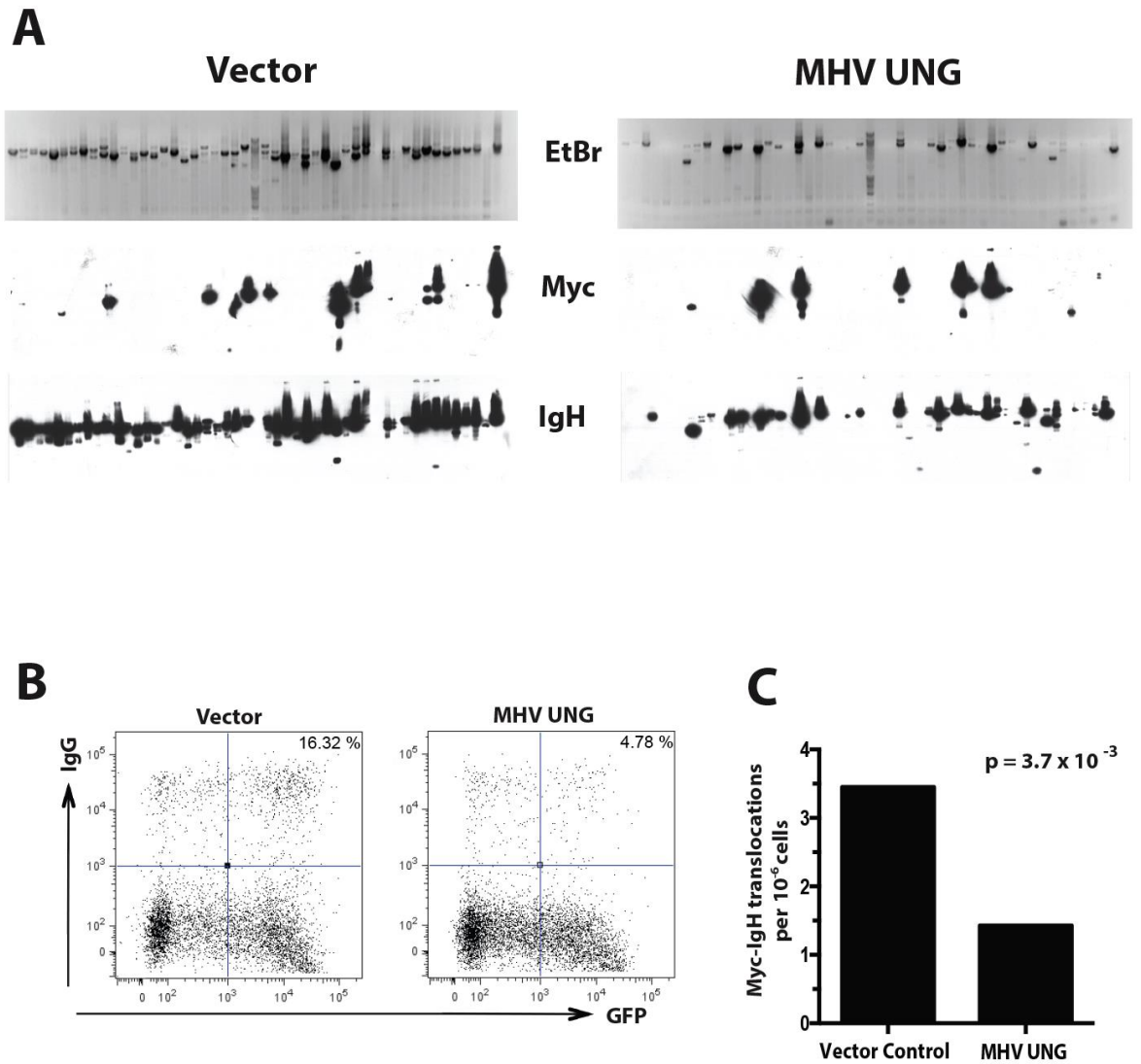


Figure 24

MHV-UNG Expression Decreases IgH-Myc Translocations in *wt* mouse B-Cells

(A) Ethidium bromide staining, anti-cMyc and anti IgH Southern blots of translocation PCR products from vector control infected, or MHV-UNG infected *wt* B-cells. **(B)** FACS analysis of cells sorted for DNA; MHV-UNG expression suppresses switch to IgG1. **(C)** Myc-IgG translocation rate per million cells, MHV-UNG expression significantly reduces translocation frequency compared to vector control. Average of four independent experiments. $p = 0.0037$ Fischers Exact test.

Table 2A

IgH-cMYC Translocation Data from Four Independent Experiments

Replicate	Gel lanes	Cell Number	Lanes with Reciprocal Translocations	Translocations per lane
1 Vector	12	1,200,000	2	0.166666667
2 Vector	8	800,000	8	1
3 Vector	16	1,600,000	4	0.25
4 Vector	48	4,800,000	10	0.208333333
Vector Total	84	8,400,000	29	0.34523
1 MHV	12	1,200,000	1	0.08333
2 MHV	8	800,000	1	0.08333
3 MHV	16	1,600,000	0	0
4 MHV	48	4,800,000	10	0.2083333
MHV Total	84	8,400,000	12	0.142857

Table 2B Statistical Analysis of Translocation Data

	Translocation	No Translocation
Vector	29	55
MHV	12	72
Total	41	127

Fischer's Exact Test P=0.0037

4.5 Viral UNGs Suppress AID Induced Reversion Mutation in NTZ-3T3 Reporter Cell

Line

The NTZ-3T3 reporter cell line system contains a GFP exon driven by a CMV promoter, however the GFP contains a premature STOP codon that prevents protein translation. If the cells are exposed to a mutagen such as AID, a small number of cells will be mutated at the STOP codon leading to GFP expression (Fig. 25). The percentage of cells that revert the GFP STOP codon can then be measured by FACS analysis. This system has been utilized by other groups to study the effect of mutations on AID function, however we used the NTZ-3T3 system in order to test for the ability of viral UNGs to suppress AID mediated mutations in the host genome (McBride, 2006).

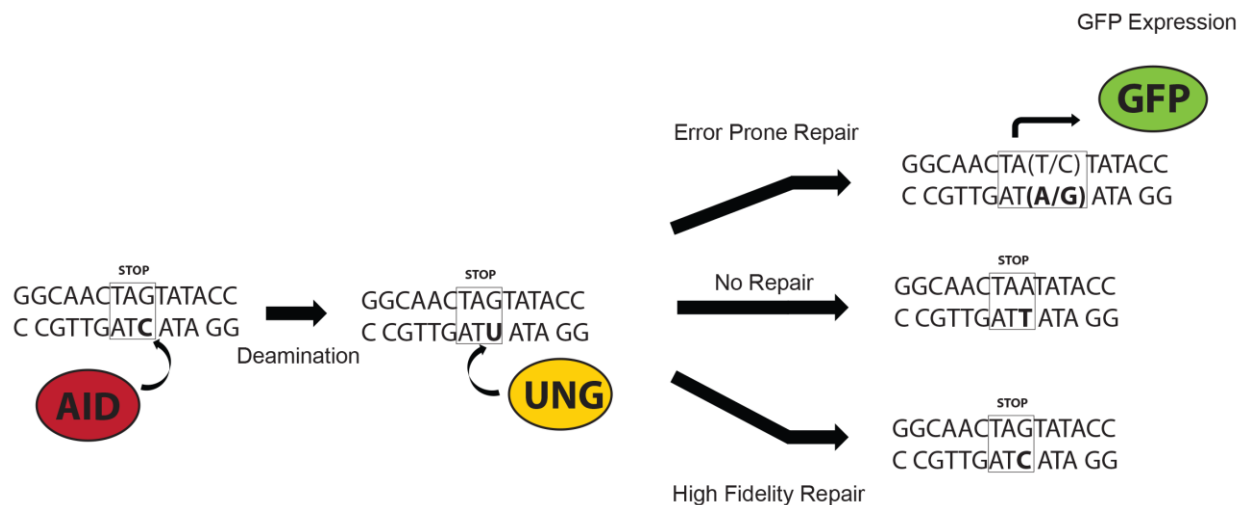


Figure 25

Error Prone Repair at the GFP-STOP Codon in NTZ-3T3 Cells is Needed to Initiate GFP Transcription After AID Deamination

After expression AID is able to deaminate the cytosine to uracil in the complementary strand opposite the STOP codon **TAG**. If the site is left unrepaired DNA polymerase will read the uracil as a thymine leading to adenine being placed in opposite strand giving a codon of **TAA**, which is still a STOP codon. If UNG recognizes the U:G mismatch, removes the base and triggers the high fidelity base excision repair pathway, the uracil is returned to a cytosine maintaining the STOP codon. However if the U:G mismatch is repaired in such a way that replaces the uracil with an adenine or a guanine, then transcription of GFP will occur driven by the CMV promoter.

To test this we infected NTZ-3T3 cells with virus containing pMX- Δ GFP vector containing viral UNG. After 48 hours the cells are subjected to puromycin selection, the cells were then placed in tetracycline free media, and then infected with virus containing pMX AID-BFP or pMX AID-mCherry. The day of AID infection is considered to be the start (day zero) of the assay (Fig. 26). The cells were kept at a low density and passaged at regular intervals, during the passaging cells are taken and measured by FACS analysis at regular intervals to measure the rate of GFP reversion. The results show that when expressed with AID all of the viral UNGs tested were able to suppress AID induced reversion mutations in NTZ-3T3 cells at comparable efficiency (Fig. 29). Over the course of the assay cells expressing AID alone show a steady increase in reversion percentage, while cells expressing any of the viral UNGs with AID show a significant reduction in the number of reverted cells (Fig. 27), (Fig. 28). From these results we can conclude that viral UNGs are fully capable of repairing AID induced deamination mutations in the host genome. Future sequencing analysis of the GFP gene will reveal if the presence of viral UNG influences the spectrum of mutations present.

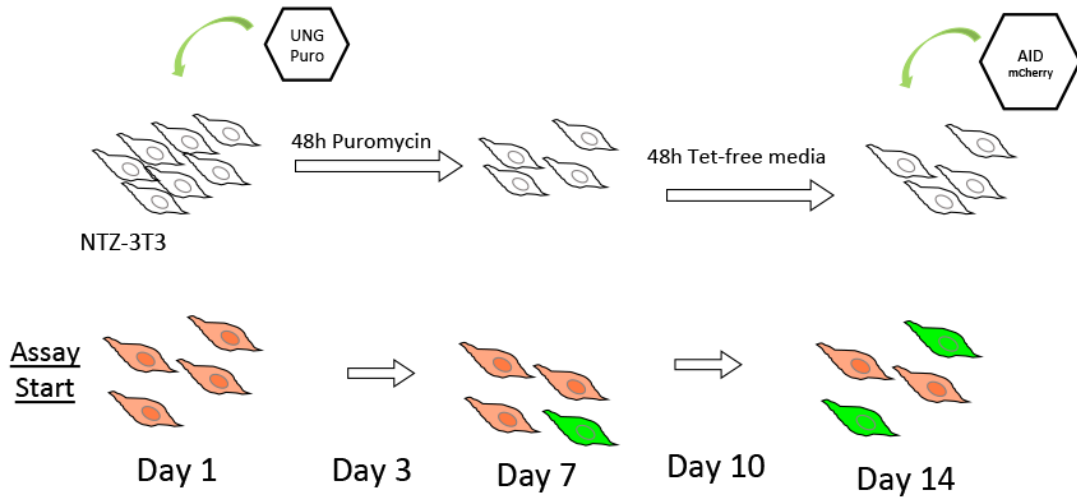


Figure 26

NTZ-3T3 Experimental Time Line

NTZ-3T3 cells are transduced with retrovirus containing pMX-vUNG, the cells are then selected for pMX expression for 48 hours using puromycin, then placed in tetracycline free media. The selected cell are then transduced with pMX AID-BFP or pMX-AID-mCherry containing retrovirus, which is considered day 0 of the assay. The cell are then passaged and scanned at regular intervals to test for GFP reversion.

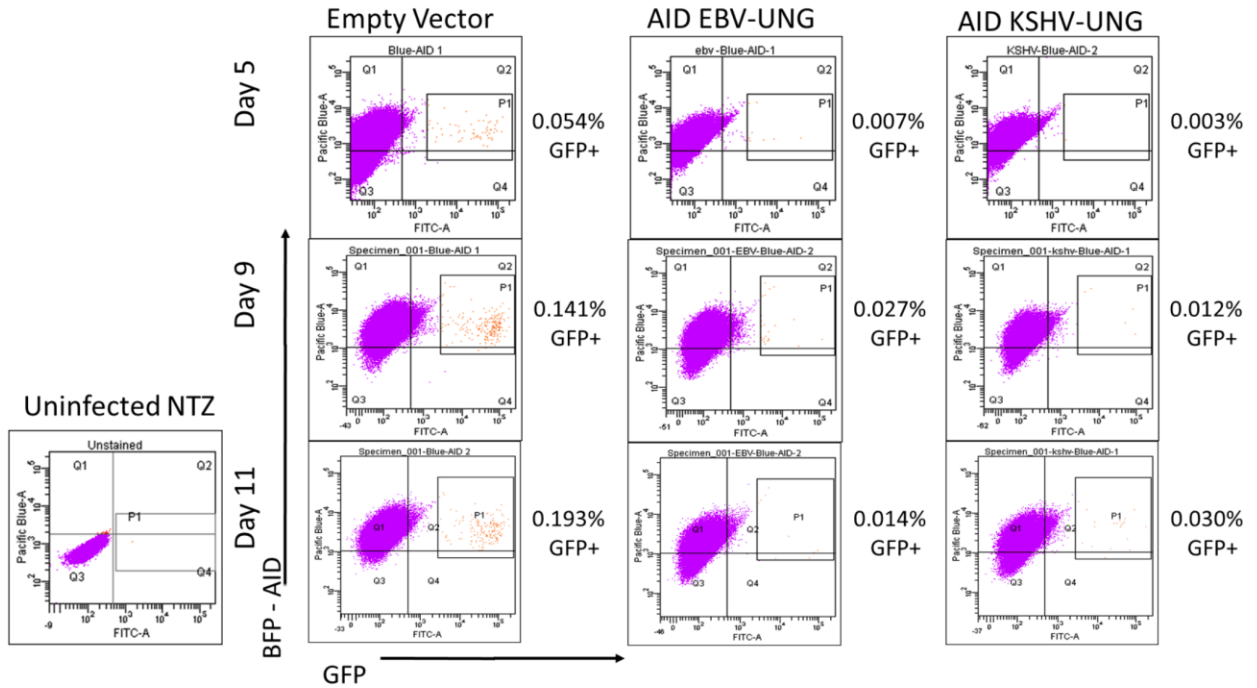
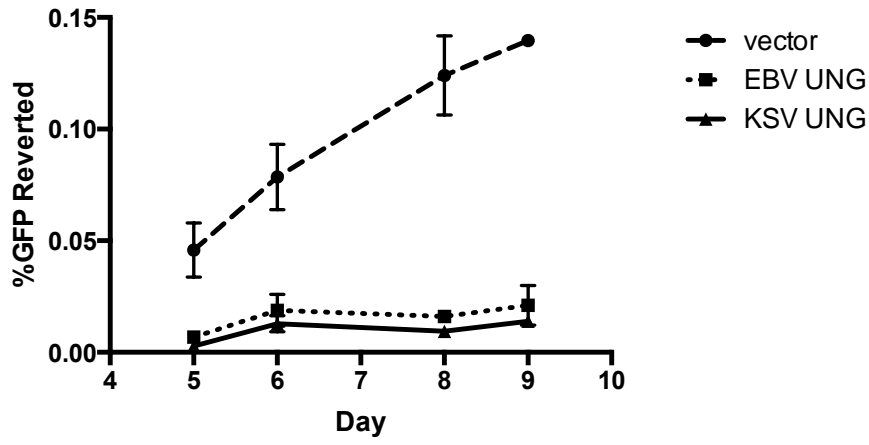


Figure 27

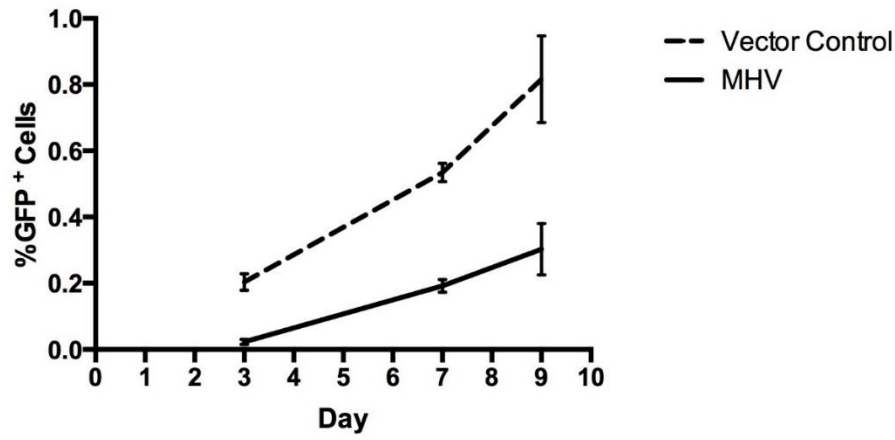
EBV-UNG and KSV-UNG Suppress AID Induced GFP Reversion Rates in NTZ-3T3 Cells Over Time

NTZ-3T3 cells infected with pMX AID-BFP and pMX EBV-UNG or pMX KSV-UNG were trypsinized and passaged at regular intervals. Representative FACS plots of cells expressing pMX-AID BFP and for the presence of GFP+ reverted cells. NTZ cells expressing pMX AID-BFP show an increase in the percentage of reverted cells from 0.054% to 0.193% over six day period. Cells expressing pMX EBV-UNG and pMX AID-BFP showed a reduction in the rate of GFP reversion from 0.007% to 0.014% over a six day period, and cells expressing pMX AID-BFP with pMX KSV-UNG showed a reduction in the rate of GFP reversion from 0.003% to 0.03% over the course of six days.

A



NTZ GFP Reversion



B



Figure 28

Expression of Viral UNGs in NTZ-3T3 Cells Suppresses GFP Reversion

(A) Graph of the reversion rates of NTZ-3T3 cells. Cells expressing EBV-UNG, KSV-UNG, or MHV-UNG showed a significant reduction in GFP reversion frequency compared to AID only controls. NTZ-3T3 cells were infected with pMX EBV-UNG, pMX KSV-UNG, pMX MHV-UNG or empty pMX control and selected using puromycin. After selection cells were infected with AID-BFP or AID-mCherry, cells were then trypsonized and scanned by FACS at various time points in order to measure reversion rates. (B) An image of a reverted NTZ-3T3 cells expressing GFP.

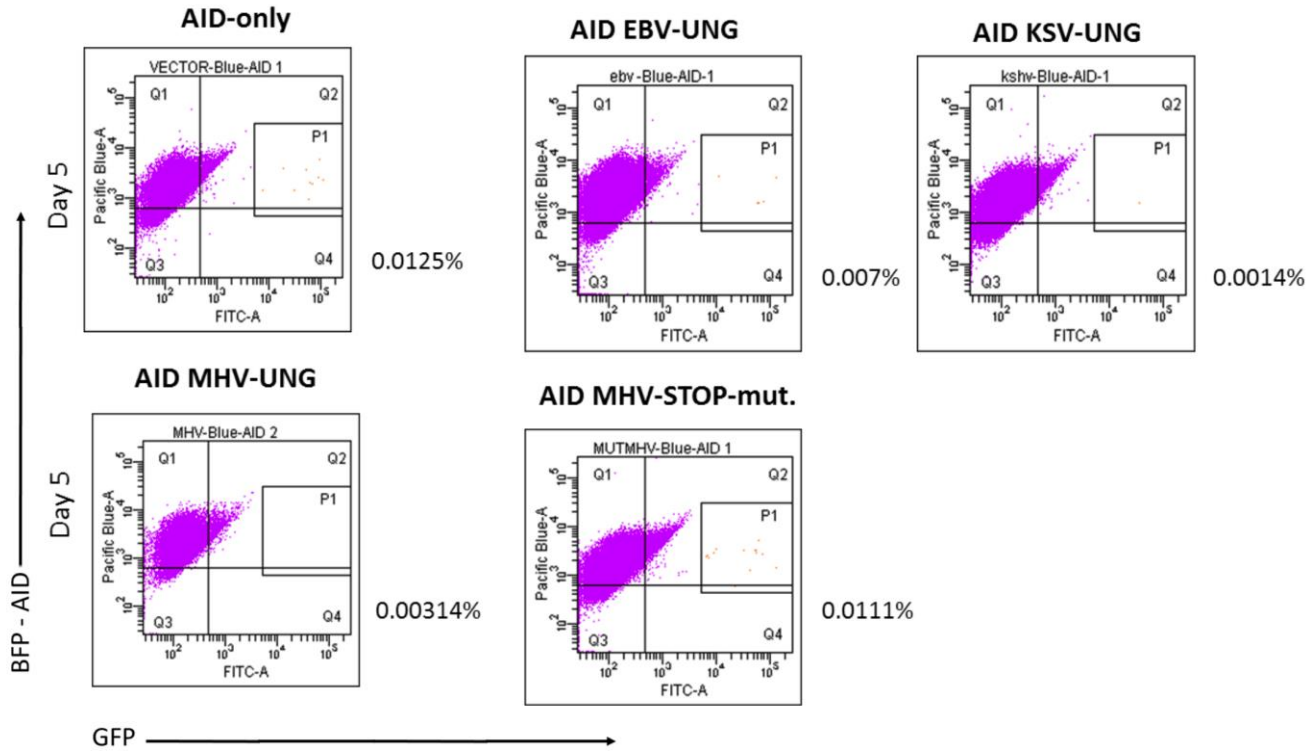


Figure 29

EBV-UNG, KSV-UNG and MHV-UNG all Suppress AID Induced GFP Reversion in NTZ-3T3 Cells

NTZ-3T3 cells infected with pMX AID-BFP and pMX EBV-UNG or pMX KSV-UNG or pMX-MHV were trypsinized and measured after 5 days. Representative FACS plots of cells expressing pMX-AID BFP and for the presence of GFP+ reverted cells. Cells expressing AID only had a reversion rate of 0.0125% while cells expressing EBV-UNG, KSV-UNG or MHV-UNG showed reduced reversion percentages. Cells expressing the truncated pMX-MHV-STOP showed similar reversion rates to the Empty vector control.

4.6 Chapter 4 Summary

During the course of our research we discovered a novel virus-host interaction mechanism. The action of viral UNG on host DNA may be an important mechanism for the survival and propagation of the herpes virus in host B-cells, as well as having implications for the development of herpes virus associated B-cell lymphomas. The expression of viral UNGs in *Ung*^{-/-} mouse B-cells was able to compensate for host UNG in the CSR process. However when expressed in wild-type mouse B-cells viral UNGs reduced CSR efficiency, demonstrating the importance of UNG levels in CSR process. Intriguingly we discovered that UNG catalytic activity is not necessary for this suppression of CSR efficiency, suggesting a potential UNG protein-scaffolding mechanism is responsible for this effect. We also discovered that the action of viral UNG on the host genome can reduce the frequency of oncogenic translocations and genomic instability, implying that viral UNG maybe playing an active role in preserving the integrity of the host cell genome. We also measured the ability of viral UNG to suppress AID generated mutations in the NTZ-3T3 indicator cell line. Later DNA sequencing analysis of these cells will allow us to determine if viral UNG alters the spectrum of mutations present in the cells, which may provide potential insight into how error prone repair of genomic uracils is triggered.

Chapter 5 - Materials and Methods

5.1 Antibodies and Reagents

- Anti-FLAG M2 antibody was used for western blots (Sigma-Aldrich, St. Louis, MO. Catalog #F3165).
- APC-rat anti mouse IgG-APC(BD pharmagen, Franklin Lakes, NJ, Catalog# 560089) was used for CSR assays.
- Anti-FLAG M2 Affinity Agaros Gel Beads (Sigma-Aldrich, St. Louis, MO. Catalog #A2220).
- Lipopolysaccharides (LPS) from *Escherichia coli* (Sigma-Aldrich, St. Louis, MO. Catalog #L2630).
- Mouse Interleukin-4 (Sigma-Aldrich, St. Louis, MO. Catalog #I1020)
- MACS anti-CD43 (Ly-48) MicroBeads (Miltenyi Biotech, San Diego, CA, Catalog# 130-049-801)
- Rabbit anti-mAID antibody 30F12 (Cell Signaling Technology, Danvers, MA, Catalog #4949)
- Goat anti-SH3BP2 antibody N-18 (Santa Cruz Bio, Dallas, TX, Catalog # sc-113954)
- Goat anti-SH3BP2 antibody C-19 (Santa Cruz Bio, Dallas, TX, Catalog # sc-8897)
- Pfu turbo DNA polymerase AD (Agilent technologies, Santa Cruz, CA. Catalog #600255).
- PI3K inhibitor LY294002 (Sigma-Aldrich, St. Louis, MO. Catalog #L9908)

5.2 Experimental Methods

Primary Splenocyte isolation

Adult mice at least six weeks of age are sacrificed, their spleens are then surgically removed and placed into a 15ml conical tube containing 5ml of phosphate buffered saline (PBS) which are then kept on ice. The spleens and PBS are then transferred to a 10cm plate inside a sterile tissue culture hood. The spleens are then placed into a 40µm nylon filter (Fischer Scientific, Waltham, MA, Catalog# 08-771-2) where they are crushed and presses through the filter using the plunger from a sterile 5ml syringe (BD pharmagen, Franklin Lakes, NJ, Catalog# 309647). The filter containing the solid spleen tissue is then discarded, and the PBS containing the primary splenocytes is transferred to a 15ml conical tube and spun at 1500RMP for 5min to pellet the cells. The majority of the PBS is aspirated off of the cell pellet, the conical tube is then raked across a tube rack in order to re-suspend the splenocyte cell pellet. 1ml of Ammonium-Chloride-Potassium (ACK) red blood cell lysis buffer is then added to the re-suspended splenocytes and allowed to incubate for 1min at room temperature. The lysis reaction is then neutralized by adding 10ml of PBS to the tube and gently mixing. The contents of the tube is then filtered through a 40µm nylon filter to separate the freely floating leukocytes from the coagulated cell debris, and placed into a new 15ml conical tube. The tube is then spun at 2300RPM for 5min in order to pellet the primary leukocytes. The cells are then re-suspended in 10ml of PBS and counted.

Isolation of naïve CD43- B-cells by magnetic activated cell sorting

Purified primary leukocytes in PBS are spun at 1500PRM for 5min in a conical tube. The cells are then resuspended at density of in 1×10^7 cells per 900µl of PBS, and 100µl of MACS anti-CD43 beads (Miltenyi Biotech, San Diago, CA, Catalog# 130-049-801) are

added and incubated with the cells on ice for 20min, with occasional mixing to prevent cell precipitation. For every 1×10^7 cells one MACS-MS column (Miltenyi Biotech, San Diego, CA, catalog # 130-042-201) is placed on a MACS magnet and stand (Miltenyi Biotech, San Diego, CA, Catalog# 130-042-108) in a sterile tissue culture hood. The MACS -MS column is washed with 1ml of cold PBS 1% FBS. To wash the cells 10ml of cold PBS is added to the tube, and it is spun at 1500RPM for 5min, the supernatant is removed and the cells are resuspended in 1ml of cold PBS 1% FBS. The resuspended cells are then added to the pre-washed MACS column, the CD43- cells that pass through the column and are collected in a new 15ml conical tube. After the flow has stopped an additional 1-2ml of PBS 1% FBS is added to the column and collected in order to collect any cells remaining in the column. The CD34- cells are then counted with a hemocytometer for plating.

Primary Mouse B-cell culture

Primary mouse B-cells are cultured at a density of 200×10^5 to 1×10^6 cells per ml in B-cell media, which consists of Roswell Park Memorial Institute media (RPMI) (Sigma-Aldrich, St. Louis, MO. Catalog #R8758) with 10% Fetal Bovine Serum (FBS) (Sigma-Aldrich, St. Louis, MO. Catalog# F6178), 1% Penicillin-Streptomycin (Sigma-Aldrich, St. Louis, MO. Catalog #P4333) 10 mM HEPES (Sigma-Aldrich, St. Louis, MO. Catalog # H0887) 10mM sodium Pyruvate (Sigma-Aldrich, St. Louis, MO. Catalog #S8636) 50 μ M 2-mercaptanol (Sigma-Aldrich, St. Louis, MO. Catalog #M3148) mouse interleukin-4 (IL-4) at 10 μ g/ μ l (Sigma-Aldrich, St. Louis, MO. Catalog# I1020) Lipopolysaccharide (LPS) at 25 μ g/ml (Sigma-Aldrich, St. Louis, MO. Catalog# L2630).

Retrovirus Production from BOSC23 cells

BOSC23 cells are grown and maintained in Dulbecco's Modified Eagle Medium (Sigma-Aldrich, St. Louis, MO. Catalog #5796) (DMEM), 10% FBS (Sigma-Aldrich, St. Louis, MO. Catalog# F6178), 1% Penicillin-Streptomycin. The BOSC23 cells are plated in a 6 well plate in 2ml of media at a density of 200-250 x10⁵ cells per well. 12-20 hours after plating the cells are transfected with pCL-ECO and PMX using the Jet-prime transfection reagent manufacturer's protocol (Polyplus, Illkirch, France, catalog#114-07)

The media on the BOSC23 viral packaging cells is changed 12 to 24 hours after Jet-prime transfection. Retrovirus containing supernatant is collected from the plate using a 5ml syringe, and then filtered through a 0.45µm low protein binding nitrocellulose filter (Millipore, Billerica, MA catalog#SLHV033RS). The virus can be used immediately, or aliquoted into 2ml Eppendorf tubes, and flash frozen on dry ice. Retrovirus containing supernatant is collected at 48 hours, 60 hours, 72 hours, and 84 hours after the initial transfection. The Frozen retro-viral supernatant is then stored at -80c for later use.

B-cell infection

Purified -CD43 mouse B-cells are plated in a 10cm plate at a density of 1 x 10⁶ cells per ml for 12-18 hours. The cells are then plated in a six well plate at a density of 1x10⁶ cells per ml in 1ml of B-cell media. 1ml of virus is the added to each well, along with 25µg/µl of LPS, 10µg/µl of IL-4, 40µg/ml 1M HEPES, and 2µl Polybrene (10mM) (Millipore, Billerica, MA catalog# TR-1003-G). The cells are then spun at 1150g for 90min at room temperature, then incubated at 37c for 12-24 hours, then 1ml of media is gently removed from the top of each well, and replaced with B-cell media.

Class Switch Recombination Assay

The infected B-cells counted daily and kept at a density of 5×10^5 per ml. At day 3 and day 4 post viral infection 1×10^6 cells are removed, transferred to a 1.5ml Eppendorf tube, pelleted at 1500RPM and washed with 1ml of PBS 1% FBS. The cells are pelleted at 1500RPM and resuspended in 200 μ l PBS 1% FBS containing 1:1000 Rat anti-mouse IgG1-APC (BD pharmagen, Franklin Lakes, NJ, catalog# 560089). The cells are stained for 20min at room temperature. The cells are then washed with by adding 1ml of PBS 1% FBS, then pelleted at 1500RPM. The cells are then resuspended in 500 μ l of PBS 1% FBS transferred to a 5ml FACS tube, and kept on ice. The cells are then scanned on a BD LSR Fortessa fluorescent cell analysis system.

IgG-cMYC Translocation Assay

30×10^6 B-cells are infected per group with retrovirus, counted daily and kept at a density of 5×10^5 per ml in 10cm plates. At day 3 post viral infection the cells are collected into a 50ml conical tube, washed with PBS and then resuspended in 4ml of PBS 1% FBS. The cells are then transferred to a 4ml BD FACS tube scanned on a BD ARIA Fusion III FACS sorter. Virally infected GFP positive cells are then sorted into a collection 15ml collection tube containing 2ml of FBS.

To extract genomic DNA the cells are then washed with PBS, and pelleted at 1500RPM, then transferred to a 1.5ml Eppendorf tube and lysed with 200 μ l of SDS Protease K digestion (Fisher scientific, Pittsburg, PA catalog# EO0491) buffer for at 12 hours at 55c. 500l of phenol is added to the tube. It is then vortexed and spun at 15000RPM (or maximum speed). The aqueous (top) layer is then removed and transferred to a new 1.5ml Eppendorf tube. The DNA is then precipitated by adding 1ml of cold ethanol to the

tube, which is then incubated on ice for 10min and spun at 15000RPM for 5min. The majority of the ethanol is carefully removed, and 1ml of 70% ethanol 30% water is then added and gently mixed to wash the DNA pellet. The tube is again spun at 15000rpm for 5min, and the majority of the liquid is carefully removed. To dry the DNA pellet completely the tubes are left open over night at room temperature. The dry DNA pellet is then dissolved in 100µl of nuclease free water, and the concentration is measured using a nanodrop 2000 (Thermo scientific).

Translocation PCR

Translocations are amplified using the Expand Long Range PCR System (Roche). 50µl Nested PCR reactions were performed using 5µl of buffer 1, 350µM of dNTPs, and 500ng of purified B-cell genomic DNA. The following derivative chromosome-15 primers were used for the first round reactions, 5'-ACTATGCTATGGACTACTGGGGTCAAG-3' and 5' -GTGAAAACCGACTGTGGCCCTGGAA-3'. Cycling conditions for the first round PCR were 29 cycles total with the first 10 cycles being 92c 10s, 60c 30s, 68c 7min. Followed by 19 cycles of 92c 10s, 60c 30s+20s each additional cycle, 68c 7min. First round PCR reactions are checked for completion on a 1% agarose gel.

1µl of first round PCR reaction is used as the template for the second round PCR, and derivative chromosome-15 primers 5'-CCTCAGTCACCGTCTCCTCAGGTA-3' and 5'-GTGGAGGTGTATGGGGTGTAGAC-3'. Cycling conditions for the second round PCR were 25 cycles total with 10 cycles of 92c 10s, 60c 30s, 68c 4min, followed by 15 cycles at 92c 15s, 60c 30s+20s per cycle, 68c 4min. Second round PCR reactions are checked for completion on a 1% agarose gel, and transferred to a nylon membrane for southern probing.

Southern Probe for IgG cMYC Translocations

Second round translocation PCRs are run on a 1.1% agarose gel at 150v. The gel is then visualized using a UV box to ensure that the second PCR worked. The gel is then placed into a bath of denature buffer (1.5 M NaCl, 0.5 M NaOH) for 30min with gentle agitation, then washed 2X with ddH₂O, then placed in a bath of neutralization buffer (1.5 M NaCl, 0.5 M Tris-HCL, 1 mM EDTA) for 30min with gentle agitation.

To transfer the DNA to the membrane a tub is then filled with paper towels or a large sponge and soaked in 20XSSC buffer, the level of buffer should not be higher than the height of the towels. A whatman filter is placed on the top of the paper towel stack. The gel is then carefully placed on the whatman and a nylon membrane is placed on top of the gel. 3 to 4 more whatmans are placed on top of the membrane, and a large stack of dry paper towels is placed on top. A large flat weight is then balanced on top of the stack, the whole apparatus is covered in cellophane wrap to prevent dehydration. The transfer apparatus is left at room temperature overnight to allow for complete transfer. After the transfer is complete the apparatus is dismantled, the membrane is then washed with 2X SSC buffer for 5min and dabbed dry with a new whatman, and then placed in to a UV cross-linker for 3min to bind the DNA to the membrane. The membrane is prepared for hybridization by incubating in 10ml of hybridization buffer (50ml formamide, 25ml 0.5M NaH₂PO₄, 15ml H₂O, 5ml 5M NaCl, 7.0g SDS) with 200l of salmon sperm DNA (100X) in a hybridization tube at 55c for at least 1 hour. 1ml of buffer is removed from the tube and 600ng of probe is added to it, the diluted probe is then added back into the tube. The membrane is probed with either a biotinylated probe against cMYC (cMYC-15 Probe

3'-GGA CTGCGCAGGGAGACCTACAGGGG-5') or against IGH (IGH-15 Probe 3'-CCTGGTATACAGGACGAACTGCAGCAG-5') probe is added and incubated at 55c with

rotation overnight. Remove the blot from the tube and wash it 2XSSC+0.1%SDS for 20min three times at 55c. The membrane is then incubated with blocking buffer (Casin, 1XTBST) for 15min, then incubated with 70µl of streptavidin-HRP (300X) for 15min. The membrane is then washed 4X with wash buffer (100mM Tris pH7.5, 150mM NaCl, 0.05% SDS) for 5min, and then put into equilibration buffer (100mM Tris pH9.5, 150mM NaCl) for 5min. To visualize the membrane excess buffer is removed, and 5ml of ECL is added, the membrane is then placed into a cassette and exposed to a film in a dark room.

NTZ-3T3 Reversion Assay

NTZ-3T3 cells are maintained in DMEM with 10% FBS, and 1% Penicillin-Streptomycin. Prior to the start of the experiment the cells are selected by treating with G418 at 1500µg/ml and Zeocin at 300µg/ml for 14 days. Cells are then removed from selection pressure for at least 48 hours before starting the assay. To start the assay 1-2 x 10⁶ NTZ-3T3 cells are plated in a 10cm plate with 8ml of media, 12-20 hours later the cells are infected with pMX-UNG-ΔGFP or pMX-ΔGFP by adding 2ml of retrovirus containing supernatant and 10µl of Polybrene (10µg/ml). To select for pMX expressing cells, 48 hours after infection the media is changed and the cells are treated with 4µg/ml puromycin (Sanata Cruz Bio, Dallas, TX, catalog #sc-108071) for 48 hours. An uninfected NTZ-3T3 control plate is also treated with puromycin to ensure that uninfected cells are killed efficiently. The media is then changed to remove the cells from selection for at least 24 hours, the cells are then passaged and replated in a 10cm plate at a density of 1-2 x 10⁶ cells per plate in 8ml of DMEM. 12-20 hours later the cells are infected with pMX-AID-mCherry 2ml of retrovirus containing supernatant and 10µl of Polybrene (10µg/ml). The addition of AID virus is considered to be Day 0, the starting point of the assay. The cells are then passaged at a sub-confluent cell density and tested for GFP reversion on day 3 or 4, day 6 or 7, day 9 or

10, day 11 or 12. To measure the percentage of GFP positive reverted cells at the aforementioned time points, 1×10^6 trypsinized cells placed into a 4ml BD FACS tube, washed with PBS 1%FBS, then resuspended with 1ml of PBS 1%FBS and scanned by a BD Aria Fusion III Flow Cytometer to test for GFP expression. At the final time point of the assay mCherry positive AID expressing cells are sorted by fluorescence activated cell sorting, and collected in 15ml conical tube containing 2ml of FBS.

NTZ-3T3 Mutational Analysis

Genomic DNA Extraction

To extract genomic DNA the cells are then washed with 8ml of PBS, and pelleted at 1500RPM, then transferred to a 1.5ml Eppendorf tube and lysed with 200 μ l of SDS Protease K digestion buffer overnight at 55c. 500 μ l of phenol is added to the tube. It is then vortexed and spun at 15000RPM (or maximum speed). The aqueous (top) layer is then removed and transferred to a new 1.5ml Eppendorf tube. The DNA is then precipitated by adding 1ml of cold ethanol to the tube, which is then incubated on ice for 10min and spun at 15000RPM for 5min. The majority of the ethanol is carefully removed, and 1ml of 70% ethanol 30% water is then added and gently mixed to wash the DNA pellet. The tube is again spun at 15000rpm for 5min, and the majority of the liquid is carefully removed. To dry the DNA pellet completely the tubes are left open over night at room temperature. The dry DNA pellet is then dissolved in 100 μ l of nuclease free water, and the concentration is measured using a nanodrop 2000.

cDNA Synthesis

cDNA library generation for the cloning of genes was done using a SuperScript IV Reverse Transcriptase Kit (Lifetechnologies, Waltham, MA, Catalog # 18090010) according to the manufacturers protocol.

High Fidelity PCR

For every 20µl PCR reaction 100ng of NTZ genomic DNA is used. Along with 100ng of forward primer CMVP-F TGACCTCCATAGAAGACACCCT and reverse primer tetGFP –R TTATGTTTCAGGTTTCAGGGGG. 100µM dNTPs, 2µl 10x Cloned Pfu AD reaction buffer, and 1µl Pfu turbo DNA polymerase AD (Agilent technologies, Santa Cruz, CA. Catalog #600255). Cycling conditions for the reaction are as follows 1X 94c 4min, 28X 94c 30s, 57c 30s, 72c 60s, 1X 72c for 4min. To add a Adenosine to the 3' end the PCR product, 1µl of Taq polymerase (Sigma-Aldrich, St. Louis, MO. Catalog #D1806) is added to the finished PCR reaction and then it is incubated at 72c for 10min.

The PCR reactions is then run on a 1% agarose gel with 1µl/ml ethidium bromide. To obtain pure GFP amplicons, PCR bands at 714bp are cut from the gel using a sterile razor blade, and then digested using a GeneElute gel extraction kit (Sigma-Aldrich, St. Louis, MO. Catalog # NA1111), and resuspended in nuclease free water.

TOPO-TA Cloning and DNA Sequencing

To isolate unique sequence clones for mutational analysis, purified GFP PCR products were ligated into a plasmid vector for sequencing using a TOPO-TA cloning kit (Lifetechnologies, Waltham, MA, catalog # 450071). To ligate the PCR product into the

vector 2µl of purified PCR product is combined with 2µl of nuclease free water, 1µl of manufacturer supplied salt solution, and 1µl of Topo vector solution. The reactions is incubated for 10 minutes at room temperature, then placed on ice. 50µl of mach-1 competent *e.coli* cells are allowed to thaw on ice. 5µl of the TOPO ligation reaction is added to the mach-1 *e.coli* cells and incubated on ice for 20min. The tube is then heat shocked for 30s at 37c, and placed on ice for 5 min. 200µl of SOCS media is added to the tube, and it is placed in a 37c shaking incubator for 1 hour. 100µl of the Mach-1 cells in media is spread on a LB agar plate containing 100µg/ml ampicillin. The plates are then incubated 12-24 hours at 37c. Individual colonies are then picked using sterile pipet tips, placed in 10ml falcon tubes, and incubated with 2ml of LB with 100µg/ml ampicillin at 37c with agitation overnight.

Topo plasmids are isolated from the overnight cultures using a GenElute plasmid miniprep kit (Sigma-Aldrich, St. Louis, MO. Catalog #PLN70). Topo plasmids are then resuspended in nuclease free water and their concentration is quantified using a nanodrop. To analyze mutations plasmids are then sent to a sequencing core for Sanger sequencing using M13 Forward primer 5'-GTAAAACGACGGCCAG-3' and M13 Reverse primer 5'-CAGGAAACAGCTATGAC-3'.

Site Directed Mutagenesis

20ng of mUNG or MHV-UNG in the pDUET plasmid were amplified by 0.5 µl of 25µM each specific primer pair needed to mutate a specific amino acid to generate catalytically inactive UNGs mixed with 5µl of 10X pfu turbo buffer, 1ul of 10mM dNTP mix, 1µl of pfu turbo enzyme, and ddH2O to 50µl. The reaction conditions were as follows 18X 94c for 30 seconds, 55c for 1 minute, and 68c for 2 minutes. PCR reactions are then treated with 11 DpnI for 1 hour at 37c. 2-10µl of each digested PCR reaction is then used to transform

competent *e.coli* cells, which are then streak plated to produce single colonies. Individual clones are analyzed by sequencing for the presence of the mutation. Once a vector has successfully taken up a mutation, the vector is subjected to a second round of site directed mutagenesis with the other primer pair and screened to produce a vector that possesses both desired mutations (Fig. 21). The sequences of the primers used to generate the mutations are as follows:

mUNG D147N-F

5'-GGTTGTCATTCTGGGACAGaATCCCTATCACGGACCTAAT-3'

mUNG D147N-R

'5-ATTAGGTCCGTGATAGGGATtCTGTCCCAGAATGACAACC-3'

mUNG H270L-F

'5-CACCATGTCCTGCAGACAGCTtCCCCTCCCCGCTGTCCGGTG-3'

mUNG H270L-R

'5-CACCGACAGCGGGGAGGGGgAGAGCTGTCTGCAGGACATGGTG-3'

MHV68 D85N-F

'5-GTTGTTATTCTGGGACAGaATCCCTATCATGGGGGCCAGGCC-3'

MHV68 D85N-R

'5-GGCCTGGCCCCCATGATAGGGATtCTGTCCCAGAATAACAAC-3'

MHV68 H207L-F

'5-CATCTTGTATTAAGGCGCAACtTCCTTCCCCCTGGCATCTC-3'

MHV68 H207L-R

'5-GAGATGCCAGGGGGGAAGGAaGTTGCGCCTTTAATACAAGATG-3'

Cell Lysis and SDS-PAGE

Frozen cell pellets are thawed on ice and resuspended in cold RIPA with protease inhibitors (Roche, Indianapolis, IN, catalog# 04693116001) pipetted to insure complete resuspension of the pellet. The suspension is then transferred to a pre-chilled 1.5ml Eppendorf tube, and placed on a rocker at 4c for 10min. The tubes are then spun at 14,000 RPM for 5min at 4c, the supernatant is removed and placed into a new pre-chilled 1.5ml Eppendorf tube on ice. The concentration of protein is then measured using a BCA protein quantification kit (Fisher scientific, Pittsburg, PA catalog # 23228). Protein lysates are then either stored at -80c or prepared for gel loading. 40g of protein per lane is mixed with 4X NuPAGE LDS Sample Buffer (Lifetechnologies, Waltham, MA, Catalog # NP0007) 3µl of NuPAGE sample reducing agent (Lifetechnologies, Waltham, MA, Catalog # NP0009) and RIPA buffer to a final volume of 30µl and mixed, then heated to at 70c for 10min. After heating the samples are loaded onto a 12% Bis-Tris gel (Lifetechnologies, Waltham, MA, Catalog # GB00125) with 20X MOPS SDS running buffer (Lifetechnologies, Waltham, MA, Catalog # NP0001), along with 20µl of Benchmark protein ladder for protein mass reference (Lifetechnologies, Waltham, MA, Catalog # NP10747-012). Once the gel is fully loaded it is run at 50mAmps for 40min or until the dye reaches the bottom of the gel.

Gel to Membrane Protein Transfer

Once the Bis-Tris gel is finished running it is carefully removed from its plastic casing and washed with Tobin's buffer (25mM Tris, 192mM glycine, 10% methanol) the gel is then placed onto a PVDF membrane that has been incubated in methanol. The gel and membrane are then placed between two towbin's soaked sponges, placed into a plastic cassette and then placed into a XCell Transfer tank (Lifetechnologies, Waltham, MA, Catalog #EI9051) containing cold tobin's buffer. The proteins are then transferred to the PVDF membrane at 400m Amps for 25min.

Western Blot

After the transfer the membrane is washed 3X in TBST (TBS 10% Tween 20), and block with 5% milk 2% BSA in TBST on a rocker for 1 hour. The membrane is then washed again with 3X with TBST. The membrane is incubated with primary antibody in 5% milk 2% BSA for 1 to 12 hours, then washed 3X with TBST for 20 min. The membrane is then incubated in secondary antibody for 30-60min in 5% milk and 2% BSA. Then the membrane is washed with TBST 3X for 20min. To visualize the membrane it is exposed to 5ml of ECL plus (Fischer Scientific, Waltham, MA, Cataloge#32132). After 1 minute of ECL exposure the membrane is drained of excess ECL, wrapped in cellophane, taped into a cassette. Films are exposed to the membrane in a dark room for 10s to 2 hours.

Two Dimensional Gel Analysis

Proteins were purified and prepared for analysis using methods previously published (Shen, 2007). Proteins were separated by isoelectric point on a pH 3-10 immobilized pH

gradient strip (Biorad laboratories, Philadelphia, PA Catalog# 163-2032), Then separated on a Criterion polyacrylamide gel (Biorad laboratories, Philadelphia, PA Catalog# 345-0127) before transferring to a nitrocellulose membrane and blotting with an anti-AID antibody (Cell Signaling Technology, Danvers, MA, Catalog #4949) one hour to overnight.

FLAG Immuno-Precipitation

After cell lysis with RIPA buffer, 1-1.5ml of cold protein lysate is combined with 20 μ l of Anti-FLAG M2 affinity agaros Gel Beads (Sigma-Aldrich, St. Louis, MO. Catalog #A2220) and incubated with rotation at 4c for 1 to 12 hours. The beads are then washed 3X with RIPA to remove non-precipitated proteins. To remove the bound protein from the beads they are then mixed with 4X NuPAGE LDS Sample Buffer (Lifetechnologies, Waltham, MA, Catalog # NP0007) 3 μ l of NuPAGE sample reducing agent (Lifetechnologies, Waltham, MA, Catalog # NP0009) and RIPA buffer to a final volume of 30 μ l and mixed, then heated to at 70c for 10min. The precipitated lysates are then run on SDS-PAGE polyacrylamide gel, and transferred to a nitrocellulose membrane for immunoblotting.

Chapter 6 - Discussion

6.1 AID Phosphorylation

Our data, as well as the work of others, suggest that phosphorylation is a major mechanism for regulating the activity of AID. Our analysis demonstrates that chromatin associated AID is likely to be highly phosphorylated (Fig. 10). From these results we can conclude AID's phosphorylation state influences its ability to associate with chromatin and act on genomic DNA. There has been notable interest in the study of AID regulation by posttranslational modification, however the majority of research has focused on two phosphorylation sites S3 and S38 (Delker, 2009). While these two sites have been shown to be important in regulating the activity of AID in SHM and CSR, the signaling pathways that lead to AID phosphorylation are not fully understood. Other studies have suggested that protein kinase A (PKA) is capable of phosphorylating AID at S38, while our results demonstrate the PI-3 kinase (PI3K) pathway can lead to phosphorylation of AID at this site. These experiments should be interpreted cautiously though, since PI3K was able to regulate AID-S38 phosphorylation in 3T3 cells but not in B-cells (Fig. 17). The modification state of a protein can be complicated by a number of factors such as the phase of cell cycle, and external growth factors, and cell type. Future study is needed if we hope to understand the signaling pathways that regulate AID-S38 phosphorylation and their biological implications.

There are however many more post translational modification sites on AID such as T150 and Y184 that have yet to be studied in detail. Our data suggest that these two sites likely play a role in the regulation of AID in the CSR process (Fig. 13). How these sites modulate AID's involvement in CSR is still unclear. It is possible that these phosphorylation sites play a role in the ability of AID to interact with binding partners. This may be an important mechanism for regulating AID complex formation, catalytic activity or cellular localization.

The development of phospho-specific antibodies that recognize AID p-T150 or AID p-Y184 will serve as an indispensable tool to study the effects of AID phosphorylation in the future. While we have demonstrated their sensitivity and specificity (Fig. 11) the conditions necessary for detection of these AID phosphorylation events are difficult to resolve. We were able to stimulate AID-Y184 phosphorylation in mouse B-cells using NaVO_4 , a pan tyrosine phosphatase inhibitor, then detect its presence by immunoblot (Fig. 12). Previous studies had detected p-Y184 AID in mouse B-cells and our data confirms its presence (McBride, 2006). Future work will focus on the determining the conditions that induce Y184 AID phosphorylation. Exposing B-cells to stimulation such as small molecule inhibitors, Toll-like receptor stimulation, or interleukins may stimulate Y184 AID phosphorylation, providing insight into its role in cellular processes.

Perhaps the most informative model system for the study of AID phosphorylation would be a knock-in mouse model system where the endogenous *Aid* is replaced with *Aid* containing a point mutation that prevents phosphorylation at the site of interest. A knock-in *Aid-S38A* mouse has already been generated, and an *Aid-T150A* or *Aid-Y184F* knock-in mouse would provide great insight into the effect of these phosphorylation events *in vivo* (Cheng, 2009). B-cells from these mice could be isolated for *in vitro* CSR experiments, which would be less artificial than the viral transduction of AID in to *Aid*^{-/-} B-cells. To detect *in vivo* CSR defects, B-cells and serum from these mice could be analyzed for shifts in the distribution of antibody isotypes. V(D)J sequences of germinal center B-cell from these mice could be analyzed to detect defects in the SHM process. A transgenic model also has the potential to produce an unexpected phenotype, providing information about the effect of AID phosphorylation on physiological processes that would otherwise have remained unknown.

AID can be targeted to the V(D)J region or different switch regions of the Ig locus depending on the factors present. Because of this AID interacting proteins are of intense interest to the field. With the assistance of the Bedford lab, we were able to identify four

potential p-Y184 AID binding proteins using a protein domain array (Fig. 14) These proteins all contain a SH2 phospho-tyrosine binding domain, and two of them are themselves tyrosine kinases known to be involved in B-cell signal transduction pathways (Zipfel, 2000). A phosphorylation specific AID binding partner would be a novel discovery. This phospho-specific AID interaction could act as a mechanism to regulate AID's dynamic roles at the Ig locus. A unique signal, phosphorylation state, and phospho-AID complex to target AID to each specific location on the Ig locus. Moreover it is still not know why AID induced uracils in the Ig locus are repaired in a low fidelity manner. The phosphorylation state of AID, and the binding partners associated with it, may serve as a switch to attract error prone repair factors to the V(D)J locus.

Though mutation of the SH2 domain containing adaptor protein SH3BP2 is associated with bone deformities in humans, its deletion from the mouse genome produced an unexpected CSR phenotype, suggesting it may play a role in antibody diversification processes (Chen, 2007). We were able to clone and isolate SH3BP2 from stimulated mouse splenocyte cDNA, confirming its expression in B-cells. Using commercially available antibodies we were able to detect SH3BP2 by immunoblotting HEK cells expressing pMX-SH3BP2. However we were unable to detect SH3BP2 protein in lysates from stimulated mouse B-cells. These results suggest that the currently available SH3BP2 antibodies are unable to detect endogenous levels of SH3BP2. This limitation in sensitivity impeded our attempts to detect p-Y184 AID SH3BP2 interaction in cells.

One strategy to overcome this limitation in sensitivity would be to detect p-Y184 AID interaction with SH3BP2 using mass spectrometry. FLAG-AID expressing B-cells could be treated with NaVO_4 to prevent AID-Y184 dephosphorylation, then FLAG immuno-precipitated. Protein precipitates could then be analyzed by mass spectrometry to identify AID interacting proteins; these results would be compared to cells expressing FLAG-AID^{Y184F} in order to identify proteins that interact specifically with p-Y184 AID.

Although *Sh3bp2*^{-/-} mice exist they have not been thoroughly evaluated for defects in CSR or SHM. An *in vitro* CSR assay using *Sh3bp2*^{-/-} B-cells would confirm the previously reported CSR defect, and germinal center B-cells could have their V(D)J sequences analyzed for defects in SHM. *Sh3bp2*^{-/-} mice could also be crossed with other mouse lines such as AID^{Y184F} to determine if any detectable defects in B-cell processes are indeed do to its phospho dependent interaction with AID.

6.2 The Role of Herpes Virus UNG

Previously it had been suggested that DNA viruses encoded UNGs in order to protect their own genome from mutations caused by uracil incorporation. This has been demonstrated *in vivo* in at least two systems in HSV-1 and MHV68 (Pyles and Thompson, 1994) (Minkah, 2015) . However, it was not known if viral UNGs were able to act on the host genome and interfere with the action of host UNG. We have demonstrated viral UNGs are capable of acting on uracils incorporated into mammalian genomic DNA in 3T3 cells, as well as primary mouse B-cells. Not only are viral UNGs capable of eliminating uracils from genomic DNA and triggering the downstream high-fidelity BER pathway, but they are also capable of participating in complex antibody diversification processes in host B-cells.

When we introduced viral UNGs into *Ung*^{-/-} mouse B-cells using a retroviral delivery system all three of the viral UNGs tested, MHV68, EBV, and KSV were able to provide compensation for the lack of mouse UNG in *in vitro* CSR assays (Fig. 18). While it is possible that different viral UNGs may have differing levels of activity on the host genome, all of the viral UNGs tested were able to induce a similar level of switch in this assay. If there is any difference in the ability of these viral UNGs to induce CSR in *Ung*^{-/-} B-cells *in vitro* perhaps an experimental system that provides a lower level of UNG protein expression would be able to reveal this difference.

Our data demonstrates that when expressed in wild-type mammalian B-cells *in vitro* viral UNG interferes with the CSR process, reducing its efficiency (Fig. 19). This unexpected result demonstrates the importance UNG protein level in the CSR process. These data suggest that there is an optimal level of UNG expression needed for efficient CSR; not enough UNG and there will be little CSR, but too much UNG and switching efficiency will be reduced.

The association of EBV infection with Burkitt's lymphoma is well established and the contribution of EBV genes such as LMP-1 and LMP-2 to EBV associated malignancies has been heavily researched (Young and Rickinson, 2004). The discovery that viral UNGs may be involved the transformation process is completely novel. Our data suggests that viral UNG may protect the host genome from oncogenic translocations such as the IgH-cMyc translocation associated with Burkitt's lymphoma (Fig. 24). It is therefore possible that a loss or down regulation of herpes virus UNG may be needed before oncogenic translocations can occur. If herpes virus UNGs are indeed playing role in protecting the host genome from mutagenic events as the data suggests, then they would be a poor choice to target with drugs to treat viral infections.

The NTZ-3T3 indicator cell line has been previous used in studies to measure the mutagenic activity of AID (McBride, 2006). As might be suspected the expression of viral UNG in this system alongside AID significantly reduced the reversion rate of the STOP codon (Fig. 27). Although it is not known if the presence of viral UNG in the system alters the spectrum of mutations produced we are currently performing a clonal sequencing analysis to address this question. The results of our CSR experiments demonstrate that UNG may have an alternate protein scaffolding function independent of its catalytic activity. In the future we plan to repeat the NTZ-3T3 mutation assay using the catalytically inactive UNG mutants in order to study what, if any, effect this scaffolding mechanism has on the

frequency of STOP codon reversion and the spectrum of mutations generated by AID activity.

These experiments suggest that herpes virus UNGs may be interfering with AID-mediated antibody diversification mechanisms such as SHM and CSR, while protecting the host cell genome from AID induced chromosomal instability. The pattern and levels of viral UNG expression in infected host B-cells *in vivo* are unknown. Ascertaining the level of viral UNG expression *in vivo* may prove to be a difficult task as there are no commercially available antibodies that specifically recognize viral UNG. One possible approach to study UNG expression levels in an *in vivo* model would be attach an epitope tag such as FLAG to UNG in an MHV68 mouse model system, then isolating particular B-cell subsets such as germinal center B-cells and immunoblotting their protein lysates using an anti-FLAG antibody.

It would also be possible to epitope tag UNG in the EBV genome in order to study its role using an immortalized human B-cell LCL system. An immortalized LCL system that expresses an epitope-tagged viral UNG could prove to be a powerful system to study the biochemistry of EBV-UNG in the presence of the full EBV viral genome and in the context of its native host cell type. This system could potentially be used to identify potential EBV-UNG interacting partners by immuno-precipitation, which would provide valuable insight into the non-catalytic mechanisms of EBV-UNG action. An EBV immortalized LCL system could also be used to study the effects of viral UNG on spectrum and frequency of mutations present in the host B-cell genome, however this may not provide as much information as a full *in vivo* system.

These data also provide insight into the molecular mechanisms of somatic hypermutation and class switch recombination. The fact that expression of viral UNG or mouse UNG in wild-type B-cells reduces switch efficiency suggests that UNG levels are tightly regulated to an optimal level in the CSR process. The intriguing discovery that UNG

catalytic activity is not necessary for this suppression of CSR efficiency suggest that UNG is performing a non-cononical function, likely recruiting factors to the Ig gene locus through protein-protein interaction. This alternate UNG mechanism may somehow contribute to the shift to low fidelity repair mechanisms at the Ig gene locus, perhaps recruiting low fidelity repair factors.

While these experiments demonstrate that it is possible for herpes virus to interfere with the antibody diversification process it is still unknown whether this interference is used as a direct mechanism to inhibit the immune response to the viral infection. It would certainly be advantageous for a virus to prevent the host immune system from effectively responding and adapting to its presence. Epstein Barr infection has been shown to be associated with autoimmune disorders, suggesting that it does interfere with antibody formation *in vivo*, and the discovery that viral UNGs interfere with antibody diversification processes in host B-cell provides a potential mechanism for the formation of EBV associated autoantibodies (Draborg, 2013). It may be possible to detect this influence of viral UNG on antibody formation *in vivo*. By infecting mice with MHV68 or MHV68- Δ UNG virus then isolating B-cell populations the antibody V(D)J sequences between these two groups could be compared. If viral UNG alters SHM *in vivo* there may be differences between the frequency and spectrum of mutations present in these two groups. Given the results from of our NTZ-3T3 indicator cell line assay one might expect the MHV68-UNG expressing group to have less mutations overall when compared to the MHV68- Δ UNG group. However it is possible that the involvement of MHV68-UNG at the Ig locus alters the spectrum of mutations present, as the mechanisms that lead to error prone repair at the Ig locus are not well understood. A mouse model may serve as a better system to understand the influence of viral UNG on mutation since cell lines such as the NTZ-3T3 cells may not express the necessary factors to initiate error-prone repair in response to the removal of uracil from DNA. This system could also be used to test for the effect of viral UNG on CSR *in vivo*. The data from *in vitro* CSR assays

suggests that the presence of viral UNG interferes with molecular mechanisms of the CSR process. However the *in vitro* assay provides limited information due to the fact that we are only measuring the efficiency of switch from one isotype to another (IgM to IgG1), and that viral UNG expression is driven off of an artificial promoter providing high protein expression. It would be possible to measure the effect of viral UNG on the CSR process *in vivo* by comparing infected B-cells from MHV68 and MHV68- Δ UNG infected mice. The frequency of different BCR isotypes expressed on infected cells could then be measured by FACS analysis. If the presence of viral UNG does indeed inhibit of the ability of B-cells to undergo CSR one might predict that B-cells infected with MHV68-UNG expression would have elevated levels of IgM expressing B-cells. An *in vivo* system such as this could also be used to test the theory that herpes virus UNG interference at the Ig locus is actively involved in suppressing ability of the host immune system to produce antibodies that recognize the virus. Serum from MHV68 and MHV68- Δ UNG infected mice could be tested for its ability to recognize MHV68 viral proteins via immunoblot assay.

Another possible explanation for the involvement of herpes virus UNG during SHM and CSR is to promote survival and proliferation of the host B-cell. Herpes viruses that target B-cells such as MHV68 and EBV possess a number of genes that stimulate growth and survival of their host cell, allowing for replication of the episomal viral genome in the process. AID expression is tightly restricted to germinal center B-cells where SHM and CSR occur. EBV genes like LMP-1 and LMP-2 mimic and augment growth and survival signals found in germinal center reaction reactions, In fact EBV LMP-1, which mimics CD40 stimulation, has been shown to up-regulate AID expression (Kim, 2013). While AID induced mutations produce a diverse antibody repertoire they can also lead to programmed cell death. We have demonstrated that viral UNG is able to reduce the frequency of oncogenic translocations (Fig. 24) that would most likely lead to apoptosis if they were to occur in wild-type cells *in vivo*. Viral UNG interference in AID-mediated processes may simply be a

means for the virus to reduce the level of potentially genotoxic mutations, enhancing the survival of the host cell and therefore the virus. This could be tested experimentally by using an *in vivo* competition assay, infecting mice with wild-type MHV68 or MHV68- Δ UNG and tracking each population with a unique label. After some length of time the ratio of wild-type MHV-UNG to MHV68- Δ UNG virus expressing cells could be measured. If the infected cells expressing MHV-UNG survive consistently longer than the MHV68- Δ UNG expressing cells it would suggest that the presence of viral UNG does indeed provide protection to the host cell.

Bibliography

Akbari, M., Pena-Diaz, J., Andersen, S., Liabakk, N.B., Otterlei, M., and Krokan, H.E. (2009). Extracts of proliferating and non-proliferating human cells display different base excision pathways and repair fidelity. *DNA Repair (Amst)* 8, 834-843.

Aloj, G., Giardino, G., Valentino, L., Maio, F., Gallo, V., Esposito, T., Naddei, R., Cirillo, E., and Pignata, C. (2012). Severe combined immunodeficiencies: new and old scenarios. *International reviews of immunology* 31, 43-65.

Amon, W., and Farrell, P.J. (2005). Reactivation of Epstein-Barr virus from latency. *Reviews in medical virology* 15, 149-156.

Anagnostopoulos, I., Hummel, M., Kreschel, C., and Stein, H. (1995). Morphology, immunophenotype, and distribution of latently and/or productively Epstein-Barr virus-infected cells in acute infectious mononucleosis: implications for the interindividual infection route of Epstein-Barr virus. *Blood* 85, 744-750.

Ascherio, A., Munger, K.L., Lennette, E.T., Spiegelman, D., Hernan, M.A., Olek, M.J., Hankinson, S.E., and Hunter, D.J. (2001). Epstein-Barr virus antibodies and risk of multiple sclerosis: a prospective study. *JAMA* 286, 3083-3088.

Baer, R., Bankier, A.T., Biggin, M.D., Deininger, P.L., Farrell, P.J., Gibson, T.J., Hatfull, G., Hudson, G.S., Satchwell, S.C., Seguin, C., *et al.* (1984). DNA sequence and expression of the B95-8 Epstein-Barr virus genome. *Nature* 310, 207-211.

Beck, J., and Nassal, M. (2007). Hepatitis B virus replication. *World journal of gastroenterology* : WJG 13, 48-64.

Begum, N.A., Izumi, N., Nishikori, M., Nagaoka, H., Shinkura, R., and Honjo, T. (2007). Requirement of non-canonical activity of uracil DNA glycosylase for class switch recombination. *J Biol Chem* 282, 731-742.

Blaskovic, D., Stancekova, M., Svobodova, J., and Mistrikova, J. (1980). Isolation of five strains of herpesviruses from two species of free living small rodents. *Acta virologica* 24, 468.

Boshoff, C., and Weiss, R. (2002). AIDS-related malignancies. *Nature reviews Cancer* 2, 373-382.

Brady, G., Macarthur, G.J., and Farrell, P.J. (2008). Epstein-Barr virus and Burkitt lymphoma. *Postgraduate medical journal* 84, 372-377.

Cai, Q., Verma, S.C., Lu, J., and Robertson, E.S. (2010). Molecular biology of Kaposi's sarcoma-associated herpesvirus and related oncogenesis. *Advances in virus research* 78, 87-142.

Caldwell, R.G., Wilson, J.B., Anderson, S.J., and Longnecker, R. (1998). Epstein-Barr virus LMP2A drives B cell development and survival in the absence of normal B cell receptor signals. *Immunity* 9, 405-411.

Cesarman, E., Chang, Y., Moore, P.S., Said, J.W., and Knowles, D.M. (1995). Kaposi's sarcoma-associated herpesvirus-like DNA sequences in AIDS-related body-cavity-based lymphomas. *N Engl J Med* 332, 1186-1191.

Cesarman, E., Nador, R.G., Bai, F., Bohenzky, R.A., Russo, J.J., Moore, P.S., Chang, Y., and Knowles, D.M. (1996). Kaposi's sarcoma-associated herpesvirus contains G protein-coupled receptor and cyclin D homologs which are expressed in Kaposi's sarcoma and malignant lymphoma. *J Virol* 70, 8218-8223.

Chang, M.H. (2007). Hepatitis B virus infection. *Seminars in fetal & neonatal medicine* 12, 160-167.

Chang, Y., Cesarman, E., Pessin, M.S., Lee, F., Culpepper, J., Knowles, D.M., and Moore, P.S. (1994). Identification of herpesvirus-like DNA sequences in AIDS-associated Kaposi's sarcoma. *Science* 266, 1865-1869.

Chen, G., Dimitriou, I.D., La Rose, J., Ilangumaran, S., Yeh, W.C., Doody, G., Turner, M., Gommerman, J., and Rottapel, R. (2007). The 3BP2 adapter protein is required for optimal B-cell activation and thymus-independent type 2 humoral response. *Molecular and cellular biology* 27, 3109-3122.

Cheng, H.L., Vuong, B.Q., Basu, U., Franklin, A., Schwer, B., Astarita, J., Phan, R.T., Datta, A., Manis, J., Alt, F.W., *et al.* (2009). Integrity of the AID serine-38 phosphorylation site is critical for class switch recombination and somatic hypermutation in mice. *Proceedings of the National Academy of Sciences of the United States of America* 106, 2717-2722.

Chiotan, C., Radu, L., Serban, R., Cornacel, C., Cioboata, M., and Anghel, A. (2014). Cytomegalovirus retinitis in HIV/AIDS patients. *Journal of medicine and life* 7, 237-240.

Cohen, J.I. (2013). Clinical practice: Herpes zoster. *N Engl J Med* 369, 255-263.

Conticello, S.G. (2008). The AID/APOBEC family of nucleic acid mutators. *Genome Biol* 9, 229.

Cortazar, D., Kunz, C., Selfridge, J., Lettieri, T., Saito, Y., MacDougall, E., Wirz, A., Schuermann, D., Jacobs, A.L., Siegrist, F., *et al.* (2011). Embryonic lethal phenotype reveals a function of TDG in maintaining epigenetic stability. *Nature* 470, 419-423.

Cyster, J.G. (2010). B cell follicles and antigen encounters of the third kind. *Nat Immunol* 11, 989-996.

Delker, R.K., Fugmann, S.D., and Papavasiliou, F.N. (2009). A coming-of-age story: activation-induced cytidine deaminase turns 10. *Nat Immunol* 10, 1147-1153.

Di Noia, J.M., Williams, G.T., Chan, D.T., Buerstedde, J.M., Baldwin, G.S., and Neuberger, M.S. (2007). Dependence of antibody gene diversification on uracil excision. *J Exp Med* 204, 3209-3219.

Diaz, M., and Storb, U. (2003). A novel cytidine deaminase AIDs in the delivery of error-prone polymerases to immunoglobulin genes. *DNA Repair (Amst)* 2, 623-627.

Draborg, A.H., Duus, K., and Houen, G. (2013). Epstein-Barr virus in systemic autoimmune diseases. *Clinical & developmental immunology* 2013, 535738.

El-Serag, H.B., and Rudolph, K.L. (2007). Hepatocellular carcinoma: epidemiology and molecular carcinogenesis. *Gastroenterology* 132, 2557-2576.

Epstein, M.A., Achong, B.G., and Barr, Y.M. (1964). Virus Particles in Cultured Lymphoblasts from Burkitt's Lymphoma. *Lancet* 1, 702-703.

Fajgenbaum, D.C., van Rhee, F., and Nabel, C.S. (2014). HHV-8-negative, idiopathic multicentric Castleman disease: novel insights into biology, pathogenesis, and therapy. *Blood* 123, 2924-2933.

Fortini, P., and Dogliotti, E. (2007). Base damage and single-strand break repair: mechanisms and functional significance of short- and long-patch repair subpathways. *DNA Repair (Amst)* 6, 398-409.

Ganguly, N., and Parihar, S.P. (2009). Human papillomavirus E6 and E7 oncoproteins as risk factors for tumorigenesis. *Journal of biosciences* 34, 113-123.

Gazumyan, A., Timachova, K., Yuen, G., Siden, E., Di Virgilio, M., Woo, E.M., Chait, B.T., Reina San-Martin, B., Nussenzweig, M.C., and McBride, K.M. (2011). Amino-terminal phosphorylation of activation-induced cytidine deaminase suppresses c-myc/IgH translocation. *Molecular and cellular biology* 31, 442-449.

Geoui, T., Buisson, M., Tarbouriech, N., and Burmeister, W.P. (2007). New insights on the role of the gamma-herpesvirus uracil-DNA glycosylase leucine loop revealed by the structure of the Epstein-Barr virus enzyme in complex with an inhibitor protein. *J Mol Biol* 366, 117-131.

Grinde, B. (2013). Herpesviruses: latency and reactivation - viral strategies and host response. *Journal of oral microbiology* 5.

Gupta, P., Suryadevara, M., and Das, A. (2014). Cytomegalovirus-induced hepatitis in an immunocompetent patient. *The American journal of case reports* 15, 447-449.

Hagen, L., Kavli, B., Sousa, M.M., Torseth, K., Liabakk, N.B., Sundheim, O., Pena-Diaz, J., Otterlei, M., Horning, O., Jensen, O.N., *et al.* (2008). Cell cycle-specific UNG2 phosphorylations regulate protein turnover, activity and association with RPA. *The EMBO journal* 27, 51-61.

Henderson, S., Rowe, M., Gregory, C., Croom-Carter, D., Wang, F., Longnecker, R., Kieff, E., and Rickinson, A. (1991). Induction of bcl-2 expression by Epstein-Barr virus latent membrane protein 1 protects infected B cells from programmed cell death. *Cell* 65, 1107-1115.

Howard, J.H., Frolov, A., Tzeng, C.W., Stewart, A., Midzak, A., Majmundar, A., Godwin, A., Heslin, M., Bellacosa, A., and Arnoletti, J.P. (2009). Epigenetic downregulation of the DNA repair gene MED1/MBD4 in colorectal and ovarian cancer. *Cancer biology & therapy* 8, 94-100.

Huff, J.L., and Barry, P.A. (2003). B-virus (Cercopithecine herpesvirus 1) infection in humans and macaques: potential for zoonotic disease. *Emerg Infect Dis* 9, 246-250.

Humme, S., Reisbach, G., Feederle, R., Delecluse, H.J., Bousset, K., Hammerschmidt, W., and Schepers, A. (2003). The EBV nuclear antigen 1 (EBNA1) enhances B cell immortalization several thousandfold. *Proceedings of the National Academy of Sciences of the United States of America* 100, 10989-10994.

Jung, J.U., Stager, M., and Desrosiers, R.C. (1994). Virus-encoded cyclin. *Molecular and cellular biology* 14, 7235-7244.

Kavli, B., Sundheim, O., Akbari, M., Otterlei, M., Nilsen, H., Skorpen, F., Aas, P.A., Hagen, L., Krokan, H.E., and Slupphaug, G. (2002). hUNG2 is the major repair enzyme for removal of uracil from U:A matches, U:G mismatches, and U in single-stranded DNA, with hSMUG1 as a broad specificity backup. *J Biol Chem* 277, 39926-39936.

Kawai, K., Gebremeskel, B.G., and Acosta, C.J. (2014). Systematic review of incidence and complications of herpes zoster: towards a global perspective. *BMJ open* 4, e004833.

Kelly, G., Bell, A., and Rickinson, A. (2002). Epstein-Barr virus-associated Burkitt lymphomagenesis selects for downregulation of the nuclear antigen EBNA2. *Nature medicine* 8, 1098-1104.

Kemmerich, K., Dingler, F.A., Rada, C., and Neuberger, M.S. (2012). Germline ablation of SMUG1 DNA glycosylase causes loss of 5-hydroxymethyluracil- and UNG-backup uracil-

excision activities and increases cancer predisposition of Ung^{-/-}Msh2^{-/-} mice. *Nucleic acids research* 40, 6016-6025.

Kim, J.H., Kim, W.S., and Park, C. (2013). Epstein-Barr virus latent membrane protein 1 increases genomic instability through Egr-1-mediated up-regulation of activation-induced cytidine deaminase in B-cell lymphoma. *Leuk Lymphoma* 54, 2035-2040.

Kitamura, K., Wang, Z., Chowdhury, S., Simadu, M., Koura, M., and Muramatsu, M. (2013). Uracil DNA glycosylase counteracts APOBEC3G-induced hypermutation of hepatitis B viral genomes: excision repair of covalently closed circular DNA. *PLoS pathogens* 9, e1003361.

Krokan, H.E., and Bjoras, M. (2013). Base excision repair. *Cold Spring Harbor perspectives in biology* 5, a012583.

Mackett, M., Stewart, J.P., de, V.P.S., Chee, M., Efstathiou, S., Nash, A.A., and Arrand, J.R. (1997). Genetic content and preliminary transcriptional analysis of a representative region of murine gammaherpesvirus 68. *The Journal of general virology* 78 (Pt 6), 1425-1433.

McBride, K.M., Barreto, V., Ramiro, A.R., Stavropoulos, P., and Nussenzweig, M.C. (2004). Somatic hypermutation is limited by CRM1-dependent nuclear export of activation-induced deaminase. *J Exp Med* 199, 1235-1244.

McBride, K.M., Gazumyan, A., Woo, E.M., Barreto, V.M., Robbiani, D.F., Chait, B.T., and Nussenzweig, M.C. (2006). Regulation of hypermutation by activation-induced cytidine deaminase phosphorylation. *Proc Natl Acad Sci U S A* 103, 8798-8803.

McHeyzer-Williams, L.J., and McHeyzer-Williams, M.G. (2005). Antigen-specific memory B cell development. *Annu Rev Immunol* 23, 487-513.

Millns, A.K., Carpenter, M.S., and DeLange, A.M. (1994). The vaccinia virus-encoded uracil DNA glycosylase has an essential role in viral DNA replication. *Virology* 198, 504-513.

Minkah, N., Macaluso, M., Oldenburg, D.G., Paden, C.R., White, D.W., McBride, K.M., and Krug, L.T. (2015). Absence of the Uracil DNA Glycosylase of Murine Gammaherpesvirus 68 Impairs Replication and Delays the Establishment of Latency In Vivo. *J Virol*.

Mol, C.D., Arvai, A.S., Slupphaug, G., Kavli, B., Alseth, I., Krokan, H.E., and Tainer, J.A. (1995). Crystal structure and mutational analysis of human uracil-DNA glycosylase: structural basis for specificity and catalysis. *Cell* 80, 869-878.

Muramatsu, M., Kinoshita, K., Fagarasan, S., Yamada, S., Shinkai, Y., and Honjo, T. (2000). Class switch recombination and hypermutation require activation-induced cytidine deaminase (AID), a potential RNA editing enzyme. *Cell* 102, 553-563.

Muramatsu, M., Sankaranand, V.S., Anant, S., Sugai, M., Kinoshita, K., Davidson, N.O., and Honjo, T. (1999). Specific expression of activation-induced cytidine deaminase (AID), a novel member of the RNA-editing deaminase family in germinal center B cells. *J Biol Chem* 274, 18470-18476.

Nakamura, M., Kondo, S., Sugai, M., Nazarea, M., Imamura, S., and Honjo, T. (1996). High frequency class switching of an IgM⁺ B lymphoma clone CH12F3 to IgA⁺ cells. *Int Immunol* 8, 193-201.

Neipel, F., Albrecht, J.C., Ensser, A., Huang, Y.Q., Li, J.J., Friedman-Kien, A.E., and Fleckenstein, B. (1997a). Human herpesvirus 8 encodes a homolog of interleukin-6. *J Virol* 71, 839-842.

Neipel, F., Albrecht, J.C., and Fleckenstein, B. (1997b). Cell-homologous genes in the Kaposi's sarcoma-associated rhadinovirus human herpesvirus 8: determinants of its pathogenicity? *J Virol* 71, 4187-4192.

Nemerow, G.R., Mold, C., Schwend, V.K., Tollefson, V., and Cooper, N.R. (1987). Identification of gp350 as the viral glycoprotein mediating attachment of Epstein-Barr virus (EBV) to the EBV/C3d receptor of B cells: sequence homology of gp350 and C3 complement fragment C3d. *J Virol* 61, 1416-1420.

Nilsen, H., Rosewell, I., Robins, P., Skjelbred, C.F., Andersen, S., Slupphaug, G., Daly, G., Krokan, H.E., Lindahl, T., and Barnes, D.E. (2000). Uracil-DNA glycosylase (UNG)-deficient mice reveal a primary role of the enzyme during DNA replication. *Molecular cell* 5, 1059-1065.

Odumade, O.A., Hogquist, K.A., and Balfour, H.H., Jr. (2011). Progress and problems in understanding and managing primary Epstein-Barr virus infections. *Clinical microbiology reviews* 24, 193-209.

Polack, A., Hortnagel, K., Pajic, A., Christoph, B., Baier, B., Falk, M., Mautner, J., Geltinger, C., Bornkamm, G.W., and Kempkes, B. (1996). c-myc activation renders proliferation of Epstein-Barr virus (EBV)-transformed cells independent of EBV nuclear antigen 2 and latent

membrane protein 1. Proceedings of the National Academy of Sciences of the United States of America 93, 10411-10416.

Portis, T., Dyck, P., and Longnecker, R. (2003). Epstein-Barr Virus (EBV) LMP2A induces alterations in gene transcription similar to those observed in Reed-Sternberg cells of Hodgkin lymphoma. Blood 102, 4166-4178.

Pyles, R.B., and Thompson, R.L. (1994). Evidence that the herpes simplex virus type 1 uracil DNA glycosylase is required for efficient viral replication and latency in the murine nervous system. J Virol 68, 4963-4972.

Raab-Traub, N. (2002). Epstein-Barr virus in the pathogenesis of NPC. Seminars in cancer biology 12, 431-441.

Ramiro, A.R., Jankovic, M., Callen, E., Difilippantonio, S., Chen, H.T., McBride, K.M., Eisenreich, T.R., Chen, J., Dickins, R.A., Lowe, S.W., *et al.* (2006). Role of genomic instability and p53 in AID-induced c-myc-Igh translocations. Nature 440, 105-109.

Revy, P., Muto, T., Levy, Y., Geissmann, F., Plebani, A., Sanal, O., Catalan, N., Forveille, M., Dufourcq-Labelouse, R., Gennery, A., *et al.* (2000). Activation-induced cytidine deaminase (AID) deficiency causes the autosomal recessive form of the Hyper-IgM syndrome (HIGM2). Cell 102, 565-575.

Riccio, A., Aaltonen, L.A., Godwin, A.K., Loukola, A., Percesepe, A., Salovaara, R., Masciullo, V., Genuardi, M., Paravatou-Petsotas, M., Bassi, D.E., *et al.* (1999). The DNA

repair gene MBD4 (MED1) is mutated in human carcinomas with microsatellite instability.

Nature genetics 23, 266-268.

Rosen, H.R. (2011). Clinical practice. Chronic hepatitis C infection. *N Engl J Med* 364, 2429-2438.

Rother, R.P., Rollins, S.A., Fodor, W.L., Albrecht, J.C., Setter, E., Fleckenstein, B., and Squinto, S.P. (1994). Inhibition of complement-mediated cytolysis by the terminal complement inhibitor of herpesvirus saimiri. *J Virol* 68, 730-737.

Rowe, M., Rowe, D.T., Gregory, C.D., Young, L.S., Farrell, P.J., Rupani, H., and Rickinson, A.B. (1987). Differences in B cell growth phenotype reflect novel patterns of Epstein-Barr virus latent gene expression in Burkitt's lymphoma cells. *The EMBO journal* 6, 2743-2751.

Schatz, D.G., and Ji, Y. (2011). Recombination centres and the orchestration of V(D)J recombination. *Nature reviews Immunology* 11, 251-263.

Schiffman, M., and Castle, P.E. (2003). Human papillomavirus: epidemiology and public health. *Archives of pathology & laboratory medicine* 127, 930-934.

Shen, H.M., Tanaka, A., Bozek, G., Nicolae, D., and Storb, U. (2006). Somatic hypermutation and class switch recombination in *Msh6(-/-)Ung(-/-)* double-knockout mice. *J Immunol* 177, 5386-5392.

Shen, J., Pavone, A., Mikulec, C., Hensley, S.C., Traner, A., Chang, T.K., Person, M.D., and Fischer, S.M. (2007). Protein expression profiles in the epidermis of cyclooxygenase-2

transgenic mice by 2-dimensional gel electrophoresis and mass spectrometry. *J Proteome Res* 6, 273-286.

Shlomchik, M.J., and Weisel, F. (2012). Germinal center selection and the development of memory B and plasma cells. *Immunol Rev* 247, 52-63.

Simas, J.P., and Efstathiou, S. (1998). Murine gammaherpesvirus 68: a model for the study of gammaherpesvirus pathogenesis. *Trends in microbiology* 6, 276-282.

Soulier, J., Grollet, L., Oksenhendler, E., Cacoub, P., Cazals-Hatem, D., Babinet, P., d'Agay, M.F., Clauvel, J.P., Raphael, M., Degos, L., *et al.* (1995). Kaposi's sarcoma-associated herpesvirus-like DNA sequences in multicentric Castleman's disease. *Blood* 86, 1276-1280.

Sunil-Chandra, N.P., Arno, J., Fazakerley, J., and Nash, A.A. (1994). Lymphoproliferative disease in mice infected with murine gammaherpesvirus 68. *The American journal of pathology* 145, 818-826.

Tichy, E.D., Liang, L., Deng, L., Tischfield, J., Schwemberger, S., Babcock, G., and Stambrook, P.J. (2011). Mismatch and base excision repair proficiency in murine embryonic stem cells. *DNA Repair (Amst)* 10, 445-451.

Tulman, E.R., Afonso, C.L., Lu, Z., Zsak, L., Kutish, G.F., and Rock, D.L. (2001). Genome of lumpy skin disease virus. *J Virol* 75, 7122-7130.

Uchida, J., Yasui, T., Takaoka-Shichijo, Y., Muraoka, M., Kulwichit, W., Raab-Traub, N., and Kikutani, H. (1999). Mimicry of CD40 signals by Epstein-Barr virus LMP1 in B lymphocyte responses. *Science* 286, 300-303.

Usherwood, E.J., Stewart, J.P., and Nash, A.A. (1996). Characterization of tumor cell lines derived from murine gammaherpesvirus-68-infected mice. *J Virol* 70, 6516-6518.

Ward, T.M., Williams, M.V., Traina-Dorge, V., and Gray, W.L. (2009). The simian varicella virus uracil DNA glycosylase and dUTPase genes are expressed in vivo, but are non-essential for replication in cell culture. *Virus research* 142, 78-84.

Watson, C.T., Steinberg, K.M., Huddleston, J., Warren, R.L., Malig, M., Schein, J., Willsey, A.J., Joy, J.B., Scott, J.K., Graves, T.A., *et al.* (2013). Complete haplotype sequence of the human immunoglobulin heavy-chain variable, diversity, and joining genes and characterization of allelic and copy-number variation. *American journal of human genetics* 92, 530-546.

Weck, K.E., Dal Canto, A.J., Gould, J.D., O'Guin, A.K., Roth, K.A., Saffitz, J.E., Speck, S.H., and Virgin, H.W. (1997). Murine gamma-herpesvirus 68 causes severe large-vessel arteritis in mice lacking interferon-gamma responsiveness: a new model for virus-induced vascular disease. *Nature medicine* 3, 1346-1353.

Who (2009). Human papillomavirus vaccines: WHO position paper. *Biologicals : journal of the International Association of Biological Standardization* 37, 338-344.

Young, L., Alfieri, C., Hennessy, K., Evans, H., O'Hara, C., Anderson, K.C., Ritz, J., Shapiro, R.S., Rickinson, A., Kieff, E., *et al.* (1989). Expression of Epstein-Barr virus transformation-associated genes in tissues of patients with EBV lymphoproliferative disease. *N Engl J Med* 321, 1080-1085.

Young, L.S., and Rickinson, A.B. (2004). Epstein-Barr virus: 40 years on. *Nature reviews Cancer* 4, 757-768.

Yu, M.C., and Yuan, J.M. (2002). Epidemiology of nasopharyngeal carcinoma. *Seminars in cancer biology* 12, 421-429.

Zipfel, P.A., Grove, M., Blackburn, K., Fujimoto, M., Tedder, T.F., and Pendergast, A.M. (2000). The c-Abl tyrosine kinase is regulated downstream of the B cell antigen receptor and interacts with CD19. *J Immunol* 165, 6872-6879.

Vita

Marc Daniel Macaluso was born in Kansas City, Missouri, in 1983 to Irene and Robert Macaluso. He grew up in the suburbs of Houston and attended Texas Tech University where he received his Bachelors of Science in Biochemistry in 2006. In 2006 he worked for Receptor Logic Inc. developing specialized antibodies. In 2007 he matriculated in the Graduate School of Biomedical Sciences at The University of Texas M.D. Anderson Cancer Center.